Remote Sensing in Water Resources Management: The State of the Art

Remote Sensing in Water Resources Management: The State of the Art

Wim G. M. Bastiaanssen

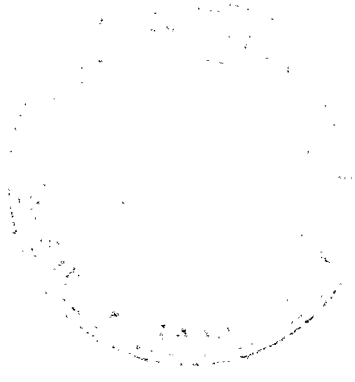

IWMI

INTERNATIONAL WATER MANAGEMENT INSTITUTE

P.O. Box 2075, Colombo, Sri Lanka

The Author: Wim G. M. Bastiaanssen is a senior agro-hydrologist assigned to the Performance Assessment Program of the International Water Management Institute (IWMI), and a visiting Associate Professor at the International Institute for Aerospace Survey and Earth Sciences (ITC) dealing with remote sensing and geographic information systems for water resources management analysis. From 1986 to 1996, he worked with the DLO-Winand Staring Centre in Wageningen on water management research issues in arid zones.

Bastiaanssen, W. G. M. 1998. *Remote sensing in water resources management: The state of the art.* Colombo, Sri Lanka: International Water Management Institute.

/ remote sensing / irrigation management / efficient water use / evapotranspiration / irrigated farming / satellite surveys / hydrology / meteorology / agronomy / soil salinity / water requirements / river basins / environment / health /

ISBN 92-9090-363-5

The International Irrigation Management Institute, one of sixteen centers supported by the Consultative Group on International Agricultural Research (CGIAR), was incorporated by an Act of Parliament in Sri Lanka. The Act is currently under amendment to read as International Water Management Institute (IWMI).

Contents

Preface

THIS REPORT FOCUSES on the applications of remote sensing that support water resources management in irrigated river basins and summarizes the major achievements. Most of the cited publications cover elements of both irrigation and remote sensing sciences. Some scientifically good remote sensing papers were omitted because they were not linked to irrigation management. Most of the papers deal with satellite remote sensing; little attention has been paid to airborne remote sensing. Although interest in using aircraft is growing in a few agricultural areas in industrialized countries, this approach is seldom feasible for operational monitoring of irrigation, particularly in developing countries. Nevertheless some aircraft studies that involve prototype radiometers scheduled for future space platforms have been given attention in this report.

Irrigation and drainage professionals unfamiliar with remote sensing techniques may find the vocabulary difficult. The aim of this report is partly to describe the current state of the science, and use of remote sensing nomenclature was unavoidable. It is not intended as an introductory remote sensing textbook for irrigation engineers.

The scientific progress of remote sensing is described in chapter 2. Readers interested only in the possibilities that remote sensing offers nowadays, rather than in the technical derivation of remote sensing determinants, can skip chapter 2. Chapters 3, 4, and 5 focus on applications and cost aspects and may be of greater interest to policy makers and managers of irrigated river basins.

An extensive list of scientific publications provides further references related to specific issues.

Summary

DURING THE LAST decade, scientists in national research programs have shown increasing interest in using data from earth observation satellites to obtain information on land surface parameters. Better understanding of land surface conditions is needed for several applications in hydrology, meteorology, and agronomy. Inspiring results have been achieved, and these insights should be utilized for the management of irrigation schemes and distribution of water within river basins. This state-of-the-art review examines pertinent articles that describe the technical application of fractional vegetation cover, leaf area index, crop type, crop yield, crop water stress, and evapotranspiration. The information can be obtained under cloud-free conditions by both high resolution (20 to 30 m) and low resolution (1.1 km) satellite measurements. Combining measurements from less frequent overpasses at high spatial resolution with measurements from frequent overpasses at low spatial resolution is advantageous.

This review includes discussion of the relevance of remote sensing in basic and applied research for irrigation management. The importance of remote sensing is found in the early detection of soil salinity and as a procedure for assessing soil moisture at the soil surface and water storage in the root zone. Additional basic research is needed to solve these issues. Remote sensing produces the spectral measurements that provide the biophysical input data needed to determine actual and potential evapotranspiration. This information can help solve basic issues on regional scale water use and water requirements. Some suggestions for intercomparison studies among remote sensing algorithms are outlined. Finally, application studies will be required to bridge the gap between scientific achievements in remote sensing for agriculture and the needs of managers and policy makers for water allocation and irrigation performance indicators. Examples demonstrate how remotely sensed data can provide key information for better management of water in irrigated river basins.

1.

Introduction

IRRIGATION IS THE largest consumer of fresh water. Seckler et al. (1998) estimate that around 70 percent of all water used each year produces 30 to 40 percent of the world's food crops on 17 percent of all arable land. As water scarcity becomes more acute and competition for fresh water intensifies, better irrigation management will be required to achieve greater efficiency in the use of this valuable resource. More knowledgeable management is essential for improving crop production per unit of water from the field level up to entire river basins.

But we lack accurate information on the conditions of irrigation systems, making performance hard to quantify (Molden 1997). And as a result, when technical interventions are made, the effects on the actual performance of the irrigation system are difficult to describe. Financial investments intended to improve productivity and make efficient use of good quality irrigation water can be economically justified only if progress becomes a measurable phenomenon. Too often, progress in water management is interpreted qualitatively and subjectively.

Achieving food security through irrigation while combating waterlogging and salinization to ensure sustainable agriculture requires quantitative and repetitive analysis of the irrigation processes. The task of providing that information on scales ranging from farm fields to command areas and entire water basins is far from trivial. Distinct spatial variations in soil properties, soil moisture status, cropping conditions, and micro-meteorology all occur within an irrigation scheme. Although information on irrigation practices can be acquired by conventional field visits, they have a subjective character, and survey methodologies usually differ from survey to survey. Moreover, field data can become outdated because changes in land and water management occur frequently. Consequently, remote sensing from space, which can regularly provide objective information on the agricultural and hydrological conditions of large land surface areas as well as small ones, has a great potential for enhancing the management of irrigation systems.

The capacity of remote sensing to identify and monitor crop parameters has expanded greatly during the last 15 years, even though several unresolved issues still exist. Many national research programs have encouraged scientists to study the spectral radiative properties of the earth's surface as measured from satellites. Rising concerns about the rapid degradation of many nonrenewable natural resources have given remote sensing investigations added impetus. The International Satellite Land-Surface Climatology Project (ISLSCP) encourages scientists to use remote sensing data to better understand natural processes on the global land surface (e.g., Sellers et al. 1995). Large-scale field experiments have been executed to validate remote sensing algorithms for estimating surface parameters and fluxes such as evapotranspiration (WMO 1988). Such studies have established that the presence of crops can be determined and several biophysical parameters can be measured with an accuracy of over 80 percent. This accuracy exceeds that of data collected in a heterogeneous irrigation environ-

ment by conventional methods. Another strength of remotely sensed data is that it allows the construction of long time series—as much as 10 to 20 years—for investigating changes in irrigation conditions.

At present, however, remote sensing is essentially a research tool and is not applied in the management of irrigated agricultural systems. The transfer of thoroughly tested remote sensing algorithms into practical management tools needs attention. This publication describes the state of the art of remote sensing in irrigated agriculture and attempts to:

- categorize global research efforts on remote sensing in agriculture
- classify research findings into degrees of applicability
- identify cost and benefits related to the application of satellite remote sensing
- offer a blueprint of future remote sensing programs for supporting water resources management in general, and irrigated agriculture in particular

Inventory

Of the nearly 500 scientific publications cited in this review, 313 that explicitly relate to irrigation management and remote sensing are categorized in table 1. These publications are far from a complete inventory of the global research on irrigation and remote sensing, however the table captures the trends and developments. Earlier reviews in this field were made by Menenti (1990), Vidal and Sagardoy (1995), and Thiruvengadachari and Sakthivadivel (1997). Their citations along with others have been used for the establishment of table 1. Most of the references have appeared in refereed journals, although some are internal reports from research laboratories.

Table 1. Categorized remote sensing publications that explicitly refer to irrigation management.

Category	Before 1986	1986–90	1991–97	Total
Irrigated area	4	21	15	40
Land use	4	16	29	49
Crop water needs	1	13	15	29
Crop water use	3	9	20	32
Crop water stress	10	2	18	30
Crop yield	3	0	12	15
Rainfall	0	2	1	3
Soil salinity	30	28	22	80
Waterlogging	1	2	8	11
Reservoir or pond mapping	0	2	6	8
Infrastructure	1	2	2	5
Reviews	1	5	5	11
TOTAL	58	102	153	313

Table 1 shows that the number of publications grew nearly three-fold from the pre-1986 period to the 1991–97 period. Most research has been dedicated to soil salinity mapping (80 publications), land use (49), and the quantification of the area under irrigation (40). Crop hydrological surveillance by remote sensing made rapid progress after 1990, although pioneering work was done in the late 1970s. Publications on crop classifications appeared more frequently in the 1990s after improved sensors onboard Landsat, SPOT (Satellite pour l'Observation de la Terre), and IRS (Indian Remote Sensing Satellite) made data with higher spatial resolution available. The leading international research centers active in irrigation and remote sensing are listed in Annex 1.

Principal Steps

Figure 1 shows the sequence of interdisciplinary steps between the raw satellite signal and end users—irrigation engineers. Satellites measure reflected and emitted radiances in narrow intervals between specified lower and upper bands in the electromagnetic spectrum. An at-

Figure 1. Disciplines and sequence of procedures needed to interpret satellite spectral measurements for use in practical irrigation management performance indicators.

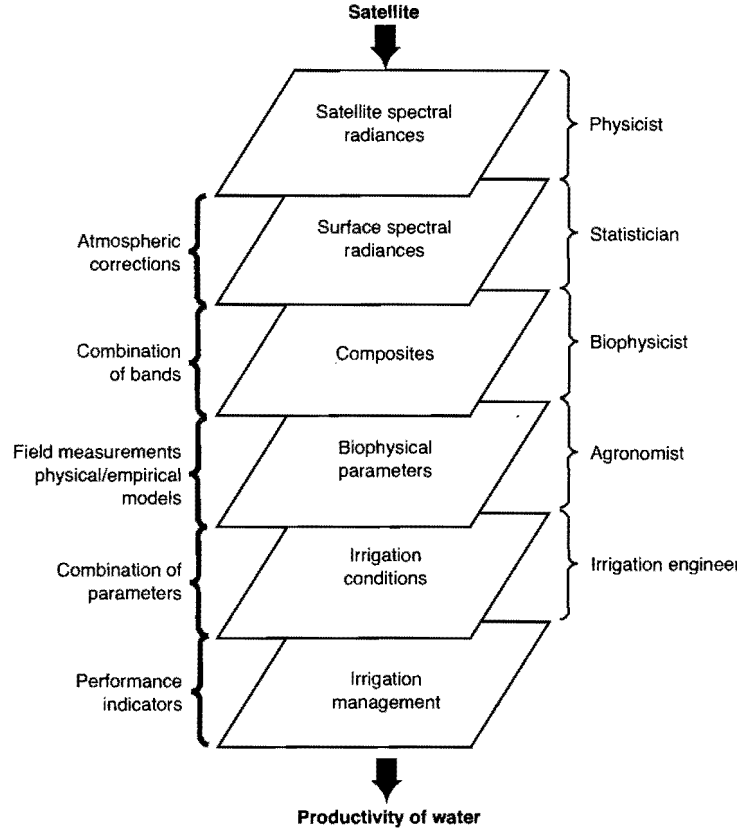

mospheric correction procedure is first needed to convert the at-satellite radiances into their at-surface counterparts, which is a discipline typically governed by radiation physicists. A geometric correction must be applied to ensure that the image coordinates of the pixels (a pixel or picture element is the smallest resolvable spatial scale in an image) agree with the topographical coordinates.

Compositing individual spectral at-surface radiances forms the basis for recognizing thematic land classes, and the identification of these classes is a typical problem addressed in statistics (first-order information). Other basic parameters such as vegetation indices, surface albedo (reflected shortwave radiation), and surface temperature can also be obtained by simply compositing individual bands. Adding information from field surveys and including physico-mathematical algorithms allows the estimation of biophysical properties and processes (second-order information). A third hierarchical order can be identified when several second-order information products are integrated to arrive at the irrigation conditions. The final stage is transferring this information into meaningful managerial tools (fourth-order information). These steps should be fully understood before applying satellite data in an operational fashion so that day-to-day or season-to-season irrigation management can be supported.

The remote sensing data source can consist of spectral information, view and illumination (bidirectional) information, spatial information, temporal information, and polarization information. Annex 2 summarizes the spectral, spatial, and temporal resolutions of current earth resources satellites. In addition to single missions, the U.S. National Aeronautics and Space Administration and the European Space Agency are planning to launch space stations that will accommodate several sensors. Annex 3 shows the rapid evolution of measurement capabilities, which is opening new avenues for quantifying and understanding land surface processes.

Detailed explanations of typical remote sensing techniques and their related vocabularies are not given in this publication, but many introductory handbooks are available that deal with remote sensing science and technological aspects in general (Curran 1985; Jensen 1986; Richards 1986; Lillesand and Kiefer 1987; and Steven and Clark 1990). For information and applications in agriculture, see Curran 1987; Asrar 1989; Hobbs and Mooney 1990; and Steven 1993, and for hydrology in particular, see Schultz 1988; IAH 1990; Barrett, Beaumont, and Herschy 1990; Engman and Gurney 1991; Azzali, Bastiaanssen, et al. 1991; Stewart et al. 1996; and Kite, Pietroniro, and Pultz 1997.

During the 1970s, satellite remote sensing was often promoted as a "solution" rather than as a tool for earth science studies. Overselling of this concept led to disappointment with the technology during the 1980s. Lack of communication impeded interdisciplinary collaboration between irrigation scientists and radiation physicists. Now, accumulated scientific achievements and improved potential make it appropriate to thoroughly review the robustness of the various remote sensing algorithms that have been developed in agricultural science. Innovation in the use of remote sensing data in agricultural water management should be stimulated to gain knowledge on the practical value of advanced technologies. Proposed methodologies should be systematically reviewed and their generic aspects and dependence on ground data critically evaluated. This report briefly describes the potential of remote sensing and outlines its limitations and capabilities. It will help irrigation scientists, engineers, and water managers understand how far this technology has progressed.

The comprehensive analysis in chapter 2 shows that certain components of satellite remote sensing could be used more profitably. Chapter 3 inventories situations in which irrigation management and its applications can fit. Chapter 4 discusses the cost-effectiveness of applications of remote sensing, which will be much better understood when projects are implemented, i.e., when images are commercially obtained and processed and the customers (the end users) participate in analyzing the images and use the information in making decisions. Chapter 5 outlines the types of future research and applications of remote sensing projects that land and water managers need.

2.

State of the Art of Remote Sensing Research in Irrigated Agriculture

SPECTRAL RADIANCES MEASURED by satellites do not directly indicate the irrigation conditions at the ground. Between satellite spectral radiances and irrigation decision making lie several levels of interpretation that must be made. Vegetation indices are, due to their simplicity, best for rapidly assessing whether or not an area is cropped. Because the definitions of vegetation indices are evolving, a brief historic overview will be presented. A further interpretation of the spectral radiances can be established by spectrally recognizing different thematic classes such as land cover, land use, and crop types. Another path of application is the interpretation of spectral radiances into key crop parameters such as surface albedo and surface resistance or the conditions of the soil such as soil moisture and soil salinity. Hydrological analysis can be made if remote sensing data are put into hydrological models to predict soil moisture profiles, surface runoff, and river discharge.

Worldwide research efforts have resulted in many different technical solutions for mapping of individual parameters, sometimes by use of the same spectral measurements. In addition, there is a wide range of spectral possibilities for determining land surface variables or hydrological processes. For agronomists and irrigation managers who have little remote sensing expertise, the last two sections of this chapter provide guidance on selecting remote sensing methodologies and information on the type of sensors that are appropriate for them.

Spectral Vegetation Indices

A vegetation index is a common spectral index that identifies the presence of chlorophyll. The index is composed of reflectance in the red spectral region (0.62 to 0.70 μm) and a portion (0.7 to 1.1 μm) of the near-infrared spectral region. Spectral satellite measurements in the red and infrared channels must be atmospherically corrected for interference from aerosols (e.g., Paltridge and Mitchell 1990; Gutman 1991). Chlorophyll has a relative low reflectance in the red part of the electromagnetic spectrum (strong absorption) and a relatively high reflectance in the near-infrared part (low absorption). Since the late 1970s, multiple combinations of the red and infrared channels have been formulated, and various crop parameters have been derived from vegetation indices using biophysics. The definitions have gradually been upgraded to improve specific analyses (table 2).

Table 2. Overview of vegetation indices used in agricultural remote sensing studies.

Indicator	Strength	Source
SR: Simple ratio	Presence of vegetation	Jordan 1969
PVI: Perpendicular vegetation index	Vegetative cover	Richardson and Wiegand1977
NDVI: Normalized difference vegetation index	Vegetative cover	Tucker 1979
TVI: Transformed vegetation index	Crop development stages	Menenti et al. 1986
SAVI: Soil-adjusted vegetation index	Insensitive to soil background	Huete 1988
WDVI: Weighted difference vegetation index	Insensitive to soil background, suited for LAI	Clevers 1988
TSAVI: Transformed soil-adjusted vegetation index	Insensitive to soil background, suited for LAI	Baret and Guyot 1991
GEMI: Global environment monitoring index	Insensitive to atmospheric influences	Pinty and Verstraete 1992
ARVI: Atmospherically resistant vegetation index	Insensitive to atmospheric influences	Kaufman and Tanre 1992
SARVI: Soil-adjusted atmospherically resistant vegetation index	Insensitive to atmosphere and soil background	Kaufman and Tanre 1992
MSARVI: Modified soil-adjusted atmospherically resistant vegetation index	Insensitive to atmosphere, soil background, and sensor view	Qi et al. 1993
MSAVI: Modified soil-adjusted vegetation index	Sensor view, solar position, crop geometry	Qi et al. 1994
NDWI: Normalized difference wetness index	Soil wetness and salinity conditions	Nageswara Rao and Mohankumar 1994
GVI: Green vegetation index Mohankumar 1994	Biomass assessment	Nageswara Rao and
TWVI: Two-axis vegetation index	Insensitive to soil background	Xia 1994
OSAVI: Optimized soil-adjusted vegetation index	Insensitive to soil background	Rondeaux, Steven, and Baret 1996

Annex 4 presents the formulas for the vegetation indices shown in table 2. TSAVI, WDVI, SAVI, and MSAVI are vegetation indices that have been improved by reformulation to minimize the backscattering of canopy-transmitted, soil-reflected radiation in partial canopies. TSAVI requires determination of the slope and intercept of the soil line in the red and near-infrared spectral spaces. The soil line is a hypothetical line in spectral space that describes the variation in bare soil reflectance and was initially developed for the perpendicular vegetation index (PVI). PVI is defined as the perpendicular distance from the soil line between the red and near-infrared reflectance of a particular pixel. Soil lines have been found useful for increasing the sensitivity of vegetation parameters. WDVI corrects only the near-infrared reflectance for soil background.

The introduction of GEMI, ARVI, and SARVI made it easier to quantify time series of vegetation indices despite continual change in atmospheric conditions. GEMI is based on red

and infrared measurements. ARVI and SARVI require additional measurements in the blue channel (0.43 to 0.475 μm) to circumvent aerosol effects in the red channel. In the description of vegetation parameters, neither ARVI nor SARVI correct for Rayleigh and ozone-scattering interference, which arises when the size of aerosols is much smaller than the waves emitted by the sun. Rondeaux, Steven, and Baret (1996) recently reviewed the merits of the most classical and updated vegetation indices recommended for application in agronomy.

Thematic Classifications

Thematic land classes can be derived digitally by grouping pixels that have similar spectral signatures from measurements of individual bands throughout the spectrum. Usually this classification is made with the visible, near-infrared, and middle-infrared part of the spectrum. The *supervised classification* approach is the most common methodology for forming classes that are similar in spectral reflectance (e.g., Settle and Briggs 1987). In this approach, pixels are assigned to classes (i.e., training classes) verified on the ground in selected areas. Because these training sets represent a small percentage of an entire satellite image and because the selection is made by the field observers, sampling is often not random and is biased by the selection procedure. The maximum-likelihood classifier is a successful criterion that is based on *a priori* probabilities (e.g., Strahler 1980). Alternative criteria for associating pixels with classes are the modified minimum Euclidean distance to mean and the Mahalanobis distance.

The *unsupervised classification* algorithm clusters pixels multispectrally into classes through the use of standard statistical approaches such as the centroid and ward methods and does not rely on assigned classes from field visits. Kiyonary et al. (1988) argued that unsupervised classification methods are better suited for classifications of natural variations without abrupt changes in spectral reflectance. Dendograms show statistically when differences in spectral reflectance blend. Cluster-analysis technique also has statistical advantages. Hybrids of supervised and unsupervised classifications are often necessary to overcome the shortage of appropriate field data.

A classification tree (e.g., Davis and Dozier 1990; Baker, Verbyla, and Hodges 1993; Vincent et al. 1995) is a statistical technique that utilizes different decision factors to arrive at a higher level in a hierarchical decision-making environment. The end branches of the tree represent the final classes.

A *principal component* analysis is a mathematical transformation, based on linear combinations of original in-band measurements, that reduces the total number of bands without losing spectrally discernable information. Bands with higher spectral variability contribute more to the development of new component images than those with higher band-to-band correlation.

A well-known phenomenon in pixel-based image classification is the "mixed" pixel, which comprises a heterogeneous land surface, i.e., two or more objects occur within a single pixel. In agricultural areas, crop variety, seeding date, and supply of fertilizer are often unevenly distributed among and within farm fields. Because of that, the spectral reflectance of a given crop may contain a wide scatter (Leguizamon et al. 1996). *Fuzzy classifications,* with more

continuous land-cover classes, have been invented to account for variations in natural conditions (e.g., Wang 1990; Pedrycz 1990). Fuzzy classifications are based on the relative strength of a class membership that a pixel has relative to all defined classes; and a fuzzy classification requires no assumption about the statistical distribution of the data. The degree of membership within a fuzzy set is a scaled number between 0 and 1. More background information is provided in Zimmerman 1991.

A different category of statistics that gives more opportunities to thematically discern land use and crop classes is *the neural network* classifier (e.g., Benediktsson, Swain, and Ersoy 1990; Hepner et al. 1990).

A pixel-based recognition of land-surface objects can be further improved by including ancillary data in the classification procedure or by adding contextual information on geometry, such as roads, canals, field boundaries, etc. Bauer et al. 1979 and Franklin and Wilson 1991 explore the possibilities of using spatial and contextual information in addition to multispectral measurements.

Irrigated area

One of the earliest publications on using satellite technologies to distinguish irrigated areas from nonirrigated areas (in India) is Thiruvengadachari 1981. In Mendoza Province, Argentina, Thome, Yanez, and Zuluaga (1988) estimated the total amount of irrigated land by means of visible and near-infrared data from the Landsat Multispectral Scanner (MSS). They concluded that the land area irrigated greatly exceeded the land area that had water rights. In the same arid viticulture landscape, Visser (1989) tested different methods to distinguish irrigated from nonirrigated areas. He found that supervised classification procedures performed better (average accuracy of 92.5%) than a multiplier of reflectance ratios in Thematic Mapper (TM) bands 3, 4, and 5 (90% accuracy) or a principal component analysis (85%). At a scheme level of 360,000 hectares, the red-infrared ratio, or simple ratio (table 2), was chosen by Visser (1989) to identify the irrigation intensity at a larger scale. Williamson (1989) used SPOT-XS in combination with airborne data to delineate irrigated orchards and vine crops in South Australia. Visser (1990) used SPOT-XS images to discern the irrigated green areas in and around the city of Riyadh in Saudi Arabia. He selected reference plots during a field visit to allow a supervised classification. The classification accuracy varied from 94 to 100 percent. This high level of accuracy resulted from the sharp spatial contrast of vegetation developments in oasis-desert systems. Lourens (1990) used a single Landsat image to map irrigated farms individually in a 50,000-hectare study area in Pretoria, South Africa. He used a principal component analysis followed by a supervised classification. The results for groundnuts were more promising than for tobacco fields because tobacco is defoliated at harvest. For well-developed canopies, the mapping accuracy can be as high as 85 to 90 percent.

Inter-state disputes on water utilization from the Cauvery river in Karnataka, India, have necessitated an accurate and timely estimate of the irrigated crop area in each season. Nageswara Rao and Mohankumar (1994) described the classification of irrigated crops through various vegetation indices (NDWI, NDVI, and GVI) derived from Landsat Thematic Mapper. They suggested that the NDWI values for water and irrigated crops are similar and that NDWI is better suited for identifying irrigated crops than NDVI.

Lantieri (1995) calculated a vegetation index from three different SPOT-XS images during December, June, and August for the Jatiluhr Project in the West Tarum area of Java (Indonesia) and made a time composite of the three dates. Rice cropping calendars were thereafter incorporated to interpret the time-composited vegetation index (TCVI) into presence of rice, rice development stages, and irrigation conditions. Lantieri (1995) found that the 20-meter-resolution SPOT data were insufficient to locate fields of 0.3 hectare, which implies that eight pixels were too few for classification of irrigated farm fields. The accuracy in irrigated land varied between 67 and 91 percent for nine tertiary unit groups.

Vidal and Baqri (1995) used a supervised classification procedure with Thematic Mapper data to detect irrigated areas of the Gharb plain in northwestern Morocco. The maps indicated significant discrepancies in area between actually irrigated fields and fields entitled to irrigation. Van Dijk and Wijdeveld (1996) used SPOT images to map the areas under spade irrigation (natural irrigation by means of a sequence of field dams) in the Tihama Basin in Yemen. Four images, covering a complete annual cycle, were sufficient to discriminate irrigated from rainfed agriculture. The analysis indicated that the irrigated agricultural area was only 50 percent of the official estimate made by conventional methods.

Hussin and Shaker (1996) classified the main land-use types in Sumatra, Indonesia, using Landsat MSS and TM data combined with radar measurements from the European Remote Sensing satellite (ERS). The spatial resolution of ERS-1 SAR was 12.5 meters with a swath width of 100 kilometers and a wavelength of 5.3 GHz or 5.6 centimeters (C-band). To classify cropping patterns, they used two JERS-1 SAR images with a spatial resolution of 12.5 meters, a swath width of 75 kilometers, and a wavelength of 1.275 GHz or 23 centimeters (L-band), and visually interpreted the ERS and JERS images. As a result, natural forests, shifting cultivation, secondary forest, and paddies could be distinguished. The overall classification accuracy of TM data was 91 percent, which is better than that of MSS data (89%). The multisensor spectral classification of TM and SAR data gave less satisfactory results, due to the speckle noise of the SAR data, although the paddy fields could be identified well. Paddy fields appeared very dark on the radar image, which is also useful for delineating irrigated rice basins when the skies are cloudy. The SAR data appeared useful for detecting swamp forest, tidal forest, rubber plantations, and coastal coconut plantations that could not be obtained from the Landsat data.

Lloyd (1989) explored temporal NDVI profiles to distinguish irrigated crops from other vegetative cover in the Iberian peninsula. Azzali and Menenti (1996) also used the temporal variation of NDVI to distinguish irrigated from nonirrigated agriculture. They first expressed time-series analysis of NDVI as a Fourier series, and then, in a related study (Verhoef, Menenti, and Azzali 1996), classified the Fourier amplitudes at different frequencies and phases (instead of different spectral bands). Irrigated agriculture seems to have a regular behavior pattern in vegetation dynamics. This combined AVHRR-Fourier technique has potential for mapping irrigated areas continentally. Table 3 summarizes the accuracies achieved by various methods for mapping irrigated land areas. It is obvious that the mapping procedure in Indonesia, which has a high fraction of permanently green vegetation, gives less satisfactory results than mapping in arid conditions (Argentina, South Africa, and Saudi Arabia in table 3). However, accuracy in areas such as the humid zones of India and Indonesia could be improved by calculating vegetation indices with data from multiple annual cycles and incorporating SAR images.

Table 3. Status of discerning irrigated crops from nonirrigated land.

County	Image	Method	Accuracy (%)	Source
Argentina	TM	Supervised classification	92.5	Visser 1989
Argentina	TM	Vegetation index	90	Visser 1989
Argentina	TM	Principal component	85	Visser 1989
South Africa	TM	Principal component	85–90	Lourens 1990
Saudi Arabia	SPOT	Supervised classification	94–100	Visser 1990
India	TM	False-color composite	90	Nageswara Rao and Mohankumar 1994
Indonesia	SPOT	Vegetation index	67–91	Lantieri 1995

Crop types

Pattern recognition with multispectral high resolution satellite images is classic remote sensing research in agriculture. Research on this issue seems never ending; spectral and spatial capabilities are continuously improving (see annex 3), and sophisticated mathematics are becoming easier to employ as computers become faster.

The hierarchy of thematic land classes consists of different objects that are inherently related to spatial aggregation levels (fig. 2). The most elementary object class is a terrain element—one specific tree or an individual plant. A larger number of canopies or plants can form a crop type (e.g., wheat, cabbage), while multiple crops can form crop communities (e.g., cereals, vegetables, fruit trees). Land cover at a coarser scale is usually associated with a broad category of physiographic appearances such as arable land, deciduous forest, orchards, swamps, and herbaceous vegetation. Land use may be perceived as land cover with human manage-

Figure 2. Relationship between scale and thematic classes in a heterogeneous irrigated agricultural landscape. A field is defined as one type of crop, and a farm consists of several fields.

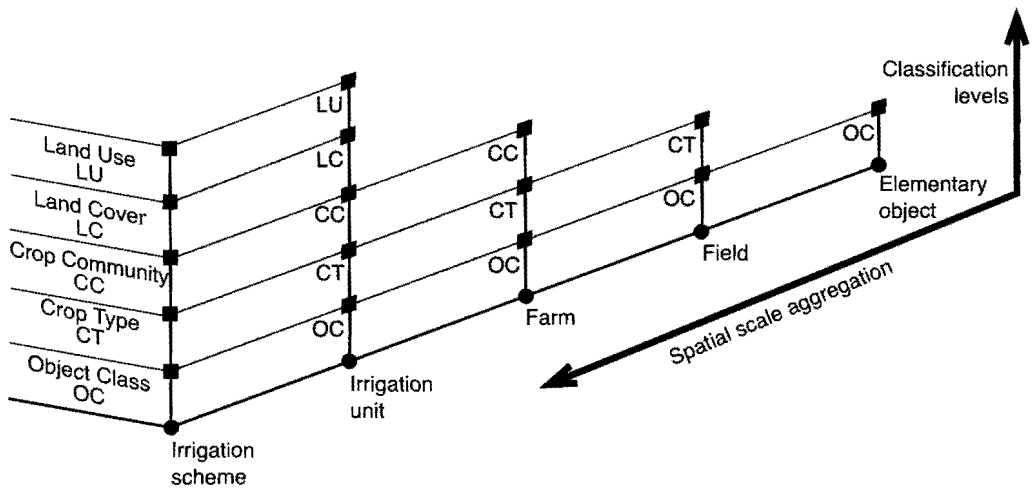

ment through such activities as irrigation, tillage, etc. The relationship between aggregation and classification hierarchies, as outlined in figure 2, is adapted from Huising (1993). Land cover and crop communities can potentially be classified with more accuracy than individual crops.

Townshend (1984), in the United Kingdom, was one of the first investigators to detect different agronomic crops using Landsat Thematic Mapper data. Newell (1989) selected SPOT images for the identification of agriculture and land use in the United Kingdom. In studies in Italy and Argentina, Menenti et al. (1986) defined a multi-index, multitemporal crop classification procedure that is based on time composites of the vegetation index. They designed a transformed vegetation index (TVI), which expresses the density of full ground cover. They combined TVI with the simple ratio to identify cropping patterns in the irrigated Po plain (Italy). Use of TVI values allowed them to correct for variations in crop development due to differences in planting dates, irrigation water supply, and farmer practices. Ground information from cropping calendars was indispensable in their study. In Mendoza (Argentina) their multiple attempts to classify different irrigated crops such as vineyards, alfalfa, olive trees, peaches, apricots, onions, garlic, carrots, and potatoes with Landsat MSS and TM data failed due to extreme variability in soil cover, crop age, and undergrowth.

Following the principles of figure 2, Dijk and van Eick (1987) and Zuluaga (1990) selected broader crop communities such as "urban," "crop 1," "crop 2," and "fallow" to map crop types in Mendoza Province, Argentina. In an attempt to obtain information on crop type, Meeuwissen (1989) tried cluster analysis in Mendoza as part of an unsupervised classification approach, and she defined classes to be used as training sets before employing a supervised classification technique based on maximum likelihood. The ward method of separating clusters proved most satisfactory for identifying vineyards, abandoned vineyards, vineyards with fruit trees, fruit trees, apricots, and vines supported by pergola. A minimum of six to nine pixels was needed for discriminating crop communities in Mendoza.

Wolters, Zevenbergen, and Bos (1991) concluded that the 30-meter spatial resolution of TM was too coarse to detect crops with different stages of growth in the small fields and fragmented land use of the Fayoum Depression, Egypt. El-Kady and Mack (1997) advocated using aerial photography to discern Egypt's minor crops, although it costs substantially more per unit area than using satellite-based classifications. They summarized Egyptian satellite-based crop-mapping studies in the Nile Valley near Beni Suef and El Minya and the middle reach of the Eastern Nile Delta: cotton, rice, and maize were identified with a maximum-likelihood method using TM bands 2, 3, 4, 5, and 7. For areas exceeding about 250,000 hectares, the classification results were well correlated with the regional statistics of the Ministry of Agriculture. For small areas, the deviations were significantly larger, but valuable detailed information could be deduced from the TM data.

Della Mana and Gombeer (1990) used TM data and an unsupervised and supervised technique to classify agricultural activities in an area of Brazil having dense natural vegetation and forests. They applied a minimum distance classifier algorithm for 21 training sets, yielding 18 land-cover classes. They concluded that agriculture and forest classes can be confused, but that water bodies and forests can be clearly separated.

A hybrid classification procedure was also applied by Jayasekera and Walker (1990) in the densely vegetated Gal Oya Irrigation Project in Sri Lanka. They worked out a principal component and unsupervised classification of Landsat MSS bands and identified five catego-

ries of paddy practices that differed in plant vigor, canopy density, and depth of the standing water. In Riyadh, Saudi Arabia, Visser (1990), using a supervised procedure, recognized patterns in urban land cover, such as palm trees, built-up areas, bare soil, roads, and water bodies. He combined SPOT panchromatic (10 m) and TM (30 m) data to take advantage of the high resolution of SPOT and the better spectral resolution of TM (see also Ehrlich et al. 1994). Waddington and Lamb (1990) used seven of the nine bands from three different Landsat MSS scenes (each scene included MSS bands 2, 3, and 4) to apply a supervised classification that used a large separability distance. Pre-processing was also done with an unsupervised classification methodology. The data were merged with additional supervised training sets.

Gong and Howarth (1992) used a supervised maximum-likelihood classification with SPOT-XS data to identify 12 land-cover types on the rural-urban fringe of Toronto. Pedley and Curran (1991) also used SPOT data for a field-by-field classification in South Yorkshire, U.K. The accuracy for 12 land-cover classes was 46 percent at pixel scale and 55 percent at field scale. The best accuracy (62%) was achieved by using measures of prior probabilities and texture within a per-field format. In Oregon, USA, Shih and Jordan (1993) used TM bands 2, 3, and 5 to distinguish among four aggregated principal land-use categories (agricultural fields, urban clearings, forest-wetlands, and water) with an unsupervised maximum-likelihood classification procedure. Vidal et al. (1996) used two SPOT images to classify land use in the Fordwah/Eastern Sadiqia irrigation system of southern Punjab, Pakistan. The size of the irrigated *killa* fields was limited and comprised only nine SPOT-XS pixels. These fields are internally nonhomogeneous, having uneven crop and soil salinity developments, which hampered use of a straightforward classification procedure. Wheat was still distinguishable from other crops with a supervised maximum-likelihood decision rule, although the accuracy was limited. In the case study by Ahmad et al. (1996), classification accuracy varied: barren, 49 percent; fallow, 81 percent; fodder, 84 percent; sugarcane, 44 percent; wheat, 89 percent. Thiruvengadachari et al. (1995) faced difficulties in detecting multiple crops in the Bhadra irrigation project in Karnataka, India. Although their aim was to identify individual crops such as groundnut, sunflower, sugarcane, and garden crops according to distribution, noncontiguous small patches reduced classification accuracy. This prompted them to define only paddy and nonpaddy crop classes, i.e., a mono-crop classification procedure.

Thiruvengadachari, Murthy, and Raju (1997) developed a crop classification methodology consisting of a new iterative supervised and unsupervised procedure. In the Bhakra canal command area in Haryana, India, they used a multi-date IRS satellite data set for the 1995-96 rabi season. They first assigned training areas on the different images and extracted a spectral signature for each image. Three overpass dates were found that would give maximum separability between spectral signatures. The supervised classification was used first, leaving 53 percent of the image pixels unlabeled. Afterward, the unclassified portions of the images were exposed to an unsupervised classification that yielded 50 "homogeneous" unlabeled clusters. The signature of each cluster was compared with reference signatures and then new training sets were formed. This process was repeated until all pixels were classified as wheat, oilseed, or other. The results were validated against a larger number of reference areas that were not used in the classification process, i.e., a residual sample procedure.

The complementary nature of microwave data to visible and near-infrared data can be used to obtain better information on regions that are frequently overcast. Microwave signals penetrate clouds and are less sensitive to atmospheric effects than visible or infrared images.

Schreier, Maeda, and Guindon (1991) compared sensor configurations and potentials for land resource surveys from the operational spaceborne microwave missions—ERS, JERS, and Radarsat. Panchromatic photos of SPOT and IRS can be used as a background to locate and update the exact position of roads and canals. Rajan (1991) demonstrated that SAR imagery has the potential to locate open water bodies, paddy fields, sparse and dense sugar palms, orchards, and swamps in the humid tropics (Songkhla, Thailand) where the application of optical remote sensing was obstructed by clouds. Use of existing land-use maps and verified field data was necessary to obtain satisfactory classification results. Examples of using radar images for classifying agricultural crops under frequently overcast skies at higher latitudes were given by Hoogeboom (1983), Brisco, Brown, and Manore (1989), and Bouman and Uenk (1992).

In the Netherlands, Schotten, van Rooy, and Janssen (1995) used eight ERS-1 SAR precision images with a 12.5-meter resolution to identify potatoes, sugarbeets, winter wheat, maize, spring barley, winter rape, beans, onions, peas, grass, lucerne, and orchards with a field-based maximum-likelihood classifier. The images were captured during the growing season between May 12 and November 3. Field size varied from 1 to 20 hectares, and an overall classification accuracy of 80 percent could be obtained only after an extensive ground survey. The lowest accuracy obtained was for onions (64%) and the highest was for lucerne (100%). A SPOT-XS image with a 20-meter resolution was used to fix the geometry of the agricultural fields prior to the classification procedure.

An example of simultaneously using SPOT (optical) and ERS-SAR (microwave) data was given by Huurneman and Broekema (1996). They used a maximum-likelihood classifier in different combinations with a neural network classifier and with optical and microwave data to reinforce the performances of both classifiers. SPOT-maximum likelihood gave an overall accuracy of 76.5 percent. Adding a neural network lowered the accuracy to 74.2 percent. The maximum attainable classification accuracy, 87.5 percent, was obtained by combining all information sources (SPOT, ERS, maximum likelihood, and neural network).

Staples and Hurley (1996) analyzed two Radarsat images with a C-band SAR at the sowing stage and at the heading stage in southeastern China. Rice paddies, banana crops, and aquaculture ponds could be identified after using ground truth information. Radarsat offers many combinations of coverage and resolution, of which the most commonly used is an image coverage of 100 kilometers with a 25-meter spatial resolution.

Janssen and Middelkoop (1992) distinguished terrain object classes using knowledge-based classification procedures. The knowledge consisted of crop rotation schemes and the geometry of the fields. Knowledge on crop rotations increased the classification accuracy of a test site by 2 to 17 percent. Field geometry was used to perform a field-based classification. The crop was correctly determined for 92 percent of the fields in the test area. Kontoes et al. (1993) demonstrated a possible 13 percent increase in classification accuracy if knowledge-based systems are applied. Ahmad et al. (1996) used the field layout of *killas* and watercourses in Pakistan to define groups of radiometric signatures. Janssen and Molenaar (1995) expanded the use of geometrical data (size, position, and shape) by means of segmentation techniques that account for a hierarchical aggregation of scales and that can create or remove physical boundaries.

Table 4 summarizes the accuracy levels attained in crop classification studies. Several of the sources in table 4 were taken from the overview of Akiyama et al. (1996). All crop classification studies that specified an accuracy level are included in the table. Less than half re-

Color Plate 1. Example of crop classification for an agricultural area in the Guadalqivir river basin near Seville, Spain. The blank areas were partially covered by clouds.

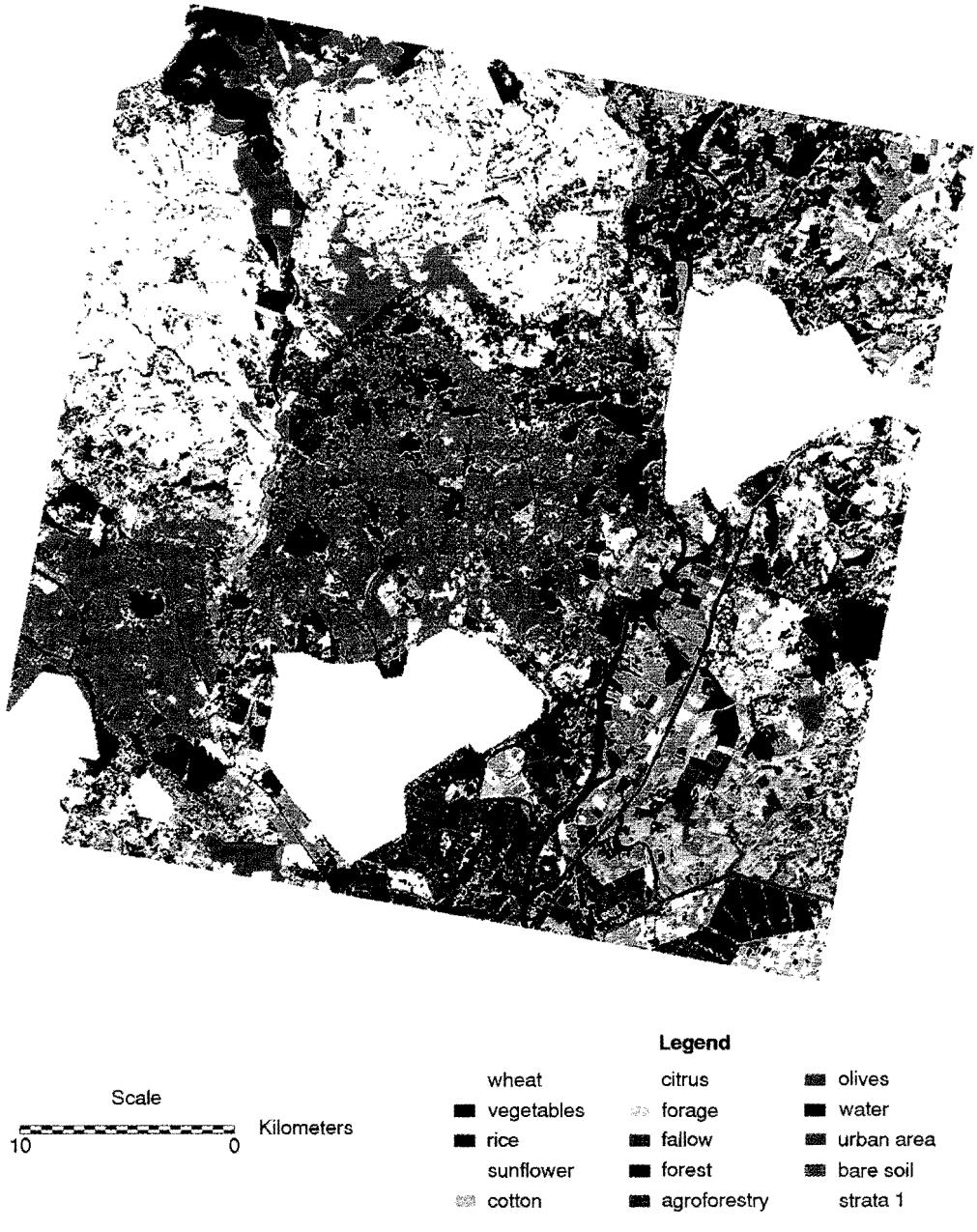

fer to irrigated land. Color Plate 1 shows an example of classified crops in a river basin, based on multiple Thematic Mapper images (after Nieuwenhuis et al. 1996). The basin contains irrigated and rainfed agricultural fields. Wheat and sunflower are the major rainfed crops, and they are located further away from the river than the small-scale irrigated fields. Rice is grown in basins; cotton and fruits have a sprinkler or pivot irrigation system.

Table 4. Accuracy levels obtained in agricultural crop classification.

Country	Satellite	Images (no.)	Identified crops (no.)	Irrigation [a]	Classification accuracy (%)	Source
USA	Landsat-MSS	2	2	no	84	Batista, Hixson, and Bauer 1985
USA	Landsat-MSS	4	4	no	90	Lo, Scarpace, and Lillesand 1986
Hungary	Landsat-MSS	4	>3	no	90	Csillag 1986
Sweden	Landsat-TM	3	7	no	20 to 70	Hall-Konyves 1990
USA	Landsat-MSS	3	3	yes	90	Waddington and Lamb 1990
Argentina	Landsat-MSS/TM	6	>3	no	80	Badhwar, Gargatini, and Redondo 1987
USA	Landsat-TM	2	8	no	75 to 96	Williams, Philipson, and Philpot 1987
Hungary	Landsat-TM/SPOT	3	3	no	82 to 91	Buttner and Csillag 1989
U.K.	SPOT-XS	4	14	no	71 to 88	Jewell 1989
Argentina	Landsat-TM	1	6	yes	91	Zuluaga 1990
Thailand	Landsat TM	3	5	yes	87 to 94	Tennakoon, Murthy, and Eiumnoh 1992
Netherlands	Landsat-TM	1	7	no	92	Janssen and Middelkoop 1992
India	IRS-LISS	1	8	yes	89	Nageswara Rao and Mohankumar 1994
Italy	Landsat-TM	4	4	no	78 to 100	Ehrlich et al. 1994
Turkey	Landsat-TM	1	2	no	85	Pestemalci et al. 1995
Netherlands	ERS-SAR	14	12	no	80	Schotten, van Rooy, and Janssen 1995
Pakistan	SPOT-XS	1	4	yes	75 to 87	Vidal et al. 1996
Pakistan	SPOT-XS	1	4	yes	49 to 89	Ahmed et al. 1996
India	IRS-1B	5	2	yes	96	Thiruvengadachari, Murthy, and Raju 1997
Avg					86	

[a]Yes = studies that reported irrigation activities.

Table 4 shows that crops can be identified with an average accuracy of 86 percent if extensive field data support the classification procedure, although there are clear limits to the total number of crops discernable at this accuracy level. Standardization of expressions related to classification performance would help to improve the evaluation of classifications. Congalton (1991) and Fitzgerald and Lees (1994) proposed the use of kappa statistics that are based on error matrices of the derived thematic land classes. D'Urso and Menenti (1996) evaluated the performance of image classifications by means of a normalized classification indicator composed of separability (signature divergence), accuracy (error), and thresholding or reliability (different confidence levels). These tools are extremely useful for post-processing and as guides for the operator in selecting the final classification procedure.

Land cover and land use

Fuller and Brown (1996) give an example of combined land-cover and land-use mapping for Great Britain derived from Coordination of Information on the Environment (CORINE), which is based on Landsat TM images. CORINE was established to help structure heterogeneous and fragmented information on land cover at the national level in Europe. Cruickshank and Tomlinson (1996) examined an application of CORINE to distinguish among agriculture, forests, semi-natural areas, and wetlands in the north of Ireland. Kite (1995) intercompared the effects of switching from Landsat MSS to AVHRR land-cover classifications for a boreal watershed. The sensors provided similar distributions of land cover for the watershed, and the standard error was only 2.98 percent. He argued that the use of larger AVHRR pixels minimizes the problem of incorrect classification of pixels. Carbone, Narumalani, and King (1996) showed the results of a land-cover classification of Orangeburg County, South Carolina (USA) with SPOT data as a pre-processing for the application of physiological crop models on a regional scale.[1] Defries and Townshend (1994) worked on a global land-cover classification.

In conclusion, a uniform classification procedure does not exist. The type of procedure that is most appropriate depends on the purpose of the classification and the information available from field visits and existing maps. Although most of the successful methods reviewed are hybrids of unsupervised and supervised classification methods, they all require field information on different growing stages. A single farm plot should be represented by at least 15 pixels. Without exception, all multitemporal image classification techniques improved the accuracy. Hence, the probability of discerning thematic land classes and determining their accuracy depends on the type of object, image material, and the availability of ancillary data.

Key Crop Parameters

Early applications of remotely sensed data relied heavily on land-use classifications. The slow dissemination of successful image-classification procedures to decision makers outside the atmospheric sciences delayed recognition of the potential for using remote sensing determinants other than classes in agronomic and hydrological studies. The rapid development of hydrologic and climatic models and the need for input data prompted scientists to focus on

[1]Areas larger than single fields or farms, but usually smaller than entire river basins.

the morphological characteristics and biophysical properties of regional land surfaces. In the last decade, the estimation of crop and hydrological parameters from satellite spectral measurements has received attention (e.g., Hall, Townshend, and Engman 1995; Xinmei et al. 1995). Reliable simulations with global hydrology models have also increased (e.g., Dickinson 1995), partially due to the contribution of remote sensing.

Biophysical crop parameters play a major role in the description of vegetation development (fractional vegetation cover, leaf area index), crop yield (leaf area index and photosynthetically active radiation) and crop evapotranspiration (leaf area index, surface roughness, surface albedo, surface emissivity, surface temperature, surface resistance, crop coefficients, and transpiration coefficients). Most of these biophysical parameters are important for irrigation management because they reflect water and production issues. Table 5 summarizes the key crop parameters scientists have reported being able to discern on a regional scale when combining remote spectral radiance measurements with field measurements and numerical models. The following sections discuss those parameters plus intermediate components of those parameters—downwelling shortwave and longwave radiation, soil heat flux, sensible heat flux, latent heat flux, and crop stress indicators.

Table 5. Biophysical crop parameters retrievable from synergistic remote sensing measurements, and their association with irrigation management.

Crop parameter	Process	Purpose
Fractional vegetation cover	Chlorophyll development, soil and canopy fluxes	Irrigated area
Leaf area index	Biomass, minimum canopy resistance, heat fluxes	Yield, water use, water needs
Photosynthetically active radiation	Photosynthesis	Yield
Surface roughness	Aerodynamic resistance	Water use, water needs
Broadband surface albedo	Net radiation	Water use, water needs
Thermal infrared surface emissivity	Net radiation	Water use, water needs
Surface temperature	Net radiation, surface resistance	Water use
Surface resistance	Soil moisture and salinity	Water use
Crop coefficients	Grass evapotranspiration	Water needs
Transpiration coefficients	Potential soil and crop evaporation	Water use, water needs
Crop yield	Accumulated biomass	Production

Fractional vegetation cover

Definition: The fractional vegetation cover (v_c) is the portion of land covered by at least one layer of plant canopies at nadir orientation.

Purpose: v_c indicates whether a surface contains vegetation; it is useful for discerning the harvested area from the crop's development throughout the year; and it regulates soil and canopy fluxes.

Because nonvegetated areas have no chlorophyll, separating nonvegetated, partially vegetated, and densely vegetated land surface becomes possible after combining visible and near-infrared multispectral measurements (Tucker 1979; Goward, Tucker, and Dye 1985). Huete, Jackson, and Post (1985) showed a high linear correlation between v_c and NDVI for a cotton crop. Ormsby, Choudhury, and Owe (1987) investigated the correlation between v_c and both SR ($r^2 = 0.90$) and NDVI ($r^2 = 0.79$). Batchily et al. (1994) monitored NDVI, SAVI, GEMI, ARVI, and SARVI during the Walnut Gulch Experiment and concluded that the seasonal dynamics of grass densities were best described by ARVI and those of perennial shrubs by SAVI. That suggests that short-lived fractional coverage changes may be related to the SAVI concept, which is potentially better than NDVI-based time series. One way to normalize v_c computations is to relate the values for soil without vegetation ($SAVI_s$) and for sparse canopies (SAVI) to the values of dense canopies ($SAVI_d$), as, for example, Choudhury et al. (1994) did:

$$v_c = (SAVI - SAVI_s)/(SAVI_d - SAVI_s) \quad (1)$$

as $SAVI_d$ and $SAVI_s$ change with crop and soil type. Equation (1) is limited to homogeneous vegetation and soil environments that have a variable canopy density. Thus the species-dependent values of $SAVI_d$ and soil-dependent values of $SAVI_s$ should be known. Equation (1) applies to a single pixel. The physical definition of $SAVI_d$ and $SAVI_s$ deteriorates if different crop types are encompassed by a single pixel, which is likely when, for instance, 1.1-kilometer AVHRR images are applied.

Alternatively, Rambal, Lacaze, and Winkel (1990) applied equation (1) with surface temperature and surface albedo, which may be favorable because the near-infrared reflectance can both increase (e.g., cotton) and decrease (desert shrub) with fractional vegetation cover (Choudhury 1991). Also, Friedl and Davis (1994) attributed spatial variations in surface temperature to fractional vegetation cover. Their approach is feasible only if the bare soil is dry and warmer than the canopy, which is not pertinent for irrigated fields. The biome type should be rather homogeneous for a set of pixels to rule out other biophysical properties that could affect surface temperature. For heterogeneous landscapes, combining the separate capabilities of NDVI and surface temperature to estimate fractional vegetation cover provides additional insights (Carlson, Gillies, and Perry 1994).

Leaf area index

Definition: The leaf area index (LAI) is the cumulative area of leaves per unit area of land at nadir orientation.

Purpose: LAI represents the total biomass and is indicative of crop yield, canopy resistance, and heat fluxes.

There have been many attempts to relate LAI to NDVI, SAVI, TSAVI, and WDVI. Most relationships between vegetation indices and LAI are perturbed by solar zenith and azimuth angles, viewing angle, ratio of diffuse to total shortwave radiation, leaf angle distribution, leaf chlorophyll content, mesophyll structure, and canopy geometry. The derived relationship be-

tween LAI and SAVI shown in figure 3 is fairly linear during the development of a crop, until a threshold value of LAI (seldom greater than 1.5 to 2) is reached. Clevers (1988; 1989) developed the simplified, semi-empirical CLAIR model for estimating LAI when there are interfering factors from red and infrared measurements. He deemed a weighted difference between the measured near-infrared and red reflectance necessary to ascertain a correction for near-infrared reflectance that is affected by soil background. Baret and Guyot (1991) simulated the relation of LAI to NDVI, PVI, SAVI, and TSAVI physically and concluded that TSAVI describes LAI better than the other vegetation indices at low to medium fractional vegetation cover. For dense canopies, the suitability of TSAVI for LAI estimates changes with the leaf inclination angle. TSAVI is suitable for dense canopies and large leaf inclination angles, but WDVI is better for dense canopies with a lower leaf inclination angle. Choudhury et al. (1994) simulated relationships between SAVI and LAI for cotton, maize, and soybeans:

$$\mathrm{SAVI} = c_1 - c_2 \exp(-c_3 \mathrm{LAI}) \tag{2}$$

The c_1, c_2, and c_3 regression coefficients of equation (2) are presented in table 6.

Table 6. Regression coefficients and correlation coefficient of the linear and nonlinear relationship between LAI and SAVI.

Crop	Country	c_1	c_2	c_3	r^2	Max. LAI[a]	Source
Cotton	USA	0.82	0.78	0.60	0.98	3.5	Huete, Jackson, and Post 1985
Maize	Italy	1.27	1.10	1.20	0.79	3.3	D'Urso and Santini 1996
Maize	USA	0.68	0.50	0.55	0.90	6.0	Daughtry et al. 1992
Soybean	USA	0.72	0.61	0.65	0.70	6.0	Daughtry et al. 1992
Wheat	USA	0.73	0.67	0.97	0.94	5.0	Choudhury et al. 1994
Fruit trees	Italy	1.34	2.70	2.40	0.39	2.6	D'Urso and Santini 1996
Winter vegetables	Italy	1.31	2.75	2.20	0.54	4.2	D'Urso and Santini 1996
Bush & grassland	Niger	0.14	0.30	–	0.95	1.2	van Leeuwen et al. 1997
Grassland	Niger	0.13	0.35	–	0.98	1.3	van Leeuwen et al. 1997
Millet	Niger	0.13	0.47	–	0.83	0.8	van Leeuwen et al. 1997
Degraded bush	Niger	0.11	0.28	–	0.96	1.0	van Leeuwen et al. 1997
All crops		0.69	0.59	0.91	–	6.0	

[a]From field observations.

Field measurements made in the typical Sahelian agroecological landscape of Niger showed that SAVI is essentially linear with LAI. LAI will not exceed 1.4, even during the rainy season (van Leeuwen et al. 1997). For these low LAI values, equation (2) can be modified to

$$\mathrm{SAVI} = c_1 + c_2 \mathrm{LAI} \tag{3}$$

Based on equation 2, the overall statistical relationship between SAVI and LAI for the crops shown in table 6 then becomes:

$$SAVI = 0.69 - 0.59 \exp(-0.91LAI) \quad (4)$$

Figure 3. Representative curves for the crop-dependent relationships between SAVI and LAI for various crop types in USA, Niger, and Italy.

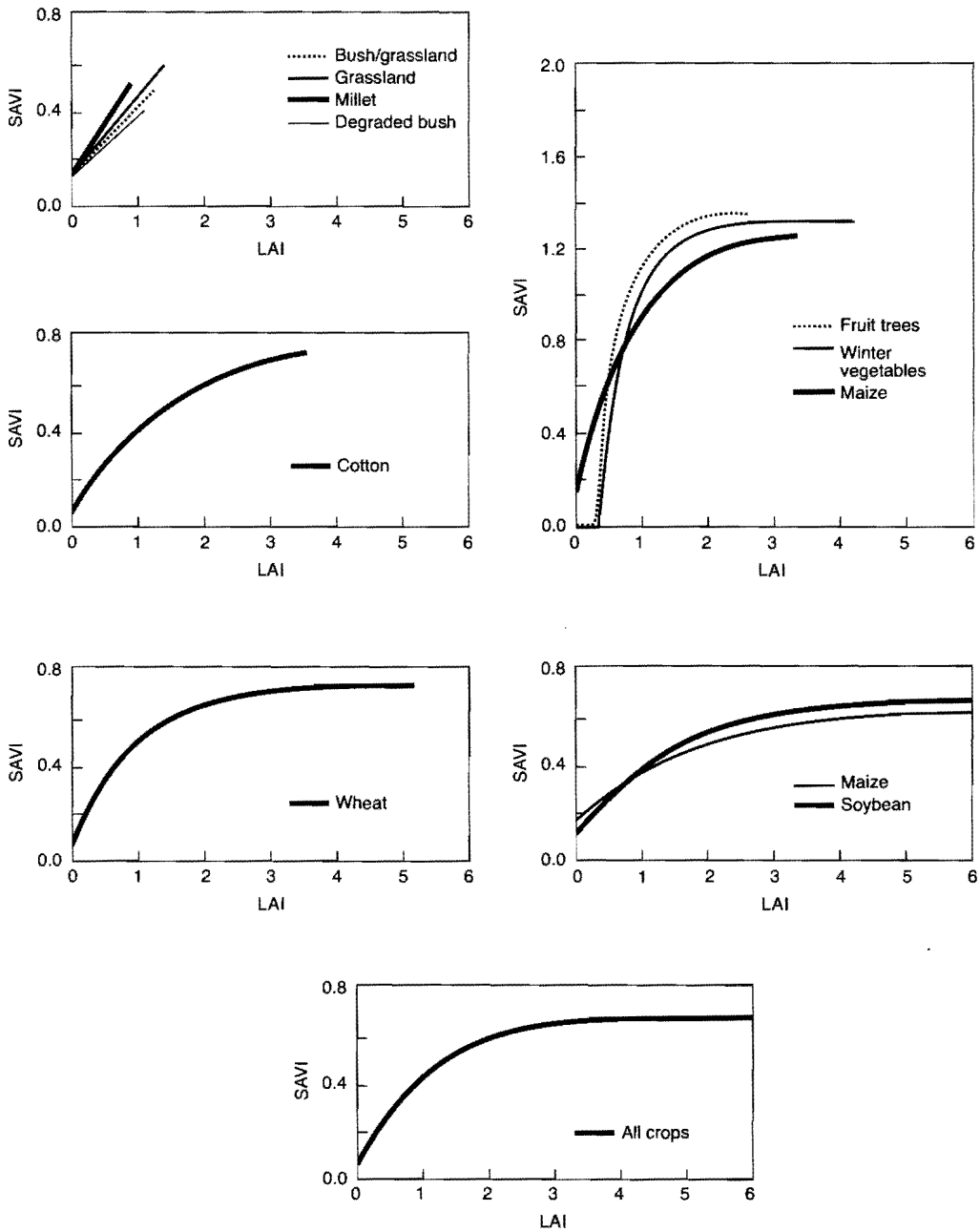

The standard error of estimate for SAVI in equation (4) is small, with 0.02 being acceptable. Figure 3 depicts all data of table 6. The "all crops" curve shows the functional relationship of equation (4) and excludes the systematically higher SAVI values of D'Urso and Santini (1996) covering maize, fruit trees, and winter vegetables.

Because vegetation attenuates the polarized emission from soil, Pampaloni and Paloscia (1986) successfully estimated LAI from the normalized differences between vertical and horizontal polarization components, using airborne passive microwave remote sensing at 10 GHz or 3.0 centimeters (X-band). Using data from the Nimbus Scanning Multichannel Microwave Radiometer (SMMR), Choudhury et al. (1990) demonstrated that a large-scale polarization difference at 37 GHz or 0.81 centimeter is also a function of LAI. Although the microwave signals are only marginally obstructed by clouds, the 25-kilometer spatial resolution of SMMR pixels is too low for applications in irrigation projects.

Photosynthetically active radiation

Definition: Photosynthetically active radiation (PAR) describes the solar radiation available for photosynthesis.

Purpose: The fraction of solar radiation absorbed by chlorophyll pigments (fPAR) describes the energy related to carbon dioxide assimilation and is derived from PAR absorbed by canopy divided by the PAR available from solar radiation.

fPAR regulates the rate of carbon dioxide flow into the leaves. The ratio of PAR to insolation is rather conservative for daily and longer time scales, irrespective of the environmental conditions (Weiss and Norman 1985). Information on the geographical distribution of PAR values is essential for assessing the primary productivity of irrigation schemes. Asrar, Myneni, and Choudhury (1992) stated that "there is now definite experimental evidence that fPAR is monotonic and a near-linear function of the NDVI" (see also Goward and Huemmrich 1992; Myneni and Williams 1994; Frouin and Pinker 1995). By means of theoretical model simulations, Asrar, Myneni, and Choudhury (1992) showed that the statement also holds for horizontally heterogeneous crop stands with a variety of fractional coverage and that the relationship is nearly unique. The relationship of fPAR to NDVI remains sensitive to the reflection properties of the background soil or litter (Hall, Huemmrich, and Goward 1990). Rondeaux (1995) claimed for this reason that TSAVI and SAVI appear to be better related to fPAR than NDVI, although NDVI is not necessarily wrong.

Surface roughness

Definition: The surface roughness (z_0) is a fraction of the crop height used as a physical reference for momentum and heat flux calculations.

Purpose: z_0 affects the shear stress between crop and atmosphere, which determines surface fluxes and the actual and potential evapotranspiration.

The roughness of the ground surface affects momentum, heat, and water vapor exchanges between land and atmosphere. Figure 4 indicates that partially covered soil has separated latent heat flux (LE) and sensible heat flux (H) for bare soil and canopy. The soil moisture regulation of latent heat flux from the bare soil is expressed physico-mathematically by means of the bare soil resistance, r_{soil}. The mechanical friction between land and atmosphere and buoyancy processes controlling the vapor removal from soil to atmosphere are expressed in the aerodynamic resistance to vapor transport, r_{av} (table 7 summarizes scientific notation used in this publication). The canopy's resistance to releasing water vapor varies with the stomatal aperture and is expressed in the canopy resistance, r_c, being physically determined by soil moisture conditions, among others. Because the atmospheric heat transfer processes differ from the transport of water vapor, the resistance to heat transfer, r_{ah}, differs from r_{av}. The LE and H fluxes depend further on the vertical differences of vapor pressure ($e_{sat} - e_{act}$) and temperature ($T_{z0h} - T_{air}$), respectively. The total flux from a sparse canopy is the sum of the individual LE and H fluxes, weighted by the fractional vegetation cover. The total LE flux is usually parameterized by an effective bulk surface resistance to evaporation, r_s, which comprises r_{soil} and r_c, and a surface temperature, T_0, which comprises T_{z0h} of soil and canopy.

Surface roughness is an essential component of aerodynamic resistance to momentum transport, heat transport, and water vapor transport (fig. 4). Total shear stress is formed by local drag over flat homogeneous surfaces and by form drag due to terrain topography. Because irrigated fields are usually flat, local drag induced by the presence of crops and wind shelters is the governing factor and form drag due to undulating terrain and mountains has less impact. The surface roughness for momentum transport (z_{0m}) is defined mathematically

Figure 4. Schematic representation of resistances to heat and vapor flow and their associated differences existing in partial canopies (see table 7 for scientific notation).

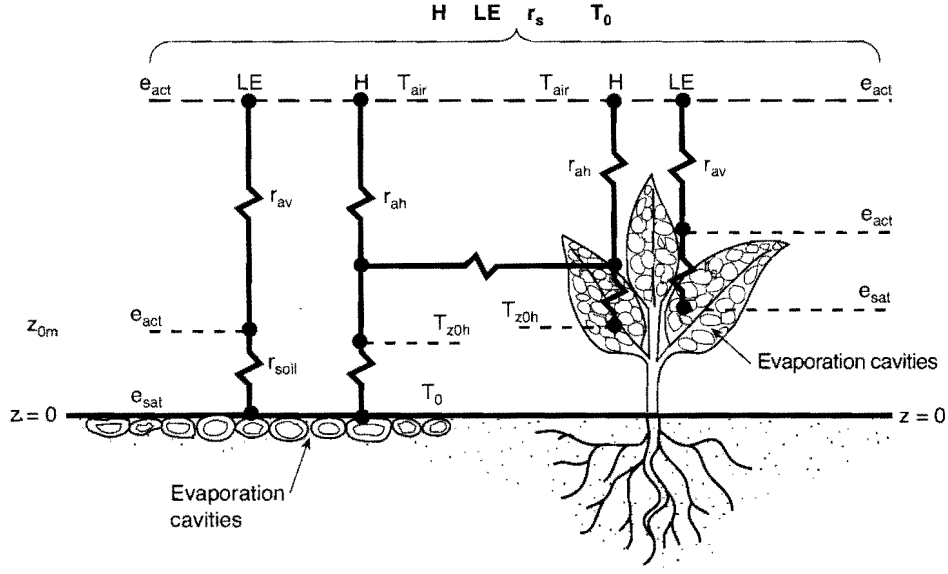

as the plane where the wind speed becomes zero. The value of z_{0m} is related to surface geometry, i.e., the vertical extent in relation to the horizontal extent of landscape elements (e.g., Hatfield 1989).

Most of the literature on z_{0m} refers to closed canopies, and z_{0m} is assessed as a small fraction of the closed vegetation height, h_v (the value of the z_{0m}/h_v ratio ranges from 0.1 to 0.2 for most crops). For partial canopies, the z_{0m}/h_v ratio is not constant. It depends on LAI and peaks at intermediate LAI values (e.g., Raupach 1994). At high LAI values, over-sheltering of canopies occurs and the surface becomes aerodynamically smoother. Vidal and Perrier (1989), for instance, gave analytical expressions for the relation of z_{0m} to LAI.

Table 7. Summary of scientific notation.

φ	= psychrometric constant (mbar/K)	P	= precipitation (mm/d)
σ	= Stefan-Boltzmann constant (W m^{-2} K^{-4})	R_n	= net radiation (W/m^2)
Λ	= evaporative fraction (dimensionless)	r_0	= surface albedo (dimensionless)
ε_0	= thermal infrared surface emissivity (dimensionless)	r_a	= aerodynamic resistance (s/m)
		r_{ah}	= aerodynamic resistance to heat transport (s/m)
ρ_{air}	= moist air density (kg/m^3)	r_{av}	= aerodynamic resistance to vapor transport (s/m)
$\rho_{air}c_p$	= heat capacity of moist air (J m^{-3} K^{-1})	r_p	= broadband planetary reflectance (dimensionless)
c_p	= heat capacity at constant pressure (J kg^{-1} K^{-})	r_s	= bulk surface resistance to actual evapotranspiration (s/m)
d	= displacement height (m)	r_s^{min}	= minimum surface resistance to maintain potential evapotranspiration (s/m)
E_{pan}	= evaporation from a class A evaporation pan (mm/d)	s_a	= slope of the saturated vapor pressure curve (mbar/K)
e_{act}	= actual vapor pressure (mbar)	T	= absolute temperature (K)
e_{sat}	= saturated vapor pressure (mbar)	T_0	= surface temperature (K)
ET_{act}	= actual evapotranspiration (mm/d)	T_{air}	= air temperature (K)
ET_{pot}	= potential evapotranspiration (mm/d)	T_{z0h}	= temperature at the surface roughness length for heat transport (m)
ET_{ref}	= evapotranspiration of a reference crop (mm/d)	t_{act}	= actual crop transpiration (mm/d)
G_0	= soil heat flux density (W/m^2)	t_c	= transpiration coefficient (dimensionless)
H	= sensible heat flux density (W/m^2)	t_{pot}	= potential transpiration (mm/d)
h_v	= height of closed vegetation (m)	U	= relative humidity (dimensionless)
$K^{\downarrow}$	= incoming broadband shortwave radiation (W/m^2)	u	= wind speed (m/s)
kB^{-1}	= correction factor for difference in roughness momentum and heat (dimensionless)	v_c	= fractional vegetation cover (dimensionless)
		Y_{act}	= actual crop yield (kg/ha)
k_c	= crop coefficient (dimensionless)	Y_{max}	= maximum crop yield (kg/ha)
k_y	= crop yield response factor (dimensionless)	z	= height (m)
L	= spectral radiation (W m^{-2} μm^{-1})	z_0	= surface roughness (m)
$L^{\downarrow}$	= incoming atmospheric broadband longwave radiation (W/m^2)	z_{0h}	= surface roughness length for heat transport (m)
$L^{\uparrow}$	= outgoing surface broadband longwave radiation (W/m^2)	z_{0m}	= surface roughness length for momentum transport (m)
l	= wavelength (μm)	z_{0v}	= surface roughness length for vapor transport (m)
l_1	= lower limit wavelength (mm)		
l_2	= upper limit wavelength (mm)		
LE	= latent heat flux density (W/m^2)		

Hatfield (1989) estimated temporal canopy heights, h_v, from the temporal NDVI profile during the progression of a cotton growing season. Moran and Jackson (1991) suggested an exponential relationship between NDVI and z_{0m} for a developing alfalfa crop. Ahmed and Neale (1996) used NDVI to assess z_{0m} and SR to assess zero plane displacement height empirically for a wheat field in Smithfield, Utah (USA). These are all examples of site-specific empirical relationships.

Menenti and Ritchie (1994) used airborne laser altimeter data to quantify canopy properties with vertical and horizontal resolutions in the centimeter range. This measurement technique is based on pulsed microwaves. The time between transmission and return is an adequate measure of the height of vegetation. The surface roughness can be derived from the vegetation height by standard deviations of the neighboring pixels. Paloscia et al. (1993) applied a multifrequency approach to detect surface roughness. They used differences in microwave brightness temperatures at 10 GHz (3 cm wavelength) and 36 GHz (0.83 cm wavelength) with a 40-degree observation angle and expressed the terrain roughness as a standard deviation of height, which allowed three roughness classes to be discerned.

For evapotranspiration calculations, the surface roughness for heat transport, z_{0h}, and vapor transport, z_{0v}, must be known. Residual energy-balance models for evapotranspiration only need z_{0h}. It has been proven that the surface roughness for momentum transport (z_{0m}) can deviate substantially from z_{0h} and z_{0v} (Beljaars and Holtslag 1991; McNaughton and van den Hurk 1995). So far, practical solutions for the ratio of z_{0m} to z_{0h} have not been found, which is a critical shortcoming in the estimation of surface heat fluxes from heterogeneous landscapes.

Broadband surface albedo

Definition: The surface albedo (r_0) is the hemispherical surface reflectance of shortwave radiation between wavelengths of 0.3 and 3 μm.

Purpose: r_0 is a measure of the amount of crop-absorbed shortwave radiation that is available for heat fluxes such as evapotranspiration.

Although surface albedo values for various crops have been tabulated (e.g., Monteith and Unsworth 1990), the values change as crop variety, development stages, and irrigation practices change. Well-watered crops usually exhibit albedo values between 10 and 20 percent. Albedo values of 15 to 25 percent are more common for water-stressed crops. Hence, crop-specific albedo values cannot be given, and measurements must be made to calculate water requirements accurately.

Satellites measure the spectral reflectance in narrow bands at the top of the atmosphere. The conversion of multiple narrowband reflectances to a single broadband reflectance (Jackson 1984) is a weighting procedure in which the spectrally incoming solar radiation of each band is proportional to the weighting factors, as shown in equation (5):

$$r_p = c_4 + c_5 r_{p\,1} + c_6 r_{p-2} + \ldots c_n r_{p\,n} \tag{5}$$

where r_p is the broadband planetary reflectance, c_4 to c_n are the weighting factors for spectrally integrating narrowband reflectance, r_{p-1} to r_{p-n} are the spectral planetary reflectances,

and n represents the number of bands in the 0.3 to 3.0 μm range. For instance, Valiente et al. (1995) suggested using $c_4 = 0.035$, $c_5 = 0.545$, and $c_6 = 0.32$ for AVHRR, which has two bands in the optical range of the spectrum. Stum, Pinty, and Ramond (1985) and Pinker and Ewing (1987) gave examples of using an expression identical in shape to that of equation (5), but they were also able to perform the spectral conversion for the geostationary satellites Meteosat, GOES, and GMS.

Several authors found that surface albedo explains the spatial variation of planetary albedo, which enables linear regressions to be drawn between them (Chen and Ohring 1984; Preuss and Geleyn 1984; Zhong and Li 1988):

$$r_p = c_7 + c_8 r_0 \tag{6}$$

where the regression coefficient c_7 is the offset in the relationship between broadband planetary albedo and broadband surface albedo (i.e., albedo of a nonreflecting surface body) and the regression coefficient c_8 is the two-way transmittance of the broadband shortwave radiation (Koepke, Kriebel, and Dietrich 1985).

Examples of using AVHRR measurements for estimating surface albedo are given by Gutman et al. (1989), Koepke (1989), Saunders (1990), and Arino, Dedieu, and Deschamps (1991; 1992). Studies with sun-synchronous satellites for derivation of albedo fields are given in Pinker 1985 (GOES), Dedieu, Deschamps, and Kerr 1987 (Meteosat), Pinty and Ramond 1987 (Meteosat), Nacke 1991 (Meteosat), Arino, Dedieu, and Deschamps 1992 (Meteosat), and Nunez, Skirving, and Viney 1987 (GMS). Thematic Mapper data are better suited for estimating the albedo of irrigated terrain—examples are given by Menenti, Bastiaanssen, and van Eick (1989), Moran et al. (1989), Daughtry et al. (1990), and Wang et al. (1995). A review on surface albedo mapping procedures may be found in Pinker 1985. Choudhury (1991) mentions a relative error (absolute error divided by absolute value) of 10 percent, which is equivalent to an absolute error of 2.5 percent when a regional average albedo of 25 percent is assumed. Pinty and Ramond (1987) also mention accuracy rates of 10 percent.

Thermal infrared surface emissivity

Definition: Thermal infrared surface emissivity (ε_0) is the efficiency with which the surface emits longwave radiation at a given temperature in the 3 to 100 mm spectral range.

Purpose: ε_0 is a dominant measure of the upwelling of longwave radiation, a component of the radiation balance. A spectral value of ε_0 is necessary to determine surface temperature from spectral radiometer measurements.

The surface radiation balance has a longwave component. The Planck function describes the emission of electromagnetic radiation at a given temperature and given wavelength. Because natural surfaces (unlike black bodies) do not emit longwave radiation with 100 percent efficiency, a correction term, e_0, has to be introduced for gray bodies (e.g., Becker 1987):

$$\varepsilon_0(l_1, l_2) = L(l_1, l_2)/\int L(l, T)\, dl \tag{7}$$

where L is spectral radiation, l *is* wavelength, l_1 and l_2 are upper and lower limit wavelengths, respectively, and T is absolute temperature. The numerator is the amount of radiation actually emitted between l_1 and l_2. It is measured by a radiometer operating in the same spectral range. The denominator is the integral of the Planck function with a black-body surface. Remotely operating thermal radiometers measure $L(l_1, l_2)$ in a narrow thermal infrared band between l_1 and l_2, and they use the principles of equation (7) to obtain the physical surface temperature by inverting the Planck function, then correcting for surface emissivity between l_1 and l_2. The presence of a relatively transparent atmospheric window in the 10.5 to 12.5 μm spectral range is the reason for the development of spaceborne thermal infrared radiometers in that spectral range.

Schmugge, Becker, and Li (1991) found that the emissivity of closed canopies is almost 1 and that closed canopies have almost no spectral variation in the thermal infrared range. However, irrigated crops are often characterized by partial canopies, so a soil contribution to emissivity can be expected. Becker and Li (1990a) indicated that estimates of surface temperature may have a 2 to 4 K error if the spectral variations, $\varepsilon_0(l_1, l_2)$, of partial canopies are not considered. In a similar study, Kornfield and Susskind (1977) found an error of 1°C if an ε_0 value of 1.0 is used instead of 0.95. Information on infrared surface emissivity values obtained in laboratories and fields is given in Buettner and Kern (1965), Wong and Blevin (1967), Griggs (1968), Idso et al. (1969), Sutherland (1986), Takashima and Masuda (1987), Elvidge (1988), Caselles, Sobrino, and Becker (1988), Hipps (1989), Nerry, Labed, and Stoll (1990), Schmugge, Becker, and Li (1991), van de Griend et al. (1991), Labed and Stoll (1991), Salisbury and D'Aria (1992a; 1992b), and Rubio, Caselles, and Badenas (1996).

Practical methods for estimating $\varepsilon_0(l_1, l_2)$ from multispectral thermal infrared measurements were proposed by Kahle and Alley (1992), Watson (1992a; 1992b), and Kealy and Hook (1993). One solution suggested by Kahle and Alley (1992) is to solve for the spectral emissivity from an assumed emissivity in one or more bands. Alternatively, the Planck radiation curve can be fitted to the measured spectral radiance curve by setting the emissivity of the highest spectral thermal radiation to 1. Watson (1992a) used the temporal constancy of emissivity for rocks and dry soils to uniquely identify spectral emissivity. He related the radiance ratio to the emissivity ratio in two contiguous thermal infrared bands.

Van de Griend and Owe (1993), Caselles et al. (1995), and Valor and Caselles (1996) proposed the use of NDVI for surface emissivity in the AVHRR thermal infrared channels. Based on earlier work of Coll, Caselles, and Schmugge (1994), Caselles et al. (1995) suggested deriving the average emissivity of AVHRR channels 4 and 5 from AVHRR-based NDVI data by using a linear relationship. Comparisons with field observations in La Mancha (Spain) show that a standard deviation of 0.003 is sufficiently precise. A theoretical justification of relationships between emissivity and NDVI is provided by Valor and Caselles (1996), and their new standard model has been validated for mid-latitudes and tropical regions, including flat and rough surfaces. The error of estimate of 0.6 percent is acceptable. This is in line with the expectations of Norman, Divakarla, and Goel (1995), who a year earlier said that considerable progress in estimating emissivity with accuracy in the range of 0.01 to 0.02 was within reach.

Surface temperature

Definition: The surface temperature (T_0) is the skin temperature of the land surface, i.e., the kinematic temperature of the soil plus the canopy surface (or, in the absence of vegetation, the temperature of the soil surface).

Purpose: T_0 describes the equilibrium between energy supply (radiation balance) and energy consumption (energy balance).

The interactive heat mechanisms between land and atmosphere are determined by radiation, conduction, and convection of energy transport processes. Surface temperature is a key parameter in the surface energy balance.

Many remote sensing studies have been devoted to estimating evapotranspiration from thermal infrared measurements. One of the first was Fuchs and Tanner 1966, which recognized that the temperature of crops was informative for growing conditions. Crop architecture (fractional vegetation cover, LAI, crop height, surface roughness), illumination (azimuth and zenith), and observation angle all create a series of different temperatures values.

Kinematic surface temperature, radiometric surface temperature, aerodynamic temperature, and thermodynamic temperature are substantially different, and a clear nomenclature such as the one presented by Norman, Divakarla, and Goel (1995) and Norman and Becker (1995) is necessary to quantify temperature correctly. The radiometric surface temperature is the temperature value for black bodies obtained from thermal infrared radiometers having a certain field of view and a finite wavelength band. The aerodynamic temperature represents the temperature at a height *equal to the surface roughness length for heat transport* (z_{0h}), which implies that it is linked to crop geometry. The thermodynamic temperature has the general property of indicating the direction of heat flow between two systems in thermal contact. In crop meteorological nomenclature, this is the temperature obtained by extrapolating air temperature profiles above the canopy to a virtual heat source, i.e., the surface roughness length for heat transport, z_{0h} (fig. 4). The difference between surface temperature (T_0) and thermodynamic temperature (T_{z0h}) can be adjusted with an additional resistance to heat transport, i.e., the theoretical kB^{-1} artifact (Carlson et al. 1995).

Methods currently being used to correct radiometric surface temperature for atmospheric interference fall basically into two categories. *Direct* methods use radiation transfer models together with atmospheric radio soundings, satellite vertical sounders, and climatological data. *Indirect* methods are based on split-window or in situ temperature observations. The split-window technique for computing the surface temperature from AVHRR has been designed to account for the absorption effects that atmospheric water vapor has on radiometric surface temperatures. It is based on similar emissivity values in the 10.3 to 12.4 μm spectral range. At present, the split-window technique (so called because AVHRR measures spectral longwave radiation in two different windows) is the most practical method for deriving surface temperature from multi-thermal band sensors:

$$T_0 = T_4 + c_9(T_4 - T_5) + c_{10} \tag{8}$$

where T_4 and T_5 are the radiation temperatures from AVHRR channels 4 and 5, respectively, at the top of the atmosphere; the regression coefficient c_9 corrects for atmospheric water vapor; and c_{10} corrects for surface emissivity in AVHRR bands 4 and 5 and for attenuations of gases and aerosols.

Kealy and Hook (1993) worked out a methodology that simultaneously gave the surface temperature and the surface emissivity from which the physical surface temperature could be derived. Norman, Divakarla, and Goel (1995) observed that if emissivity is properly corrected for, the uncertainty in surface radiation temperature is 1 to 2°C. Carlson et al. (1995) reported inaccuracies of 1°C if local atmospheric radio soundings are used, but errors due to instrument calibration, angular effects, and emissivity are 2 to 3°C, at best. Atmospheric corrections c_9 and c_{10} or corrections from single channels, such as Thematic Mapper and VISSR, can be done with 90 percent accuracy if ground or atmospheric data are available. Examples of research dedicated to the retrieval of surface temperature from satellite sensors are abundant: Chen et al. (1983), Shih and Chen (1984), Wetzel, Atlas, and Woodward (1984) for GOES-VISSR; Abdellaoui, Becker, and Olory-Hechninger (1986) for GMS-MSR; Price (1984), Wan and Dozier (1989), Becker and Li (1990b), Sobrino, Coll, and Caselles (1991), Vidal (1991), Kerr, Lagouarde, and Imbernon (1992), and Ulivieri et al. (1994) for NOAA-AVHRR; Kahle (1987) for TIMS; Lathrop and Lillesand (1987) and Wukelic et al. (1989) for Landsat-TM; and Prata (1993) for ERS-ATSR (annex 5 contains a list of acronyms).

Surface resistance

Definition: Surface resistance (r_s) is the resistance of vapor flow between the evaporation front inside the soil pore and the surface roughness of vapor transport above the soil surface or between the evaporation front inside the stomatal cavity and the surface roughness of vapor transport above the leaf surface.

Purpose: r_s represents the effect of soil moisture and solute concentration on actual evapotranspiration and indicates stress caused by crop water deficit or salinity.

Information on actual evapotranspiration is indispensable for estimating effective use of irrigation water and assessing crop water stress. Irrigation is meant to enhance evapotranspiration, and the surface resistance is the link between them. Because r_s is impossible to quantify directly from remote sensing measurements, it is customary to compute evapotranspiration as the residual of the surface energy budget:

$$\mathrm{LE} = R_n - G_0 - H \tag{9}$$

where LE is the latent heat flux, R_n is net radiation, G_0 is the soil heat flux, and H is the sensible heat flux (other approaches are discussed later). Net radiation in equation (9) is the energy supplier for the surface heat fluxes. Latent heat flux is used by meteorologists to express the energy consumed for the vaporization of water, i.e., actual evapotranspiration. Surface resistance controls the passage of moisture from the soil matrix to the overlaying atmosphere (fig. 4). The canopy resistance (for canopies alone) or surface resistance (for mixed canopy and soil elements) relates r_s physico-mathematically to LE:

$$LE = [\rho_{air} c_p / \varphi(r_{av} + r_s)][e_{sat}(T_0) - e_{act}] \tag{10}$$

where $\rho_{air} c_p$ is the heat capacity of moist air, φ is the psychrometric constant, r_{av} is aerodynamic resistance to vapor transport, r_s is surface resistance to actual evapotranspiration, e_{sat} is saturated vapor pressure at the evaporation front, and e_{act} is actual vapor pressure at observation height. Stomatal and canopy resistance are controlled by, in addition to soil moisture, shortwave solar radiation, saturation deficit, leaf area index, foliage temperature, leaf age, and leaf mineral nutrients, which all affect the stomatal aperture (Jarvis 1976). Although Sellers, Heiser, and Hall (1992) related inverse surface resistance (i.e., surface conductance) directly to spectral vegetation indices, it is customary to determine the surface resistance through equations (9) and (10). That implies that net radiation, soil heat flux, and sensible heat flux need to be determined first.

Radiation balance. Combining shortwave measurements (surface albedo) and longwave measurements (surface emissivity, surface temperature) of the earth's surface permits quantification of the radiation balance of irrigated crops:

$$R_n = (1 - r_0)K^{\downarrow} + L^{\downarrow} - L^{\uparrow} \tag{11}$$

where R_n is the net radiation of upwelling and downwelling wave radiative fluxes at the surface, r_0 is the surface albedo, $K^{\downarrow}$ is the incoming broadband shortwave solar radiation between 0.3 and 3.0 μm, and $L^{\downarrow}$ and $L^{\uparrow}$ are, respectively, the incoming and outgoing broadband longwave thermal radiation emitted between 3 and 100 μm. In remote sensing of agricultural areas, the major modulator of R_n for cloudless sky conditions is the surface albedo. Once the surface temperature, T_0, is known, broadband longwave radiation, $L^{\uparrow}$, can be quantified according to the Stefan–Boltzmann law, which substitutes for Planck's law when all wave-emitted radiation is considered:

$$L^{\uparrow} = \varepsilon_0 \sigma T_0^4 \tag{12}$$

where ε_0 represents the spectral integration of $\varepsilon_0(l_1, l_2)$ and σ is the Stefan–Boltzmann constant. Equation (12) can be used for the determination of both $L^{\downarrow}$ and $L^{\uparrow}$ given in equation (11). Note that equation (12) is related to equation (7) through $\int L(l, T)\, dl = \sigma T^4$ when l_1 is 0.3 μm and l_2 is 3.0 μm. Equation (11) can be solved using partial remote sensing data (r_0, ε_0, T_0) in combination with ancillary ground data on $K^{\downarrow}$ and $L^{\downarrow}$ (e.g., Jackson, Pinter, and Reginato 1985; Moran et al. 1989; Daughtry et al. 1990; Kustas et al. 1994; Pelgrum and Bastiaanssen 1996) or entirely from remote sensing where $K^{\downarrow}$ and $L^{\downarrow}$ are derived from the procedures described below.

To get a better picture of the behavior of shortwave radiation, $K^{\downarrow}$, in a global perspective, international initiatives such as ERBE, WCRP, and ISCCP have been undertaken. ERBE (Earth Radiation Budget Experiment) is a global satellite program that measures radiation budget components simultaneously (Barkstrom et al. 1989). WCRP (World Climate Research Program) has launched a special project on global shortwave surface radiation budget data sets (Whitlock et al. 1995). Downwelling shortwave radiation, $K^{\downarrow}$, and longwave radiation, $L^{\downarrow}$, at the ground are also estimated and validated with global data sets in the framework of the ISCCP

(International Satellite Cloud Climatology Project) (Zhang, Rossow, and Lacis 1995). Considerable progress has been made in assessment of incoming shortwave radiation from geostationary satellite data and algorithms. The physically based algorithms consist of correcting the satellite radiances for scattering, reflection, and absorption through the involvement of radiation transfer models (e.g., Gautier, Diak, and Masse 1980; Diak and Gautier 1983; Pinker and Ewing 1987; Dedieu, Deschamps, and Kerr 1987). Other simplified and more or less empirical retrieval procedures have been developed and tested by Raschke et al. (1973), Tarpley (1979), Nunez, Hart, and Kalma (1984), Moser and Raschke (1984), Darnell et al. (1988), Darnell et al. (1992), Li and Leighton (1993), Lourens et al. (1995), and Diak, Bland, and Mecikalski (1996).

At present, the 24-hour integrated incoming shortwave radiation can be computed from satellite observations with an accuracy of 10 percent (Raschke and Rieland 1989; Diak, Bland, and Mecikalski 1996). Rossow and Zhang (1995) and Zhang, Rossow, and Lacis (1995) mentioned a difference in incoming shortwave radiation at individual sites of 9 W/m^2 with a deviation of 8 W/m^2 at a scale of 100 × 100 kilometers. Stuhlmann (1996), in a more careful analysis, found deviations of 5 to 10 percent on monthly basis. An excellent review on this theme has been synthesized by Pinker, Frouin, and Li (1995). Although the temporal resolution of geostationary satellites within 0.5 hour is attractive, it must be noted that the spatial resolution is only 5 kilometers at the equator. It is, however, far better than relying on ground weather stations with a coarse observation network or than using hours of sunshine when solar radiation measurements are unavailable

Longwave radiation incident on the land surface, $L^{\downarrow}$, originates from atmospheric emissions and varies with the atmospheric water vapor content. Abundance of water vapor can be determined from radiation measurements by estimating the amount of water vapor absorbed at wavelengths that are relatively free of other effects. Water-vapor abundance profiles can be produced from the multi-wavelength infrared measurements of instruments such as the High Resolution Infrared Radiation Sounder (HIRS) on NOAA under cloud-free conditions. NOAA's TIROS Operational Vertical Sounder (TOVS), containing 27 optical and microwave channels, provides estimates of atmospheric characteristics at several levels within the atmosphere. Comparisons of monthly mean maps of atmospheric water vapor from HIRS and the SSM/I microwave imager indicates an 80 percent agreement (Wittmeyer and vonder Haar 1994). Detailed study results can be found in Satterlund (1979), Schmetz, Schmetz, and Raschke (1986), Frouin, Gautier, and Morcrette (1990), Gupta (1989), Tuzet (1990), Darnell et al. (1992), Zhang, Rossow, and Lacis (1995), and Rossow and Zhang (1995). The review by Sellers, Rasool, and Bolle (1990) reveals that the accuracy of downward longwave fluxes, $L^{\downarrow}$, has a root mean square error of 14 to 20 W/m^2. Ellingson (1995) gives a critical review of the determination of surface longwave fluxes from satellite observations.

Soil heat flux. Heat flow into the soil, G_0, is driven by a thermal gradient in the uppermost topsoil. This gradient varies with fractional vegetation cover and leaf area index because light interception from, and shadow formation on, the bare soil determine radiative heating of the bare soil surface. The surface temperature and the thermal gradient in the top layer of soil react to net radiation. Surface moisture conditions affect soil thermal conductivity—moist soils are better at conducting heat. Moisture also affects soil evaporation and the energy partitioning of bare and partially covered soils. It is common to relate G_0 to R_n and soil moisture by simple substitutes for them (table 8). All solutions in table 8 are, without exception, empirical

and need to be calibrated locally. Minor light interception in partial canopies makes the essence of G_0/R_n more relevant for partial canopies ($G_0/R_n > 0.2$) than for closed conditions ($G_0/R_n < 0.05$). G_0 may be ignored for time integrations longer than a solar cycle.

Table 8. Remotely sensed dependent variables chosen to express the spatial variation of the instantaneous soil heat flux.

	Dependent variables[a]					
Source	h_c	LAI	SR	NDVI	T_0	r_0
Menenti 1984					●	
Reginato, Jackson, and Pinter 1985	●					
Clothier et al. 1986			●			
Choudhury, Idso, and Reginato 1987		●				
Moran et al. 1989				●		
Kustas and Daughtry 1990			●	●		
Zhang, Rossow, and Lacis 1995				●		
Bastiaanssen et al. 1994				●	●	●

[a]LAI = leaf area index, SR = simple ratio, NDVI = normalized difference vegetation index. See table 7 for other definitions.

Sensible heat flux. In figure 4, a crop is composed of the energy balance of the canopy and bare soil. Sensible heat, H, released from the bare soil, can flow into the canopy to enhance the transpiration process and act as an interactive heat-regulating mechanism between the soil and canopy. When a partial canopy is insufficiently irrigated, i.e., soil moisture is less than the amount optimally required, the stomata close, increasing the surface resistance, so that cooling is no longer optimal. As a result, the canopy temperature rises, modulating the H/LE ratio. Supplying irrigation water keeps the root zone moist, holding the surface resistance and the H/LE ratio at a level low enough for optimum growth. Hence, *the primary purpose of irrigation is to keep the surface resistance of the crop canopy within certain preferred limits, thereby enhancing vapor release and carbon dioxide intake.*

It follows from the physics depicted in figure 4 that state variables (the environmental variables that adjust continuously due to the energy-balance process) at reference heights (such as surface temperature, air temperature, and actual vapor pressure) may not be specified independently from fluxes and resistances. The sensible heat flux, H, is proportional to the difference between surface and air temperature ($T_0 - T_{air}$), while the aerodynamic resistance to heat transport, r_{ah}, is determined by wind speed, surface roughness, displacement height, and the thermal instability of the atmosphere. The reference heights for temperature and aerodynamic resistance must be identical to express sensible heat flux as an Ohm-type law:

$$H = (\rho_a c_p / r_{ah})(T_0 - T_{air}) \tag{13}$$

Due to space limitation, the physical background of turbulent transfer mechanisms will not be presented. Surface temperatures can be used synergistically with a vegetation index or surface albedo, or both, to extract information on the difference between T_0 and T_{air} from multispectral satellite measurements. Hope et al. (1986), Goward and Hope (1989), Nemani and Running (1989), Price (1990), Carlson, Perry, and Schmugge (1990), Nemani et al. (1993), and Carlson, Gillies, and Perry (1994) used the synergism between surface temperature and NDVI to get information on partitioning between H and LE. Moran et al. (1994) used SAVI similarly. In contrast, Menenti et al. (1989), Bastiaanssen, Hoekman, and Roebeling (1994), and Bastiaanssen, Menenti, et al. (forthcoming) devised a procedure for using the shape formed by the relation of surface temperature to surface albedo.

Figure 5 shows that the surface temperature of evaporating surfaces (either vegetated or bare soil) rises with increasing albedo and decreasing NDVI. These relationships can be explained by the depletion of moisture from soil and vegetation and the subsequent higher ratio of H to LE and higher equilibrium surface temperatures. The inverse proportionality between surface temperature and surface albedo when r_0 exceeds 0.27 can be established only if the role of evaporation is ruled out. Then surface temperature becomes entirely controlled by net radiation, and an increase in albedo results in lower net radiation values yielding to lower equilibrium surface temperatures. This essentially occurs when vegetation is absent, or when NDVI approaches minimum values. The relationship between T_0 and r_0 can be utilized to delineate pixels that have a negligible evapotranspiration (i.e., LE = 0). After solving H according to equation (13), actual evapotranspiration, LE, can be estimated on a pixel basis using the residual approach of equation (9). The surface resistance can then be obtained by solving equation (10).

Other approaches. Besides the LE-residual approach outlined in equations (9) to (13), other approaches for determining latent heat flux or evapotranspiration have been attempted. Retrieval of regional evapotranspiration with remote sensing data using physical algorithms that have different degrees of complexity are discussed by Choudhury (1989), Baily (1990), Schmugge and Becker (1991), Moran and Jackson (1991), Engman and Gurney (1991), Menenti (1993), Norman, Divakarla, and Goel (1995), Bastiaanssen et al. (1996), and Kustas and Norman (1996). Pioneering work on utilizing thermal infrared observations to estimate evapotranspiration has been carried out by Idso et al. (1975) and Jackson, Reginato, and Idso (1977). The large number of remote sensing evapotranspiration algorithms that subsequently were developed and tested differ mainly in the type of land-use information required, the wavelength and ancillary micro-meteorological data used, and the need for numerical models. Table 9 outlines the history of the estimation of evapotranspiration from irrigated and nonirrigated fields.

Most of the algorithms in papers listed in table 9 have been applied on a limited basis in irrigated fields and river basins. But there are some exceptions. Among the algorithms that have been fairly widely tested in irrigated agriculture are the simplified daily surface energy-balance model of Jackson, Reginato, and Idso (1977) and upgraded versions proposed by Seguin and Itier (1983) and Hurtado, Artigao, and Caselles (1994), which have been applied in irrigation schemes in USA, Spain, France, and Morocco. More complex instantaneous surface energy-balance descriptions have been validated by Kustas et al. (1994) who applied their model in USA and by Bastiaanssen, Pelgrum, Wang, et al. (forthcoming) who applied the SEBAL algorithm on irrigated areas in Egypt, Spain, Italy, Argentina, China, Niger, USA,

Figure 5. Observed relationship between surface albedo and surface temperature (above) and between Normalized Difference Vegetation Index and surface temperature (below) from Thematic Mapper data over part of the Rio Grande Basin and the Chihuahuan shrub and grassland vegetation in the vicinity of Las Cruces, New Mexico, USA, September 25, 1995.

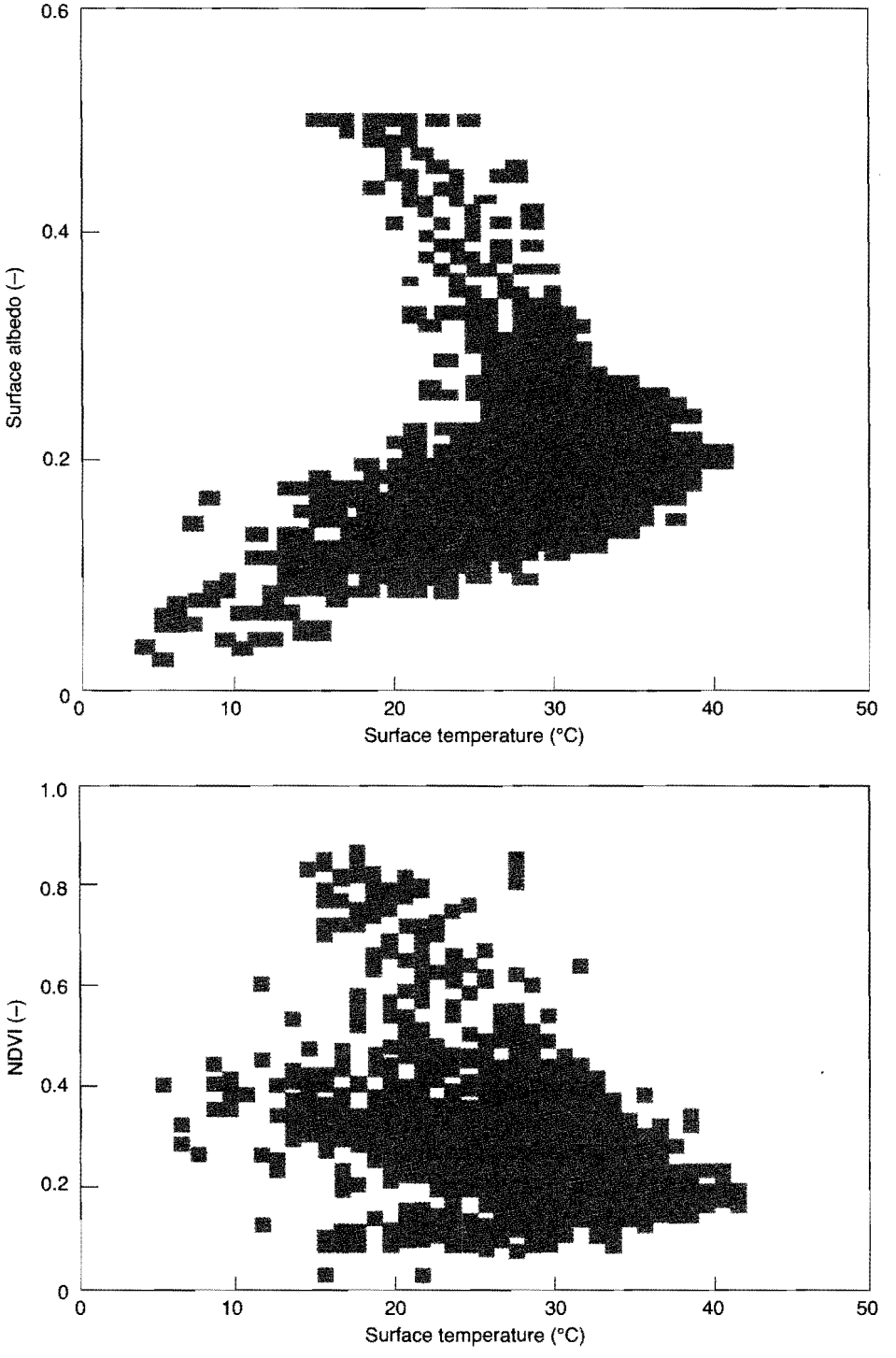

Table 9. Selected bibliography on remote sensing evapotranspiration algorithms indicating their spectral range and the required field information.

Source	Irrig[a]	Land[b]	Num[c]	Spectrum[d]					Field data needed[e]																		
				vis	nir	tir	pmw	rad	h_c	U	u	T_{air}	soil	LAI	r_s^{min}	z_0	R_n	E_{pan}	P	ε_0	r_0	PBL	$L^{\downarrow}$	$K^{\downarrow}$	z_{0h}	z_{0m}	r_a	d
Jackson, Reginato, and Idso 1977; Jackson et al. 1981	●	●		●		●			●	●	●	●					●							●				
Soer 1980		●	●	●	●	●			●	●	●	●	●				●		●		●		●	●				
Hatfield, Reginato, and Idso 1984	●	●				●			●	●	●	●				●	●				●		●	●				●
Nieuwenhuis, Smidt, and Thunnissen 1985		●		●	●	●			●		●	●																
Taconet, Bernard, and Vidal-Madjar 1986		●	●			●			●		●	●	●	●	●													
Abdellaoui, Becker, and Olory-Hechninger 1986			●			●				●	●	●	●											●				
Seguin et al. 1989	●	●				●					●	●				●	●											
Kerr et al. 1989			●	●	●													●	●									
Vidal and Perrier 1990	●	●				●			●		●	●		●			●											
Smith and Choudhury 1990			●	●	●		●						●					●	●									
Diak 1990			●			●														●	●	●						
Cihlar, St-Laurent, and Dyer 1991		●	●	●	●							●	●						●									
Hall et al. 1992		●		●	●	●					●	●										●	●	●	●			
Deblonde and Cihlar 1993		●	●	●	●							●	●										●					
Braden and Blanke 1993		●	●	●	●	●				●	●	●							●				●	●				
Hurtado, Artigao, and Caselles 1994	●	●		●	●	●			●		●	●		●			●											
Kustas et al. 1994				●	●	●				●	●	●												●		●		●
Choudhury 1994				●	●																							
Norman, Kustas, and Humes 1995		●	●	●	●	●			●		●	●					●											
Vidal and Baqri 1995	●	●				●			●			●		●			●											
Ottle et al. 1996		●	●	●	●	●		●	●	●		●	●	●										●			●	
Bastiaanssen, van der Wal, and Visser 1996	●			●	●	●			●																			
Granger 1997		●		●		●				●		●					●											

[a]Study conducted in irrigated land.

[b]Algorithm requires information on land use (crop type) to assign biophysical model parameters.

[c]Numerical models require data on soil hydraulic and thermal properties.

[d]vis = visible, nir = near infrared, tir = thermal infrared, pmw = passive microwave, rad = radar.

[e]LAI = leaf area index, PBL = PBL radio soundings, soil = soil physical properties. See table 7 for other definitions.

Color Plate 2. Bulk surface resistance to evaporation (s/m), derived from all bands of Landsat Thematic Mapper using the SEBAL algorithm, June 1991, Guadiana River Basin, Castilla La Mancha, Spain. The irrigated areas appear in bright green and blue (r_s <200 s/m). The blue areas consist mainly of pivot irrigation systems in addition to a few reservoirs.

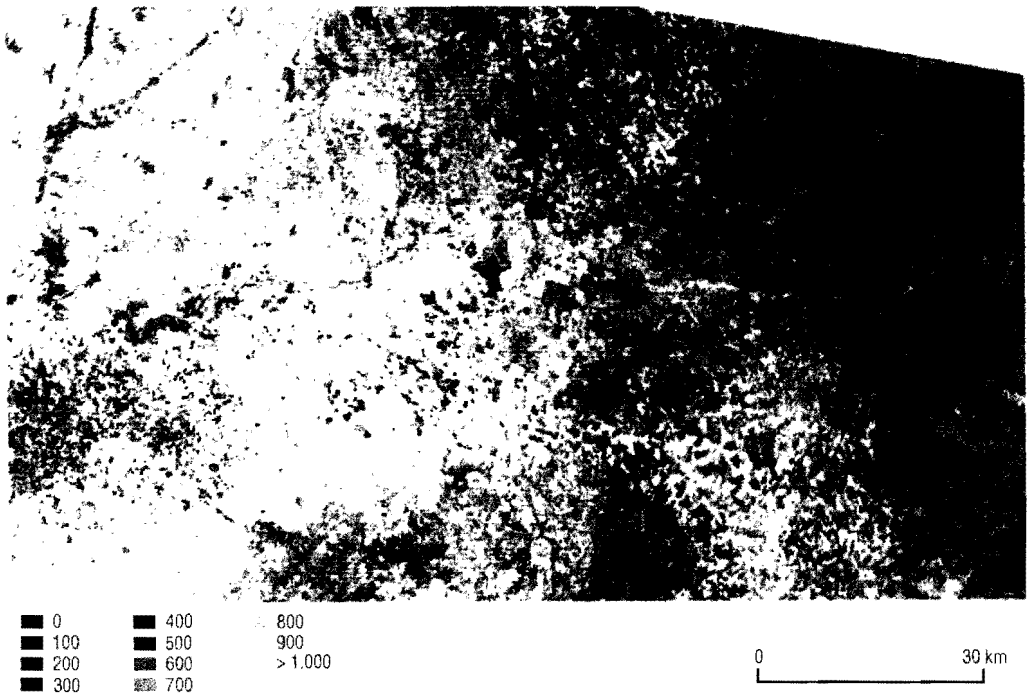

Sri Lanka, India, Pakistan, Kenya, Ethiopia, and Zambia. Validation efforts for SEBAL have shown that the error at a field scale of 1 hectare varies between 10 to 20 percent and that the uncertainty diminishes when multiple fields are included. For an area of 1,000 hectares, the error diminishes to 5 percent, and for regions comprising 1,000,000 hectares of farmland, the error becomes negligibly small. The pixel-by-pixel residual latent heat flux from equation (9) can be inverted in equation (10) to determine the surface resistance for any of the methods in table 9 that explicitly solve for R_n, G_0, and H:

$$r_s = [\rho_a c_p / \varphi (R_n - G_0 - H)][e_{sat}(T_0) - e_{act}] - r_{av} \tag{14}$$

Color Plate 2 is an example of a surface resistance map determined according to equation (14).

An alternative approach for computing surface resistance is relative evapotranspiration. Relative evapotranspiration is defined as the ratio of actual to potential evapotranspiration and can be derived from crop stress indicators (table 10). Although this approach does not explicitly provide a value for actual evapotranspiration, it may be determined if potential evapotranspiration can be obtained independently. Morton (1983) described wet-environment evaporation in the complementary relationship between actual and potential evapotranspiration. He concluded that radiation type of expressions for evaporation in a wet environment, such as

irrigated terrain, are sufficiently accurate to compute the maximum possible water consumption from crops. Caselles and Delegido 1987 provides an example of calculating potential evapotranspiration from radiation-type equations. They obtained the potential evapotranspiration for green grass on the basis of remote sensing estimates of incoming solar radiation and air temperature. Watts et al. (1995) produced daily solar radiation maps from GOES-7 data in southern Sonora, Mexico, and computed potential evapotranspiration by applying the radiation-type equation of Makkink (Stewart et al. 1995). Both Bastiaanssen, van der Wal, and Visser (1996) and Roerink et al. (1997) used net available energy ($R_n - G_0$) as a safe proxy for potential evapotranspiration.

Relative evapotranspiration can be linked analytically to surface resistance for decoupled soil-atmosphere systems by means of the ratio of Penman-Monteith denominators at different resistance levels:

$$LE_{act}/LE_{pot} = [s_a + \varphi(1 + r_s^{min}/r_a)]/[s_a + \varphi(1 + r_s/r_a)] \quad (15)$$

Table 10. Selected literature describing the detection of crop water stress from remotely sensed multispectral measurements.

Source	Crop stress indicator	Principle
Hiler and Clark 1971	Number of stress days	Accumulated relative evapotranspiration
Jackson, Reginato, and Idso 1977	Stress degree day	Accumulated surface minus air temperature
Jackson et al. 1981; Jackson, Kustas, and Choudhury 1988	Crop water-stress index	Spreading of surface minus air temperature
Luvall and Holbo 1989	Thermal response number	Thermal inertia, moisture availability
Menenti and Choudhury 1993	Surface energy-balance index	Surface temperature and mixed layer conditions
Shibayama et al. 1993	Derivative of reflectance	Spectral canopy reflectance at 960 nm
Moran et al. 1994	Water deficit index	Trapezoid formed by surface temperature and SAVI
Bastiaanssen, van der Wal, and Visser 1996	Evaporative fraction	Relationship of albedo and surface temperature
Mogensen et al. 1996	Spectral reflectance index	Accumulated number of stress days

where LE_{act} and LE_{pot} are actual and potential latent heat flux, respectively, s_a is the slope of the saturated vapor pressure curve, r_s^{min} is minimum surface resistance to maintain potential evapotranspiration, i.e., the resistance when actual and potential evapotranspiration coincide, r_a is aerodynamic resistance, φ is the psychrometric constant, and r_s is bulk surface resistance to actual evapotranspiration. Equation (15) is based on the assumption that the atmospheric vapor pressure deficit is similar for r_s and r_s^{min}.

Jackson et al. (1981) defined a crop water-stress index (CWSI) for full canopy conditions ($\nu_c = 1$) when bare-soil evaporation is ruled out:

Figure 6. Relationship between vegetation index and surface temperature conditions for a single crop (above, after Moran 1994) and for a heterogeneous landscape (below, after Lambin and Ehrlich 1996).

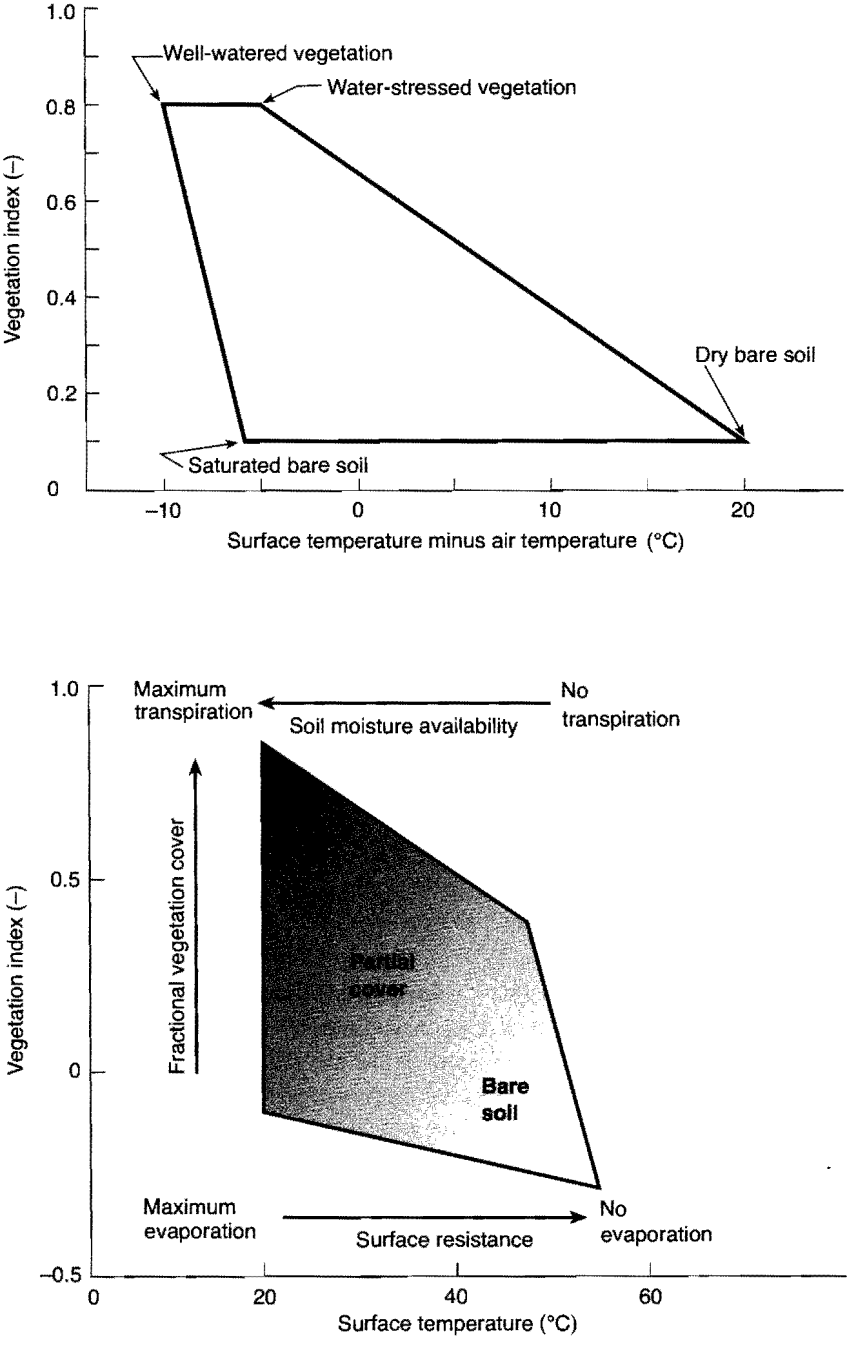

$$\mathrm{CWSI} = 1 - (t_{act}/t_{pot}) \tag{16}$$

where t_{act} and t_{pot} are actual and potential crop transpiration, respectively. CWSI has been obtained from thermal infrared field measurements (e.g., Idso, Reginato, et al. 1981):

$$\mathrm{CWSI} = (T_0 - T_{0min})/(T_{0max} - T_{0min}) \tag{17}$$

where T_{0min} is the surface temperature when the canopy resistance is minimum ($t_{act} = t_{pot}$) and T_{0max} occurs when the stomata are entirely closed ($t_{act} = 0$).

To normalize the measured temperatures for radiation and wind speed, Jackson, Kustas, and Choudhury (1988) replaced surface temperature (T_0) values in equation (17) with vertical differences in surface and air temperature ($T_0 - T_{air}$). Because CWSI is limited to the transpiration of closed crops ($v_c = 1$) with a given fixed vegetation index, Moran et al. (1994) suggested the use of a water deficit index (WDI) based on solutions of CWSI at different levels of fractional vegetation cover ($v_c = 0$ to 1). In their work, fractional vegetation cover is represented by SAVI. When a full range of fractional vegetation cover values is considered, a trapezoid between SAVI and $T_0 - T_{air}$ arises (fig. 6). Mathematically, then:

$$\begin{aligned} \mathrm{WDI}_{SAVI} &= [1 - (\mathrm{ET}_{act}/\mathrm{ET}_{pot})]_{SAVI} \\ &= [(T_0 - T_{air}) - (T_0 - T_{air})_{min}]_{SAVI}/[(T_0 - T_{air})_{max} - (T_0 - T_{air})_{min}]_{SAVI} \end{aligned} \tag{18}$$

where ET_{act} and ET_{pot} are actual and potential evapotranspiration, respectively. The minimum and maximum values for the difference between T_0 and T_{air} must be solved for SAVI = 0 and SAVI = max. Because instantaneous $\mathrm{ET}_{act}/\mathrm{ET}_{pot}$ values for thermal infrared measurements are identical to $\mathrm{LE}_{act}/\mathrm{LE}_{pot}$, surface resistance can be obtained from WDI, r_s^{min}, and r_a using equations (15) and (18).

From the perspective of equation (15), $\mathrm{LE}_{act}/\mathrm{LE}_{pot}$ is entirely controlled by soil hydrology (r_s). Physics prescribes, however, that soil-water-crop-atmosphere systems are a continuum, which implies that atmospheric vapor pressure deficit in the Penman-Monteith equation changes through r_s with soil water status (e.g., Morton 1983; de Bruin 1989). This feedback is what Bouchet (1963) described when he showed that the relationship between the actual and potential evapotranspiration rates (for a constant net radiation) is an inverse one. Because of the feedback mechanism between moisture in the soil and atmosphere, on the one hand, and the energy available for heat- and moisture-exchange processes, on the other, evapotranspiration cannot exceed the net available energy ($R_n - G_0$) during the time between two successive irrigation turns, except, by at most a small amount, at the physical boundaries between dry and wet areas. Heat flux measurements with eddy correlation devices in well-irrigated fields confirm that LE is approximately $R_n - G_0$ when both terms are integrated over time (Dugas et al. 1991; Ahmed and Neale 1996; Wang et al. 1994). Thus $R_n - G_0$ probably is a good substitute for ET_{pot}, and the evaporative fraction (latent heat flux divided by net available energy, or $\mathrm{LE}/[R_n - G_0]$) is consequently physically similar to relative evapotranspiration. The benefit of using the evaporative fraction is that crop stress can be obtained from simple flux ratios rather than from aerodynamic and surface resistances as proposed in equation (15). Equation (15) implies that evapotranspiration algorithms that have been tested and

validated at the regional scale (all studies listed in table 9) can be used to assess LE_{act}/LE_{pot} and r_s regionally. This is a step forward as compared with using LE_{act}/LE_{pot} for a particular crop or SAVI value. When expressed as a latent heat flux residual, the expression for the evaporative fraction, Λ, becomes:

$$\Lambda = [(R_n - G_0 - H)/(R_n - G_0)] \sim (LE_{act}/LE_{pot}) = 1 - WDI \quad (19)$$

Bussières and Goita (1997) evaluated different strategies for estimating evapotranspiration from remote sensing measurements when skies are overcast. The strategies are based on assuming the value for the evaporative fraction found on cloud-free days and on cloudy days is the same and the synergetic use of passive microwave data. Courault, Lagouarde, and Aloui (1996) worked on the application of satellite remote sensing for frequent cloudy days in a maritime catchment. They suggested estimating evapotranspiration with a crop water-balance model if image acquisition fails.

Calculation of most indicators of crop water stress listed in table 10 requires, in addition to remotely sensed surface temperature, ancillary data such as air temperature and aerodynamic resistances, which are difficult to quantify. To avoid the problem of defining micrometeorological conditions adjacent to the surface, where they manifest a distinct spatial variation, Menenti and Choudhury (1993) suggested measuring the state variables of the planetary boundary layer from an altitude where vapor pressure deficit, temperature, and wind speed are well mixed and thus independent of surface features.

Crop coefficients

Definition: The crop coefficient (k_c) is the ratio of potential evapotranspiration for a given crop to the evapotranspiration of a reference crop, usually grass or alfalfa.

Purpose: k_c permits calculation of water requirements for a particular crop in a certain development phase, using prevailing meteorological conditions measured from a standard weather station.

The crop coefficient is a traditional concept for relating water needs of a particular crop to those of a standard crop (van Wijk and de Vries 1954):

$$k_c = ET_{pot}/ET_{ref} \quad (20)$$

The selection and definition of the reference crop has been subject to changes over time. Penman (1948) used open water surfaces to design his famous expression. Applications for irrigated agriculture were basic to Penman's derivation, thus he selected water as the reference surface in studies of plant evapotranspiration. Later, the reference became the crops alfalfa and grass (Doorenbos and Pruitt 1977), and recently progress was made toward a more accurate physical definition of grass as the reference crop after a Consultation Meeting at FAO (Allen et al. 1995). Because the biophysical conditions used for the various reference crops were not identical, applications of tabulated k_c values should be made with caution. The bio-

physical crop properties and state variables affecting potential evapotranspiration and causing the difference between ET_{pot} and ET_{ref} are

- surface albedo (for net shortwave radiation corrections)
- infrared surface emissivity (for net longwave radiation corrections)
- surface temperature (for net longwave radiation and soil heat flux corrections)
- surface roughness for momentum, heat, and vapor transport (for aerodynamic resistance corrections)
- displacement height (for aerodynamic resistance corrections)
- leaf area index (for minimum canopy resistance and soil heat flux corrections)

For partial canopies, it is important to include the radiative properties of the soil (soil albedo, soil infrared emissivity) and the physical properties of the soil (hydraulic conductivity, thermal conductivity, and vapor diffusivity), as well as soil temperature and soil roughness for momentum and heat transport in the correction between ET_{ref} and ET_{pot}.

As indicated earlier, surface albedo, infrared surface emissivity, surface roughness, displacement height, and minimum canopy resistance can be derived individually from SR and NDVI. Tabulated crop coefficients have therefore also been related to vegetation indices such as PVI (Jackson et al. 1980; Heilman, Heilman, and Moore 1982), NDVI (Bausch and Neale 1987; Neale, Bausch, and Heeremann 1989), and SAVI (Bausch 1993; Neale et al. 1996). Investigations carried out by Bausch and Neale (1987) refer to the basal crop coefficient of maize (Wright 1982), which is defined as crop conditions under which transpiration is unlimited and soil evaporation is essentially nil. This definition eliminates uncertainties associated with soil physical corrections. It is interesting to note that the remote sensing measurements of Neale et al. (1996) were done with a low-altitude aircraft, which enabled them to concurrently monitor the need to supply irrigation water over large areas. They determined the accuracy in estimating tabulated k_c values from SAVI to be more than 90 percent. Azzali, Menenti, et al. (1991) and Meeuwissen (1989) assigned k_c values to groups of crops (crop class coefficients) that had uniform canopy development. To identify uniform canopy development, they employed a hybrid classification technology, rather than using vegetation indices for a particular crop. All these methods rely on spatial interpretation of tabulated and, hence, pre-fixed k_c values that have been derived for a reference crop with other possible biophysical properties.

D'Urso and Santini (1996) attempted to derive k_c analytically from remotely sensed estimates of albedo (using r_{p-l}), surface roughness (using SR), and r_s^{min} (using LAI). The advantage is that, unlike applications involving tabulated k_c coefficients, crop types and their development phases do not have to be known. This approach deserves more attention because indications are growing that tabulated k_c values give biased potential evapotranspiration values for larger areas, such as heterogeneous command areas.

Transpiration coefficients

Definition: The transpiration coefficient (t_c) is the fraction that results from dividing unstressed transpiration by potential evapotranspiration.

Purpose: t_c separates potential evapotranspiration into potential soil evaporation and potential crop transpiration components.

A cropped area is usually composed of a portion of canopies and a portion of bare soil. Irrigation water is ideally supplied if the root zone has easily available soil moisture, allowing unlimited crop water uptake (Doorenbos and Pruitt 1977). If the soil surface remains dry, water losses from soil evaporation will be limited.Although soil evaporation is often regarded as an unavoidable loss from an irrigation system because the soil must become wet to let surface water infiltrate, modern irrigation techniques such as drip systems can prevent the soil between crop rows from becoming moist. Soil evaporation losses can be as large as crop transpiration on an annual basis when the crop is sprinkled regularly. Irrigation scheduling should aim at keeping the topsoil dry without inducing a moisture deficit in the root zone. This concept affects the definition of required and actual crop water consumption and the computation of water-use efficiencies. And it demands some careful consideration: only for closed canopies (which occur during only one part of the seasonal growing cycle) are the differences between total evapotranspiration and crop transpiration irrelevant.

Separation of potential transpiration from potential evapotranspiration usually involves the transpiration coefficient, t_c. Ritchie (1972) and Al-Kaisi, Brun, and Enz (1989) parameterized t_c to vary exponentially with LAI. Choudhury et al. (1994) incorporated data from rangelands and from fields containing oats, millet, soybean, sunflower, cotton, sorghum, and maize, using the relationship

$$t_c = t_{pot}/ET_{pot} = 1 - \exp(-c_{11}LAI) \tag{21}$$

and concluded that when the regression coefficient $c_{11} = 0.6$, the data points fit satisfactorily (fig. 7). They found an average accuracy of 75 percent is reached when the LAI values range from 2.5 to 5.0. The range for c_{11} lies between 0.5 and 0.8, depending on crop type and the moisture conditions of the surface of the bare soil (Feddes 1987). Because the relationships between LAI and SAVI and between LAI and t_c are both nonlinear, Choudhury et al. (1994) showed a linear relationship between t_c and SAVI to be theoretically justified. Because LAI can be determined from remote sensing data according to equation (4) and because ET_{pot} can be found from either crop factors (k_c) or a radiation type of expression for potential evapotranspiration, unstressed transpiration can be obtained from satellite measurements by combining LAI and ET_{pot}. For stressed conditions, Troufleau et al. (1994) suggested incorporating radar data (SAR) to infer near-surface soil moisture and to qualitatively assess the ratio of actual soil evaporation to potential soil evaporation.

Figure 7. Observed relationship between transpiration coefficient and leaf area index for various crop types (Choudhury et al. 1994).

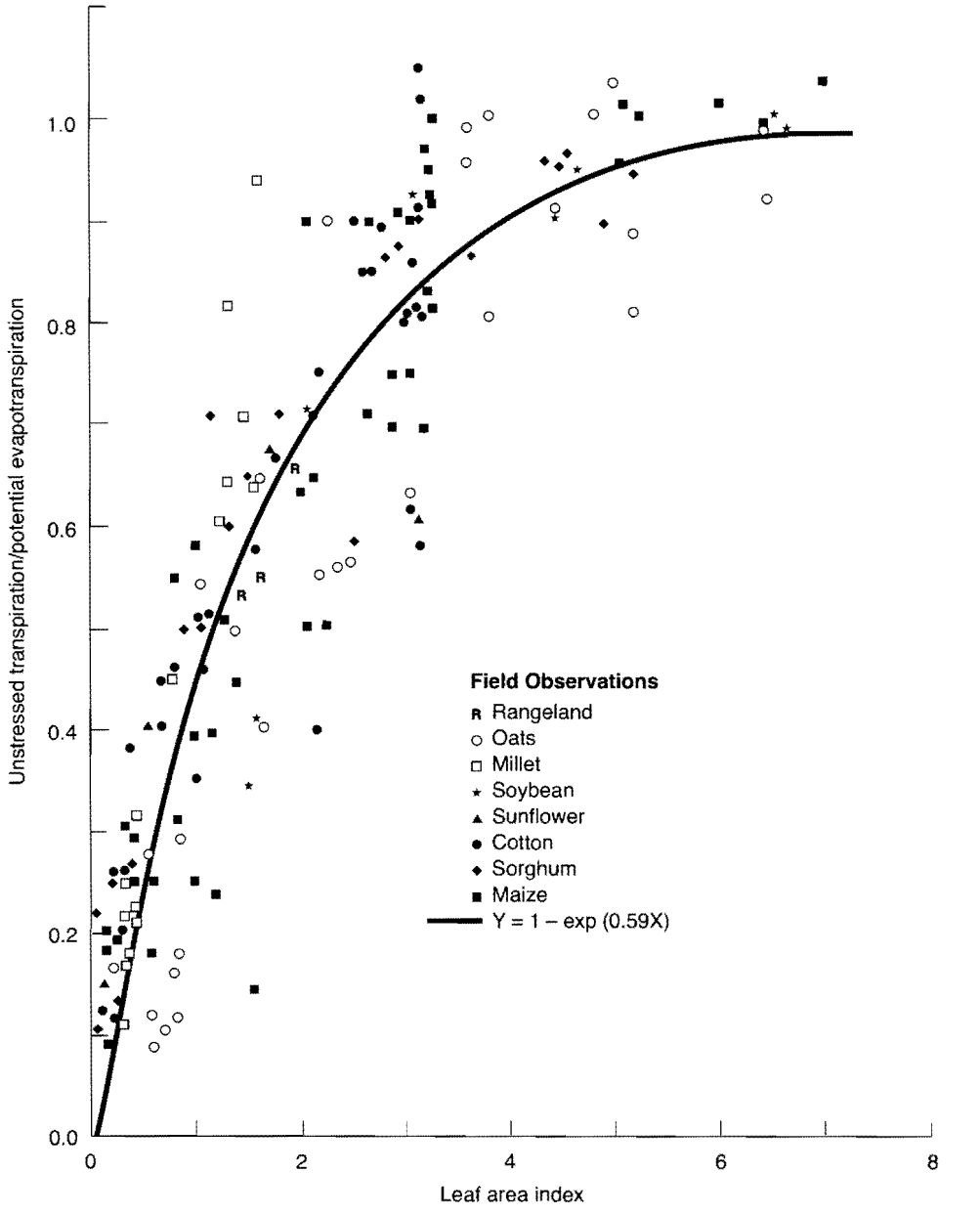

Crop yield

Crops open their stomatal apertures to receive atmospheric carbon dioxide and release vaporized soil moisture. Accumulated dry matter production is a final result of the crop's lifetime carbon dioxide intake, soil moisture uptake, and net photosynthetic assimilation. If LAI and

fPAR can be obtained from vegetation indices, it is likely that net primary production can be extracted from vegetation indices as well.

Daughtry et al. (1992) confirmed that the production of maize and soybean can be satisfactorily related to vegetation indices. Waddington and Lamb (1990) made successful predictions of potato yield using SR obtained from Landsat MSS data. Steven, Biscoe, and Jaggard (1983) estimated regional yields of sugarbeets. Tucker et al. (1980; 1981), Ashcroft et al. (1990), Rudorff and Batista (1991), Singh et al. (1992), Sharma et al. (1993), Benedetti and Rossini (1993), Dubey et al. (1994), Pestemalci et al. (1995), and Thiruvengadachari, Murthy, and Raju (1997) related NDVI to the yield of wheat. Thiruvengadachari, Murthy, and Raju (1997) applied a linear regression analysis between peak NDVI during the heading of wheat and wheat yield observed at the end of the growing season. They obtained the yield of wheat from in situ crop-cutting experiments in 157 plots scattered across the study area and showed a statistical relationship between wheat yield and NDVI to be a valid approximation of crop yield ($r^2 = 0.86$). Earlier, Hatfield (1983) had shown that NDVI at the heading stage can be a suitable substitute for crop yields.

Estimates of rice yields were obtained in Japan (Yamagata and Akiyama 1988; Mubekti, Miyama, and Ogawas 1991; Shibayama and Akiyama 1991), India (Patel et al. 1991; Murthy et al. 1996) and Thailand (Tennakoon, Murthy, and Eiumnoh 1992), using multiple regression analysis to relate two or more spectral reflectances to yields. Murthy et al. (1996) showed that grain yield of rice in Karnataka, India, can be linearly related to NDVI at the heading stage or to a time-composited version of NDVI ($r^2 = 0.77$). It is interesting to note that even NOAA-based NDVI values were suitable for estimating the yields of millet (Rasmussen 1992), cotton, maize, and rice (Quarmby et al. 1993), wheat (Barnett and Thompson 1983), and wheat, soybean, and maize (Kerdiles et al. 1995). Kerdiles et al. (1995) identified the maximum greenness stage to be the ideal time for assessing crop yield. Apparently simple yield indicators at one moment in time can correlate well with actual yield, but the selection of the moment remains critical. It would be worthwhile to globally intercompare yield (NDVI) relationships for separated and mixed crops.

Maas (1991) and Bouman (1992) obtained crop yields from remote sensing by assimilating satellite observations into plant-physiology simulation models. These models account for carbon dioxide intake, vapor release, photosynthesis, respiration, and dry matter assimilation. A simulated growth curve of LAI obtained from the crop growth model predictions can be verified through remote sensing estimates of LAI at a limited number of acquisition dates. Estimates of LAI were made at locations within Europe to investigate Europe's food production and security (Laguette, Vidal, and Vossen 1995).

Recent data collected from satellites include actual evapotranspiration to verify water-balance computations in crop growth models (e.g., Moran, Maas, and Pinter 1995; Nieuwenhuis et al. 1996). Moran, Maas, and Pinter (1995) applied an iterative procedure for a simple biomass production model. The model manipulates the initial conditions and parameters, so that they converge with remotely sensed estimates of actual evapotranspiration and LAI at several periods in the growing season. The model was tested for an irrigated alfalfa field and a rangeland watershed, both in Arizona (USA). Nieuwenhuis et al. (1996) followed a similar approach at the provincial level in southern Spain.

Because assimilation of carbon dioxide and transpiration are linked, dry matter accumulation should be a function of the actual crop transpiration and total evapotranspiration. The

classical FAO-Stewart yield model (Doorenbos and Kassam 1979) is based on this principle and assumes linearity between relative evapotranspiration and relative crop yield for closed canopies:

$$[1 - (ET_{act}/ET_{pot})]k_y = 1 - (Y_{act}/Y_{max}) \quad (22)$$

where Y_{act} and Y_{max} are actual and maximum crop yields, respectively, and k_y is the yield-response factor. Equation (22) can be used with reasonable accuracy to predict crop yield if moisture deficits are not more than 50 percent. For partial canopies, it is best to use the relative transpiration, t_{act}/t_{pot}, because soil evaporation does not provide clues on crop growth (e.g., de Wit 1958; Hanks 1974). Examples of using relative evapotranspiration for crop yield assessments are given for wheat by Idso, Jackson, et al. (1981), for cotton by Pinter et al. (1983), and for sugarcane by Vidal and Baqri (1995). The disadvantage of equation (22) in comparison with single $NDVI_{max}$ values is that it requires seasonally integrated values for ET_{act} and ET_{pot}, which in turn require a large data set of images.

Soil Conditions

Soil moisture

Because moisture controls the surface energy balance and partitioning between infiltration and surface runoff, many attempts to retrieve soil moisture data from airborne and spaceborne multispectral measurements have been reported (table 11). Among the first were approaches based on calculating instantaneous and time-integrated surface temperature arrays of the daily amplitude of surface temperature (thermal inertia), e.g., Wetzel, Atlas, and Woodward (1984). Recent attempts to convert thermal infrared measurements into soil moisture maps are based on surface resistance (Bastiaanssen, Pelgrum, Droogers, et al. 1997) or use of the evaporative fraction to assimilate soil moisture in soil-vegetation-atmosphere-transfer (SVAT) models (van den Hurk et al. 1997).

The large contrast between the dielectric constant of water (~80) and that of dry soil (3.5) produces different propagation characteristics of the electromagnetic wave in soils that have different moisture levels. For describing soil moisture under given conditions, wavelengths between 0.3 centimeter (100 GHz) and 30 centimeters (1 GHz) are the most effective.

Passive microwave techniques, using microwave radiometers, measure the naturally emitted radiation that can be expressed as microwave brightness temperature (Jackson, Schmugge, and O'Neill 1984), microwave emissivity (Wang and Schmugge 1980), or the ratio between the microwave brightness temperature and the physical surface temperature (Paloscia et al. 1993). Microwave radiometry reflects the moisture conditions in the top 10 centimeters of soil. The use of microwave emission is perturbed by surface roughness, attenuation and microwave emission by canopies, and to a lesser degree by soil texture. The potentials of passive microwave technology were reviewed recently by Choudhury et al. (1995) and Njoku and Entekhabi (1996). Airborne microwave radiometry, which has spatial resolutions of a few meters, has shown great success (Chanzy et al. 1997), but spaceborne passive microwave has

Table 11. Selected studies on the retrieval of soil moisture data with remotely operated radiometers.

Source	Spectrum[a]	Approach	Absolute error[b] (cm^3 water/cm^3 soil)
Idso et al. 1975	tir	Statistical with diurnal temperature range	–
Heilman and Moore 1980	tir	Statistical	–
Wang and Schmugge 1980	pmw	Microwave emissivity	0.0 to 0.09
Ulaby, Aslam, and Dobson 1982	amw	C-band radar	0.0 to 0.08
Bernard et al. 1982	amw	C-band radar	0.0 to 0.08
Rosenthal, Harlan, and Blanchard 1982	tir	Antecedent precipitation index	–
Wetzel, Atlas, and Woodward 1984	tir	Thermal inertia	–
Jackson, Schmugge, and O'Neill 1984	pmw	Microwave brightness temperature	0.0 to 0.17
Carlson 1986	tir	Thermal inertia	0.07 to 0.11
Schmugge, Wang, and Asrar 1988	pmw	Microwave brightness temperature	0.0 to 0.10
Choudhury and Golus 1988	vis, nir, pmw	Antecedent precipitation index	0.05
Perry and Carlson 1988	tir, amw	Thermal inertia, scattering coefficient	0.02 to 0.16
Owe, Chang, and van de Griend 1992	pmw	Microwave emissivity	0.00 to 0.10
Paloscia et al. 1993	pmw	Multifrequency passive microwave	0.00 to 0.10
Shih and Jordan 1993	tir	Statistical	0.01 to 0.08
Jackson et al. 1994	pmw	Microwave brightness temperature	0.00 to 0.06
Cognard et al. 1995	amw	Statistical	0.00 to 0.12
Dubois, van Zyl, and Engman 1995	amw	SVAT model	0.00 to 0.08
van Oevelen, Hoekman, and Feddes 1996	amw	Inverse integral equation method	0.03 to 0.08
Ottle et al. 1996	vis, nir, tir, amw	SVAT model	0.05
Bastiaanssen, Pelgrum, Droogers, et al. 1997	vis, nir, tir	Inverse surface resistance	0.00 to 0.07

[a]vis = visible, nir = near infrared, tir = thermal infrared, pmw = passive microwave, amw = active microwave.
[b]Dash indicates no information available.

spatial resolutions of a million hectares, which is too large an area for application in irrigation management.

Radar instruments, which are *active microwave* sensors, are being used more frequently because of their improved spatial resolution. Radar transmits a pulse of electromagnetic energy and then measures the backscatter. However, the sensitivity of the backscattering coefficient of the radar beam to soil moisture, leaf moisture, soil salinity, and surface roughness prevents a straightforward signal interpretation. Radar sensors are onboard the ERS, JERS, and Radarsat satellites. Van Oevelen, Hoekman, and Feddes (1996) estimated soil moisture at field scale from radar measurements supported by information on variations in soil moisture at different depths and on surface roughness, leaf water content, type of mineral, etc. Musiake et al. (1995) conducted an intercomparison study between microwave radars onboard ERS (C-band) and JERS (L-band) for determining the soil moisture of agricultural fields. They obtained a correlation coefficient of 0.93 between the two radiometers. Engman and Chauhan (1995) prepared a summary of applications using microwave remote sensing, including radiometry, to detect soil moisture. An application that operates without information on field conditions is under technical development, but more research is required before it will be feasible.

Soil salinity

Rising water tables, due to recharge from irrigation canals and watered fields, or naturally poor groundwater quality, due to rock weathering, may cause soil salinity problems. In irrigated landscapes, features indicating salinity are, in order of increasing severity, stunted crop growth, poor and patchy germination, crop stress, death of crop, encroachment of halophytic species, bare soils with efflorescence, and salt crust development. The fact that reflectance from a single leaf changes as its composition and morphology changes can be used to detect salinity effects at an early stage. Mougenot, Pouget and Epema (1993) noted that "visible reflectance of leaves from plants growing on salt-affected soils is lower than reflectance of non-salt-affected leaves before plant maturation and higher after. Near-infrared reflectance increases without water stress due to a succulent (cell thickening) effect and increases in other cases."

In general it can be remarked that bands in the near- and middle-infrared spectral bands give information on soil moisture and salinity (e.g., Mulders 1987; Agbu, Fehrenbacher, and Jansen 1990). Steven et al. (1992) confirmed this finding by showing that near- to middle-infrared indices are proper indicators for chlorosis occurring in stressed crops (normalized difference for TM bands 4 and 5). This new ratio is immune to color variations and provides an indication of leaf water potential. The work of Steven et al. (1992) showed that chlorotic canopies could be distinguished from healthy canopies. As compared with a healthy crop, the response of the biophysical parameters of a salty environment is manifested in a low fractional vegetation cover, low LAI, high albedo, low surface roughness, and high surface resistance.

Remote sensing investigations on soil salinity can be divided into (1) the delineation of salt-affected and cropped soils and (2) the distinction of mineralogy. Salinized and cropped areas can be identified with a salinity index based on greenness and brightness that describes

Table 12. Literature development on detection of soil salinity.

Source	Study area	Sensor	Methodology
Chaturvedi et al. 1983	South Dakota, USA	PMW	Brightness temperature
Mulders and Epema 1986	Tunisia	TM 5, 7	Digital classification
Menenti, Lorkeers, and Vissers 1986	Tunisia	TM 5, 6, 7, albedo	Digital classification
Everitt et al. 1988	Texas, USA	Video imagery	False-color composite
Sharma and Bhargava 1988	Uttar Pradesh, India	MSS	False-color composite
Singh and Dwivedi 1989	Uttar Pradesh, India	MSS	Supervised classification
Timmerman 1989	Qattara Depression, Egypt	TM 5, 6, albedo	Supervised classification
Singh and Srivastav 1990	Gujarat, India	PMW, C-band	Brightness temperature
Saha, Kudrat, and Bhan 1990	Uttar Pradesh, India	TM	Digital classification
Zuluaga 1990	Mendoza, Argentina	TM 4, 5, 7	Classification
Rao et al. 1991	Uttar Pradesh, India	TM 2, 3, 4	False-color composite
Steven et al. 1992	USA	TM 4, 5	Near/mid infrared difference
Wiegand, Everitt, and Richardson 1992	USA	XS	Multiple regression
Joshi and Sahai 1993	Saurashtra Coast, India	MSS, TM	False-color composite
Goossens, El Badawi, et al. 1993	Western Delta, Egypt	MSS, XS, TM	Supervised classification
Casas 1995	Tamaulipas, Mexico	XS 3, TM 5	Brightness, supervised classification
Brena, Sanvicente, and Pulido 1995	El Carrizo, Sonora, Mexico	TM 2, 3, 4	Multiple regression
Mirabile et al. 1995	Mendoza, Argentina	TM 3, 5	Kauth-Thomas index
Vincent et al. 1995	Gharb Plain, Morocco	XS 1, 2, 3	Greenness, brightness, classification tree
Vincent et al. 1996	Punjab, Pakistan	XS	Greenness, brightness, classification tree
Dwivedi 1996	Uttar Pradesh, India	MSS 1, 2, 3, 4	Principal component
Vidal et al. 1996	Punjab, Pakistan	XS	Greenness, brightness, classification tree

leaf moisture as influenced by salinity, with classical false-color composites of separated bands, or with a computer-assisted land surface classification (Kauth and Thomas 1976; Hardisky, Klemas, and Daiber 1983; Steven et al. 1992; Vincent et al. 1996).Essentially, a brightness index is meant to detect brightness appearing at high levels of salinity. The contributive power of false-color composites and visual interpretations is demonstrated in most studies from India in table 12. The unique patterns of geomorphologic shapes are thought to be helpful in discriminating the salinization process from a geometric perspective. Although the interpretation of aerial photographs is often mentioned as a suitable solution, that falls outside the scope of this review on satellite remote sensing.

Table 12 shows that TM bands 5 and 7 are frequently used to detect soil salinity or drainage anomalies (Mulders and Epema 1986; Menenti, Lorkeers, and Vissers 1986; Zuluaga 1990; Vincent et al. 1996). Apparently, the physiological status of the crop is best manifested at TM 5 and 7, while TM bands 3 and 4 are better suited to describe the overall crop development. Most of the studies in table 12 are based on MSS and TM data because SPOT and IRS have no bands in the spectral range greater than 1.7 μm. Joshi and Sahai (1993) found that TM, which had an accuracy of 90 percent for soil salinity mapping, was better than MSS (74%). Similarly, Goossens, Goossens, et al. (1993) and Goossens, El Badawi, et al. (1993) compared the accuracy of TM, MSS, and SPOT and found TM to be the superior multispectral radiometer for soil salinity mapping.

Johnston and Barson (1990) reviewed remote sensing applications in Australia. They found that discrimination of saline areas was most successful during peak vegetation growth. In other periods the low fractional vegetation cover of salinized areas could not be distinguished from areas that were bare due to overgrazing, erosion, or plowing. Siderius (1991) concluded the opposite. He found that salinity is best expressed at the end of the irrigation or rainy season when the plots are bare. Goossens, Goossens, et al. (1993) analyzed the beginning, middle, and end of the growing season in the western Nile Delta. They said that mono-temporal images are suitable for detecting severely salinized soils but that more gradations can be determined through a multitemporal approach. Along the same line, Venkataratnam (1983) used temporal MSS images of pre-monsoon, post-monsoon, and harvest seasons to map soil salinity in the Indian Punjab. He concluded that the spectral curves of highly and moderately saline soils change considerably throughout the annual cycle, which significantly complicates the time-compositing procedure.

The investigations of Vidal et al. (1996) in Morocco and Vincent et al. (1996) in Pakistan are based on a classification-tree procedure. In this procedure, the first treatment is to mask vegetation from nonvegetation using NDVI. Then the brightness index is calculated to detect the moisture and salinity status on fallow land and abandoned fields. The approach of Vincent et al. (1996) was suitable for locating blocks that had malfunctioning drainage networks. Two classes based on levels of soil salinity could be mapped with an accuracy of 70 percent. Areas of high salinity were 66 percent accurate and nonsaline areas were 80 percent accurate.

Interesting studies were conducted by Chaturvedi et al. (1983) and Singh and Srivastav (1990) using microwave brightness and thermal infrared temperatures synergistically. The interpretation of the microwave signal was done physically by means of a two-layer model with fresh and saline groundwater. Synergetic use of satellite measurements to map soil salinity physically is a new concept, and although the results were not perfect, the integration of multiple sensor data has set new directions for research on soil salinization. The physical

conditions of the surface soil can be obtained with optical and passive microwave data. Larger wavelengths (L-band, P-band) are capable of penetrating the soil and retrieving information from a soil layer rather than just from the soil surface.

Goossens, El Badawi, et al. (1993) presented an example of a contextual classifier for soil salinity mapping. They built a GIS to link the location of the irrigation feeders and drainage master canals in the western Nile Delta with digital elevation data and satellite classifications. Soil salinity risks are considered to be proportional to the distance of fields from the main irrigation canals, as well as to the fields' elevation differences with the main irrigation canals. Thematic Mapper bands 2, 3, 4, 5, 6, and 7 were used to classify three different stages of waterlogging according to a simple supervised procedure.

Although the combined GIS-remote sensing approach published by Cialella et al. (1997) for predicting soil drainage classes does not focus on soil salinity, it is methodologically worth mentioning. They studied soil drainage classes by means of a classification-tree analysis using airborne NDVI data, digital elevation data, and soil types.

Salt mineralogy

Salts remaining in solution precipitate into minerals after exceeding a threshold solute concentration. The spectral signature of salt minerals is widely studied in laboratories and under field conditions. Examples for the spectral region between 0.4 and 2.5 mm for halite, gypsum, alunite, jarosite, thenardite, borax, and calcite, and some of the crusts and efflorescences they produce are shown by Hunt (1977) and Mougenot, Pouget, and Epema (1990).

The retrieval of narrowband spectral reflectances have led to partial success in mapping different salt minerals. The reflectance of salt crusts (commonly NaCl) or puffed surfaces (Na_2SO_4) differs considerably. The surface moisture content affects the spectral signature under practical conditions (Epema 1990). Because surface moisture immediately affects the evaporation of saline soils and regulates the surface temperature, inclusion of thermal bands in the mapping of salt minerals has proved to be effective for hyper-saline areas in Tunisia, Libya, and Egypt (Menenti 1984; Menenti, Lorkeers, and Vissers 1986).

Hydrological Processes

Precipitation

Rainfall patterns are highly variable in space and time, and generally rain gauge networks in river basins and catchments do not accurately measure regional and seasonal rainfall (Rango 1990). Griffith et al. (1978) recognized the transient evolution and extent of cloud-top temperatures as a tool to infer convective activity. Dugdale and Milford (1986) developed the concept of cold cloud duration (CCD), using the thermal channel of Meteosat, to generate time series of cloud temperatures for tropical altitudes, where most rainfall comes from large convective storms. They suggested that the duration above a threshold temperature value is representative of the amount of rain that is generated. The success of the regression between CCD and rainfall varies with the threshold temperature above which rain occurs (e.g., Stewart

et al. 1995). Although there is an essential amount of empiricism included in this methodology, it helps to interpret rainfall intensities at unsampled locations between gauges in a network of rain gauges. Successful applications have been reported in Zambia (Huygen 1989), Mexico (Negri et al. 1993), the Sahel (Rosema 1990), and the Nile Basin (Attia, Andjelic, and Klohn 1995). Attia, Andjelic, and Klohn (1995) found that measurement of inflows to the High Aswan Dam and regulation of flow rates through the Nile river could be improved by monitoring rainfall-runoff processes upstream. Recent progress in rainfall estimations from thermal infrared images has been made by Hsu et al. (1997) who used neural networks to model complex nonlinear relationships between rainfall and cloud temperature. Petty (1995) summarized the current status of retrieving rainfall information from satellites.

Because microwave optical depth is substantially smaller for clouds and rain than for clear skies, radar measurement techniques offer a way to assess rainfall intensity. In an overview paper, Simmer (1996) compared three radar measurement techniques: passive high-frequency (over 60 GHz), passive low frequency, and low frequency. Passive high-frequency measurement has the advantage that interference from soil moisture levels can be ruled out. Also, absorption-emission-scattering features are better marked at higher frequencies. The spatial resolution of 30 to 50 kilometers is insufficient to detect small individual rainfall events. The rain radar can be installed at ground stations and on satellites such as the planned Tropical Rainfall Measuring Mission (TRMM). Simmer (1996) concluded, "the determination of rain rate at the surface from satellite measurements is still an unsolved problem."

Runoff

Ragan and Jackson (1980), Hawkins, Hjemfelt, and Zevenbergen (1985), and Zevenbergen et al. (1988) used a simple expression of fractional vegetation cover to account for the role of vegetation in holding hillside water and preventing water from running off. They established simple though useful relationships between curve numbers, which form a basic parameter in the rainfall-runoff model of the Soil Conservation Service (1972) and the simple ratio, SR.

Combining remotely sensed data on vegetation type and on the condition and extent of cover, using physically based models of hillside hydrology and erosion, improves the assessment of erosion risk for arid lands under different management options. For instance Sharma et al. (1996) used the SWAMREG transient one dimensional finite-difference model to describe the partitioning of precipitation among surface runoff, soil moisture storage, and deep percolation. Thematic Mapper data have been used by Sharma et al. (1996) to define fractional vegetation cover geographically, and these data were linked to a digital elevation model. Also Schultz (1993) has been successful in using remote sensing data to improve descriptions of catchment runoff and other hydrological processes.

River discharge

Imhoff et al. (1987) mapped flood boundaries along the lower Ganges River by using L-band radar data in association with Landsat MSS data. More recently, spaceborne altimeters were used to estimate river levels, which are extremely useful for assessing river discharges (e.g., Koblinsky et al. 1993). An interesting example of using 37 GHz passive microwave data from

Nimbus 7 to evaluate river drainage within the Amazon basin was presented by Vorosmarty et al. (1996). They linked differences between horizontally and vertically polarized brightness temperatures at 37 GHz with the dimensions of the riverbed carrying water as a direct expression of river discharge on a monthly time scale. Statistical predictions based on remote sensing were compared against forecasts of a calibrated water-balance and transport model that uses on-ground meteorological data, giving good results.

Preferred Methodologies

The literature reviewed in this chapter reflects the overall scientific achievements made by physicists, statisticians, biophysicists, and agronomists in remote sensing for irrigated agriculture. *Remote sensing clearly is more than an option for clarifying land-use patterns.* Certain algorithms can be recommended for describing irrigation processes on a regional scale. But the feasibility of routinely transferring surface spectral radiances into composites, biophysical parameters, and irrigation conditions (fig. 1) is constrained by

- the degree of empiricism involved in the remote sensing algorithms posed
- the need for field surveys and collecting ancillary hydrometeorological field data
- the need to involve physico-mathematical simulation models
- the small number of reported applications and validations

Composites of spectral information

Spectral at-surface radiances are the basis for recognizing thematic land classes (table 13). In arid climates, irrigation intensities or cultivated areas can be mapped straightforwardly on the basis of time profiles of fractional vegetation cover, which do not require field data from prescribed sites. The methodology is not self-evident for humid climates although there have been some successful studies. In humid climates, longer time series of fractional vegetation cover must be used to improve the delineation of irrigated land from surrounding perennial vegetation. Accuracy can be improved through the inclusion of synthetic amperature radar data and using a supervised classification, but the disadvantage is that training sets have to be allocated.

Classification of irrigated crops in developing countries that are characterized by small fields (under 0.5 ha) varying in soil wetness, soil salinity, and crop development is complex. Table 13 summarizes the possibilities for classifying various object classes. Ground truth is imperative for upgrading information from spectral radiances to crop types or land cover. The use of finer spatial resolutions (such as the 20 m resolution of SPOT) yields more local variances of spectral radiances. Although a large number of variances may allow more thematic classes to be distinguished, that does not always lead to greater classification accuracy. The growth of GIS has greatly enhanced opportunities for integrating conventional data with re-

Table 13. Derivations of object classes from remote sensing that are useful for irrigation management.

Object classes	Accuracy	Need for field data	Preferred principle
Cartography	high	none	Panchromatic images
Irrigated area	high	none	SAVI time series
Mono-crop types	good	high	Hybrid, multitemporal, contextual, ancillary
Multiple crop types	moderate	high	Hybrid, multitemporal, contextual, ancillary
Crop communities	moderate	high	Hybrid, multitemporal, contextual, ancillary
Land cover and use	good	moderate	SAVI time series, unsupervised classification

mote sensing data and for developing digital expert systems that incorporate mathematical functions.

Based on the literature reviewed in this publication, the transferability of methods seems limited. Hence, a general guideline for classifying cropping patterns, crop communities, land cover, and land use cannot be given. As an alternative, a set of potentially successful ingredients can be suggested:

- ground truth on crop types across the entire classification domain
- multitemporal, high resolution images
- at least 15 pixels per field
- hybrid classifications that are based on unsupervised and supervised classifications
- GIS-based aerial and contextual classifiers
- spectral bands in the near-infrared, middle-infrared, and microwave spectral range
- definition of fuzzy classes for conditions with variable cultivation practices

Whether these ingredients improve the accuracy of discerning and mapping land classes can only be judged afterwards by employing sound criteria such as kappa statistics or normalized classification indicators.

Biophysical parameters

Various stress agents, such as soil moisture, solutes, and nutrients can delay crop development, which affects the crop biophysical parameters. Vegetation indices are indicative of biophysical parameters, but the drawbacks of empiricism due to biome type, architecture, composition, and senescence stage should not be underestimated. The literature favors SAVI, TSAVI, and WDVI as the best indicators for describing LAI (e.g., Bausch 1993), though no

general rule can be set because of the dependence on leaf orientation angle. If no auxiliary field data on LAI are available, then the numerous investigations done on relationship between LAI and SAVI for various crops (table 6) could be used. Applications of equation (4) reveal a general relationship that, for some major crops, implies an error of 10 to 30 percent. The large number of investigations that have been made on the relationship of PAR to NDVI and of k_c to SAVI suggest that NDVI should be favored for calculating PAR and that SAVI should be favored for calculating crop coefficients. The crop coefficients in table 14 are considered moderately accurate because they are validated on a small scale (with lysimeters) but applied on a large scale (command areas).

The use of remote sensing data in crop growth models is an attractive concept because it improves estimates of actual crop yield. Simplified relationships between NDVI, at the heading stage, and final crop growth can also be obtained with simple crop growth models. In the absence of such models or adequate input data, simplified statistical relationships have to be found. It is practical to integrate NDVI over time, although single NDVI scenes have been useful.

It should be noted that selection of a vegetation index to obtain biophysical parameters is to a certain degree redundant because field measurements have proven that most vegetation indices exhibit a similar spatial behavior (e.g., Bausch 1993; van Leeuwen et al. 1997). For this reason, SAVI should be considered the best indicator of crop biophysical parameters for irrigation management.

Table 14. Derivations of biophysical parameters from remote sensing that are useful for irrigation management.

Biophysical parameter	Accuracy	Need for field data	Preferred principle
Fractional vegetation cover	high	none	SAVI, eq. (1)
LAI	good	none	SAVI, eq. (4)
PAR	good	none	NDVI
Surface roughness momentum	high	none	Laser-altimeter
Surface roughness heat	low	high	Unresolved
Surface albedo	good	low	Two-way transmittance, eq. (6)
Thermal infrared surface emissivity	good	none	Valor and Caselles (1996)
Surface temperature	good	low	Eq. (8) or single-way effective transmittance
Surface resistance	good	none	Eq. (14)
Crop coefficients: tabulated	moderate	none	SAVI
Crop coefficients: analytical	moderate	high	LAI, albedo, roughness, displacement, minimum surface resistance
Transpiration coefficients	good	none	Eq. (21)

Accuracy levels for surface albedo (absolute error: 0.03), thermal infrared surface emissivity (absolute error: 0.01), and surface temperature (absolute error: 2 K) have improved

considerably due to the research attention these surface radiation parameters have received over the last 15 years. Microwave techniques, although airborne, appear to have physically better prospects for identifying surface roughness than optical measurements that are associated with empirical relationships. Research using microwave data from C-band SAR on ERS, L-band SAR on JERS, and MOS on IRS should be pursued for determining surface roughness for momentum transport. The roughness for heat transport seems impossible to quantify.

Irrigation conditions

The close dependence of surface temperature on latent heat flux makes thermal remote sensing a suitable method for estimating actual evapotranspiration. The SEBAL algorithm does not need land-use maps and ancillary micrometeorological ground data. Because it can be applied with both TM and AVHRR images and has been thoroughly tested for center pivot systems, sprinkler systems, and surface irrigation systems, it should be considered a robust algorithm.

A classical way to circumvent the need to solve for the surface energy balance completely is to quantify crop stress indicators. The disadvantage is that evapotranspiration is not expressed qualitatively in planning and performance studies. Use of the water-stress index, equation (18), relies on linear interpolations between the four corners of the trapezoid formed by SAVI and $T_0 - T_{air}$. The WDI algorithm seems to be more rigorously tested than other algorithms, although it requires an automatic weather station to gather the data needed.

Methods for using remote sensing data to derive soil moisture for irrigation scheduling are in their infancy. Remote sensing estimates of the water content of the surface soil are feasible from airborne passive microwaves, but the root zone of some crops is 1 to 2 meters deep. Because topsoil moisture content cannot be straightforwardly linked to moisture deeper in the profile, root-zone soil water content cannot be obtained from present remote sensing techniques. However, water allocation decisions can be made from crop water-stress indicators (which ultimately reflect the moisture conditions of the root zone), which are perhaps even more suitable than indicators related to soil moisture. Information on topsoil moisture and on LAI, acquired at the same time, should be recognized as suitable parameters for partitioning actual evapotranspiration into actual evaporation and actual transpiration for field conditions. The combined use of reflective, thermal, and microwave sensors appears to be promising for assessing soil moisture from satellites, although not much research has been done.

State-of-the-art salinity mapping allows saline areas to be separated from nonsalinized areas. The soil dielectric constant varies with soil salinity in addition to soil moisture, which implies that P-band microwave measurements with longer wavelengths should indicate the salinity status of the subsurface. Most authors were able to distinguish only two or three classes of soil salinity, even after consulting geomorphologic or soil degradation maps or conducting conventional laborious field surveys. Current sensors and interpretation algorithms do not allow the detection of intermediate to medium salinity levels. Remote sensing is merely a spatial extrapolation technique for soil salinity rather than being an early detection system.

Precipitation and runoff need to be considered when catchments are taken as an appropriate scale for water management. Increasingly, precipitation studies use spaceborne and ground-based remote sensing data to estimate area-integrated precipitation. To compute cold cloud duration, most current studies utilize thermal infrared time series from the geostation-

ary satellites Meteosat, GMS, and GOES. Although spaceborne rainfall radars such as TRMM seem to be more accurate, they are costly. Surface runoff predictions can only be made through simple empirical models or more mechanistic ones in combination with remotely sensed data. The management of a particular watershed does not necessarily require a complex deterministic model if a parametric model with information on land cover and vegetation density based on remote sensing can suffice. The accumulated surface runoff brings together river discharge, which, if the river mouth is sufficiently wide, is manifested as a difference between horizontally and vertically polarized brightness temperature.

Selection of Images

Satellites are the only sure means of obtaining consistent, routine data sets on irrigation conditions. A renewed look at irrigation management is required to maximize the extractable information from multispectral measurements. The selection of satellite images differs from application to application, so a general guideline cannot be given. The spectral requirements of certain applications depend on the methods and algorithms employed.

The high spatial resolution of SPOT (10 m) and IRS-1C (5.8 m) in the panchromatic band makes them potentially attractive for retrieving information on irrigation and drainage infrastructure. This capability is significant because large areas in developing countries are not mapped at a scale of 1:50,000 or smaller. To use satellite images in real time for concurrent monitoring would require fast delivery of multispectral measurements. However, in practice, the long turn-around time for image delivery limits the use of high resolution images to the onset, middle, and end of the irrigation season. They can, together with Thematic Mapper images, be used for crop identification and for crop yield assessments. Now that Wide Field Sensor (WiFS) data are available every 5 days from IRS-1C, it will be easier to satisfy irrigation engineers' desire for concurrent agronomic monitoring. Evapotranspiration and crop water-stress algorithms have shown promise for use in scheduling irrigation of fields that have partially or fully closed canopies. At present this can only be done with high spatial precision by using the thermal bands of Thematic Mapper.

The availability of daily AVHRR images at most national meteorological institutions should be explored to create time composites of fractional vegetation cover, leaf area index, relative evapotranspiration (evaporative fraction, surface resistance), and actual evapotranspiration on a weekly or 10-day basis.

3.

Prospective Applications of Remote Sensing in Irrigated River Basins

THIS CHAPTER DEALS with the application of technical advances in remote sensing research to improve water resources management. There are a number of potential areas of application for which at least a minimum list of parameters can be assessed with a good or high accuracy.

One group of applications relates to typical irrigation management issues such as the planning of water allocation and the performance of irrigation and drainage systems. The productivity of water (crop yield per unit of water consumed) is the critical measure of management successes. A second group of applications concerns irrigated agriculture in the context of catchment hydrology and water flow through basins. This group is dealt with separately to emphasize that remote sensing data can contribute the analysis of hydrological processes in general. Such analysis is essential for improving knowledge of spatio-temporal variation in water availability on a regional scale. A third group of applications connects environment and health to irrigation, recognizing that greater water availability, which enhances crop growth and increases land wetness, changes the environment and that such environmental changes may alter the impact of insects and disease. Finally, based on the data needs of irrigation managers and on the number of land surface parameters whose accuracy remains low to moderate, priorities for future basic and applied research can be suggested.

Irrigation Management

Irrigation tightens the intimate relationship of people (farmers, gatekeepers, water policy makers), crops (irrigated areas, crop type, LAI development, yield), and water issues (crop water needs, crop water use, land wetness, waterlogging). The practical value of remote sensing for retrieving information about these complex and spatially distributed topics varies with the type of application and the algorithm selected. Tables 13 and 14 list a number of practical remote sensing research approaches—those indicated to have good to high accuracy—which can be advantageously used by individuals engaged in irrigation planning and monitoring or in watershed management.

The potential usefulness of selected remote sensing applications for day-to-day and season-to-season management of water resources in large irrigation schemes is summarized in table 15. Table 15 relates to the fifth hierarchical order in figure 1, where the retrieval of

managerial information for irrigation schemes is described. Specific biophysical crop parameters (fourth hierarchical order) are no longer elaborated at this level but are part of the derivation of the irrigation conditions.

Concurrent and seasonal irrigation water allocation

Proper hydraulic design of canals is based on the peak flow necessary to meet all or a certain fraction of the crop water requirements. Computations of the maximum discharge, seasonal water allocation, and water delivery per rotation interval all rely on information on the area irrigated, on the type of crop, and ideally on crop water demands that prevent crop water stress from occurring. But irrigation departments' records on irrigated areas can deviate substantially from the real situation because water and land use are constantly changing. Also, the usefulness of records is diminished when staggered plantings result in blocks or fields that are in different crop development phases and require different water amounts and when farmers alter their cropping patterns over time.

Table 15. Water management information that can be derived from remote sensing data.

Parameter	Accuracy	Need for field data	Preferred principle
Precipitation	moderate	high	Cold cloud duration and rain gauge network
Surface runoff	low	high	Curve number method
River discharge	low	high	Polarization differences, altimetry
Potential evapotranspiration	moderate	low	Two-step Penman-Monteith equation with crop coefficient
Potential evapotranspiration	moderate	low	One-step Penman-Monteith equation
Potential evapotranspiration	good	low	Radiation type of expression
Potential transpiration	moderate	low	Transpiration coefficients
Potential evaporation	moderate	low	Difference between potential evapotranspiration and potential transpiration
Actual evapotranspiration	high	low	SEBAL algorithm
Actual transpiration	low	moderate	LAI, transpiration coefficient, and SAR
Actual evaporation	low	moderate	Difference between actual evapotranspiration and actual transpiration
Crop stress indicators	good	low	Water deficit index
Crop yield	good	moderate	NDVI at heading stage
Relative yield	moderate	low	Time-integrated relative transpiration
Topsoil moisture	moderate	moderate	C-, L-band radar
Root-zone moisture	low	high	Inverse surface resistance and LAI
Soil salinity	low	high	vis, nir, tir, mw synergy
Salt minerals	low	high	Hyperspectrometry

Remote sensing applications can improve water delivery in a wide range of irrigation systems. In rigid distribution systems, pre-season planning can be based on interpretations of remotely sensed water distribution data from the preceding season combined with the recorded deviations between actual and intended water supply. In flexible systems, remote sensing information should facilitate adjusting water distribution from rotation to rotation, and on-demand systems should be able to respond immediately.

Wolters, Zevenbergen, and Bos (1991) stated that satellite remote sensing cannot be effectively utilized for the operation of irrigation systems. They said the low frequency of high resolution images was incompatible with the flexibility that canal operations require. No doubt their conclusion holds for rigid water distribution systems. But systems that are able to direct distribution swiftly, such as in the Greater Mae Klong system in Thailand (Sriramany and Murthy 1996), have the capability for immediately mitigating crop stress or waterlogging problems that have been spotted by the satellite eye. AVHRR images have a daily coverage, and this information is available in real time at almost no cost. Costly, high resolution Landsat, SPOT, and IRS images acquired on a few occasions during the growing season are better devoted to assessing irrigated areas, cropping intensities, and crop types and making early predictions of crop yield. Table 16 relates potentially useful applications to the sensors that provide the most suitable data. Research published over the last 15 years has shown that some sensors may be more suitable than others, depending on the application.

Irrigation performance

Because productivity per unit of water is the focal point for evaluation of irrigation management, regional yield data must be linked to regional consumptive use of water. The advantage of using remote sensing determinants is that they are based on standard international diagnostic techniques and that time-series measurements can be obtained from repetitive satellite coverage.

Knowledge of the performance indicators within and among irrigation schemes can help policy makers and managers wisely allocate funds for interventions and rehabilitation. As water losses attract growing public concern, means to raise irrigation efficiencies will receive increasing attention. A framework of standardized performance indicators, such as those in table 17, are required. Because geometric patterns of the pixel-based performance indicators can be identified, actual water distribution patterns can be studied, especially when the spatial structure is linked to the conveyance network through a GIS environment that allows canal distances to be computed.

Drainage performance

Particularly in arid and semi-arid climatic conditions, many irrigated fields have, or are in need of, surface and subsurface drainage systems. Besides discharging excess water, drainage systems remove salts from the root zone. Because drainage systems have high construction costs and quickly deteriorate if not well maintained, their functioning needs to be monitored. A drainage system performs well if the water table dynamics, soil moisture, and soil salinity remain within a pre-defined range. Build-ups of water and salts should be prevented.

Table 16. Sensors or satellites[a] that produce images suitable for irrigation management.

Purpose	SPOT	IRS	TM	MSS	AVHRR	ERS-SAR	Radarsat	ERS-ALT	ATSR	Meteosat	GOES	GMS	JERS-SAR
Cartographic information	●	●											
Irrigated area	●	●	●	●	●								
Cropping pattern		●	●			●	●						●
Land cover			●	●	●								
Leaf area index	●	●	●	●	●								
Crop coefficient	●	●	●	●									
Transpiration coefficient	●	●	●	●	●								
Surface roughness						●		●					●
Crop yield	●	●	●	●	●								
Potential evapotranspiration			●		●				●	●	●	●	
Actual evapotranspiration			●		●				●				
Surface moisture						●	●						●
Root-zone moisture			●		●				●				
Soil salinity			●			●							●
Water logging	●	●	●	●		●							●
River discharge						●		●					●
Precipitation										●	●	●	

[a]See Annex 2.

Table 17. Performance indicators derived from remote sensing algorithms (supplemented by needed ground data).

Indicator[a]	Remote sensing derived parameters					
	Area irrigated	Crop area	Crop yield	Water needs	Water use	LAI
Irrigation intensity	●					
Crop yield/irrigated area	●	●	●			
Annual yield/irrigated area	●	●	●			
Yield/water supplied	●	●	●			
Yield/water evapotranspired (ET_{act})	●	●	●		●	
Yield/water transpired (t_{act})	●	●	●		●	●
Water supply/actual evapotranspiration (ET_{act})	●				●	
Water supply/actual transpiration (t_{act})	●				●	●
Relative water supply (total supply/ET_{pot})	●			●		
Relative irrigation supply (irrigation supply/[ET_{pot} – rainfall])	●			●		●
Field moisture deficit (ET_{act}/ET_{pot})		●			●	●
Crop stress (t_{act}/t_{pot})	●			●	●	●
Consumed fraction (ET_{act}/total surface and subsurface inflow)	●				●	●
Relative yield (crop yield relative to ET_{act}/ET_{pot})	●		●	●	●	●

[a]Amended from the classical definitions in IIMI's list of minimum performance indicators (Perry 1996) to permit use of remote sensing data.

Because the water table cannot be detected from satellite observations, the best integrative environmental indicators currently are crop stress (t_{act}/t_{pot}) and field moisture deficit (ET_{act}/ET_{pot}). Shibayama et al. (1993) showed that the drainage performance of paddy fields could also be monitored with near-infrared and middle-infrared reflectance measurements. The derivative of the canopy reflectance at 960 nm detects more pronounced water-stress conditions than the traditional vegetation indices do.

If field moisture deficits and surface resistance (r_s) fall outside an optimal range, explanations must be found. Shallow water tables exhibit an increase in surface moisture, which can be detected from visible reflectance and microwave emissivity. Salinization affects the leaf angle orientation (leaf roll) and increases chlorosis, both of which are best observed in the near-infrared and middle-infrared bands. The final stage of soil salinization results in increased brightness, which is detectable from the visible part of the spectrum (LAI = 0, albedo high).

Uniformity in water consumption

Pixel-by-pixel quantification of the performance indicators in table 17 will permit more uniform analysis of irrigation performance. Bastiaanssen, van der Wal, and Visser (1996) investigated the uniformity of water consumption (latent heat flux) and field moisture deficits (evaporative fraction) in the Nile Delta using Landsat TM data. Nonuniform consumptive use of water is an indication of spatial variations in irrigation water supply if the contributions from rainfall and groundwater to evapotranspiration are irrelevant or evenly distributed. The uniformity of Egyptian irrigation districts was determined with remotely estimated data, and a coefficient of variation of 0.10 was found. That was only slightly smaller than the variation within irrigation districts (cv = 0.15), which is unexpectedly small, because farmers rotate canal water among their fields. This example of surveying and analyzing irrigation water rotations shows the power of remote sensing for studies of actual farm management practices.

Field moisture deficit is another irrigation performance indicator. Farm plots that have received sufficient irrigation water do not exhibit field moisture deficit. In their Nile Delta study, Bastiaanssen, van der Wal, and Visser (1996) analyzed the evaporative fraction for the gross area (including homesteads), the conveyance network, and built-up areas. They found that in 48 out of 53 irrigation districts, the evaporative fraction exceeded 0.75, which implies that the evaporation for cultivated fields is even higher. The uniformity of the evaporative fraction (cv = 0.10) and its high value reveals that Egyptian irrigation practices prevent the soil matrix from suffering any serious moisture deficits. The absence of moisture deficits can only be achieved by supplementary irrigation with ground and drainage water.

Uniformity of yield

Crop yields reflect the net result of administered irrigation water supply and the farmer's skill in adjusting to environmental and canal supply conditions. Besides being important for measuring yield per unit of water, crop yield is indicative of ambient factors (rainfall, seepage, and soil salinity), farmer skills, and market mechanisms. In a remote sensing study in Haryana, India, Thiruvengadachari, Murthy, and Raju (1997) demonstrated that the yield of wheat di-

minished when smaller areas of wheat were sown. Apparently, farmers avoid wheat cultivation if the yield becomes controlled by prevailing hydrological conditions (e.g. seepage, groundwater quality), and they sow less wheat when wheat growing conditions are poor. When growing conditions are favorable, with sufficient rainfall, irrigation water, or nonpolluted groundwater, all farmers tend to grow wheat. Yield can also reflect the farmer's socioeconomic environment, such as favorable cost-benefit ratios.

Water use legislation

Some countries are experiencing water crises and others soon will (Seckler et al. 1998). The exploitation of fresh water should be done with utmost care. It is common to allocate irrigation water on the basis of water rights: when a farmer or landowner acquires irrigated land, he acquires the right to receive irrigation water, as well. This system can be undermined by illegal removal of water from irrigation canals or withdrawal of groundwater through tubewells. If remote sensing measurements of fractional vegetation cover are combined with a geographic database on water rights, legal and illegal irrigation practices can be detected. Water charges can be paid in proportion to the total irrigated area, and variations within crop types can be verified with remote observations. Where governments enforce laws that forbid the growing of crops that have high water demands (sugarcane and rice, for example, require significantly more water than wheat and maize), measurements of fractional vegetation cover and crop types can help to verify officially reported land areas. In areas where, to prevent mining of aquifer systems, farmers pay for a certain quantum of water, estimations of accumulated evapotranspiration made by remote sensing over a growing season can be used to control the permitted groundwater extractions.

Project impact assessment

Construction and rehabilitation of irrigation and drainage projects are costly, but their impact on crop yield, water table control, or other environmental parameters is not always measurable. To evaluate the impact of these projects, irrigation conditions (table 15) must be compared before and long after a project is completed. Archived satellite data allow long, continuous time series on irrigation conditions to be assembled. From these sequences, an environmental monitoring system can be created. AVHRR time series go back as far as 1981. Inspection of changes in irrigation intensity, crop yield, crop water stress, field moisture deficit, and consumed fraction can be highly relevant for assessing the impact of certain projects. Many project donors now demand environmental impact assessments before a project begins. This requires a thorough and quickly executed regional study. Remote sensing measurements can be an essential component of such an assessment.

Selection of pilot areas

Pilot areas are often established to prove the effects of specific land and water management interventions on crop yield and land degradation before the interventions are introduced on a large scale. The successful use of pilot areas requires that the selected areas be representative

of a wider region. Remote sensing determinants of regional irrigation conditions can help to identify and select fields that represent average values for crop physical parameters such as fractional vegetation cover, LAI, and surface resistance.

Water Basin Management

Delineation of agroecological zones

Oftentimes, centrally made irrigation decisions control water management practices with little attention to different environmental needs. When there is competition for scarce water, water resources have to be distributed among competing sectors in an equitable manner. Managers should consider different water allocations for agroecologically different areas within a water basin. The first step is identification of agroecologically homogeneous units.

Regional vegetation dynamics within Karnataka State in India were described by Thiruvengadachari and Gopalkrishna (1995) using multi-year NDVI time profiles. They found a group of 10 characteristic profiles and matched administrative units (*tahsils*) to the grouped vegetation zones. Because vegetation reflects climate, compatible vegetation zones can be used to delineate agroclimatological and agroecological zones. In Thiruvengadachari and Gopalkrishna 1995, NDVI behavior corresponded with growing periods, phytophenological variables, rainfall patterns, and biomass development.

Menenti et al. (1993), Verhoef, Menenti, and Azzali (1996), and Azzali and Menenti (1996) also found that NDVI dynamics reveal agroecologically different classes. They studied long-term time series of NDVI, based on AVHRR-GAC data (7.8 km spatial resolution), and expressed long-term climatological trends of vegetation dynamics in Fourier components. This method compressed long data arrays into a few numbers. A classification of iso-growth zones was made for South America, South Africa, and Western Europe, using the annual mean NDVI and the amplitudes in NDVI at frequencies of 6 and 12 months.

Maselli et al. (1996) used monthly maximum NDVI and surface temperatures from AVHRR to divide Tuscany (Italy) into agroecological zones. Using 2 years of continuous observations, they subdivided the water basin into 10 agroecological zones.

River basin efficiency

Water is not necessarily lost if it leaves an irrigated field plot without being taken up by the crop. Leaking water may traverse into the groundwater system and be pumped up again by downstream or tail-end farmers who are short of canal water. Water-balance components can deviate considerably within a larger system where leakage and seepage zones exists. One method for appraising "beneficial losses" in an irrigation scheme is to estimate the contribution that groundwater makes to the actual evapotranspiration. Roerink et al. (1997) compared daily actual evapotranspiration rates obtained from remote sensing (SEBAL algorithm) with canal water supply rates for the Tunuyan River Basin in Mendoza Province, Argentina. They concluded that actual evapotranspiration exceeded the canal water supply by 15 percent on average. Because canal water is not effectively utilized at 100 percent, the real groundwater

contribution to evapotranspiration must be more than 15 percent. At a tertiary unit efficiency of 70 percent and a groundwater contribution of 40 percent, evapotranspiration becomes 15 percent more than the surface water contribution. Hence, by combining canal discharge measurements with estimates of evapotranspiration from remote sensing, the contribution of groundwater to crop water use can be assessed, if rainfall is eliminated.

Hydrological basin models

Models of large catchments, drainage basins, watersheds, and water basins are constantly under development for diverse applications:

- hydrological responses at catchment scale (e.g., Abbott et al. 1986)
- rainfall runoff and drainage studies (e.g., Beven, Wood, and Sivapalan 1988)
- erosion and sediment transport (e.g., de Roo 1996)
- river-discharge predictions (e.g., Vorosmarty et al. 1996)
- large-scale land-atmosphere interactions (e.g., Kite, Dalton, and Dion 1994)
- environmental impact assessments (e.g., Arnold and Williams 1987)
- planning irrigation water allocation (e.g., Schuurmans and Pichel 1996)
- ecological responses to land and water resources management (e.g., Hatton, Pierce, and Walker 1993)
- reservoir operation (e.g., Attia, Andjelic, and Klohn 1995).

These models have different degrees of complexity, and all need spatially distributed biophysical and hydrological input parameters (Rango et al. 1983). Beven and Fisher (1996) recognized that remotely sensed soil moisture, evapotranspiration, and snow cover estimates are necessary for scaling the hydrological processes in hydrological basin models. Wood et al. (1993) gave an example of using surface soil moisture estimates from passive and active microwave measurements to meet the regional data demand in infiltration and overland-flow modeling. Wood and Lakshmi (1993) used NDVI values based on Thematic Mapper data to describe patterns and density in vegetation development. Kite and Kouwen (1992) used Thematic Mapper data to discern land-cover classes, and then they applied a hydrological model to each land-cover class to predict the hydrograph of a larger watershed. Ustin et al. (1996) used a Thematic Mapper image to estimate peak summer LAI, density of vegetation, and fractional vegetation cover and to classify the type of ecosystem.

Environment and Health

Environment

Lambin and Ehrlich (1996) worked out a methodology to detect land-cover zones over the African continent and traced changes in the zones over a 10-year period. They used a seasonal time trajectory of different biome types in the NDVI-temperature space. The inverse tangent of the ratio of surface temperature to NDVI was used to describe yearly variabilities in environmental conditions from areas where irregularities occurred. The variability relates to changes in environmental conditions.

Joseph (1997) studied the environmental impact of the Indira Gandhi Canal in Rajasthan, India, with multi-date IRS LISS II and NOAA-AVHRR data. By comparing images from October 1975 against the images from October 1995, changes in cropped and waterlogged areas were detected. The waterlogged areas were recognized from reflectance in the visible part of the spectrum.

Health

Because environmental information can be partially obtained from satellite technologies, there is a growing appreciation by veterinary epidemiologists of remote sensing to help control diseases. The larval habitats of *Anopheles albimanus* and other vectors of malaria are associated with certain environmental conditions such as surface temperature, vapor pressure deficits, land types (marshes, river margins, herbaceous wetlands), and soil moisture conditions. For instance Rejmankova et al. (1995) used SPOT images to delineate land-cover classes with an unsupervised classification technique (82% accuracy) to survey outdoor aggregations of mosquitoes. Their study indicated that 89 percent of the predictions of increased risk was due to proximity to herbaceous wetlands. Rogers (1991) describes the application of remote sensing to detect environments with trypanosomes, which cause sleeping sickness in man and trypanosomiasis in domestic animals. The distribution and abundance of the tsetse fly, the vector of trypanosomiasis, is essential to explain livestock mortality rates, which correlated with mean monthly NDVI values in a transect of approximately 700 kilometers across a range of eco-climatic conditions in West Africa. The author made a plea for further exploration of NOAA data as a means to combat tropical diseases. Shutko (1991) summarized the capabilities of microwave radiometry for determining soil moisture variations, vegetation biomass, object temperature, and salinity of open water or soil in order to help identify general habitat conditions. Applications of cold cloud duration techniques for assessing patterns of rainfall are complementary to sparser ground observations. These techniques, mentioned by Thomson et al. (1996), have been used to help monitor patterns of malaria transmission, predict epidemics, and plan control strategies. Time profiles of surface temperature, field moisture deficit (evaporative fraction), and surface resistance (absolute soil moisture) indicate wet and cold regions. Application studies in this area should be pursued.

Basic Research Needs

Based on the data needs of irrigation managers and the present low to moderate accuracies of remotely sensed measurements of land surface parameters, priorities for future basic research can be set. They include the analysis of potential evapotranspiration, surface and deep soil moisture, and soil salinity.

Potential evapotranspiration

The energy-balance combination equations of the Penman-Monteith type (Penman 1948; Monteith 1965; Allen et al. 1995), require, besides crop-dependent radiation information, data on aerodynamics, such as surface roughness and displacement height, and minimum surface resistance to evapotranspiration. Crop coefficients (k_c) adjust for all these effects through a single phenological correction factor, which after being linked to "standardized" meteorological data, can be applied to obtain crop-specific potential evapotranspiration.

The number of remote sensing applications describing k_c is growing (e.g., Bausch 1995). However, crop coefficients at the regional scale have not yet been physically confirmed. That confirmation is needed because ET_{pot} estimates for heterogeneous regional land surfaces comprising different crops and crop development stages are not straightforward. Moreover, each time the definition of reference crop has undergone biophysical changes, k_c values should have been updated but were not. Data from new field measurement techniques (eddy correlation and scintillometer devices) have exposed physical inconsistencies in energy balances when tabulated crop coefficients for different crops were applied at horizontal scales of about 1 or 2 kilometers (Stewart et al., 1995). Simple ET_{ref} models, described by Makkink (1957), Priestley and Taylor (1972), and Hargreaves and Samani (1985), demonstrated that net available energy ($R_n - G_0$) is easier to implement in heterogeneous irrigated landscapes because such models do not depend on crop parameters (surface roughness, displacement height, and minimum surface resistance to evapotranspiration). However, the validity of this more simplified and robust approach on a regional scale has not been widely tested experimentally and physically. Therefore understanding of evapotranspiration in nonhomogeneous terrain is still unsatisfactory. Basic research requires one-dimensional or three-dimensional coupled PBL-SVAT models to explore feedback mechanisms between moisture in soil and atmosphere and to test the implication of using either energy-balance combination equations or the simple radiation-based formulations of ET_{pot}.

Surface and deep soil moisture

Most remote sensing studies on soil moisture have been directed toward bare soil and very sparse canopy conditions. The progress with high resolution airborne microwave radiometry is encouraging, but the spatial resolution of 50 kilometers with current spaceborne sensors is far from adequate. MERIS on Envisat, which has a microwave radiometer with a resolution of 300 meters, is only 2 years away from operational observations. Continuing basic radar research with spatial resolutions on the order of 10 to 25 meters will be productive because improved sensors (ASAR on Envisat, ESTAR on EOS) will be launched in the near future.

These SAR systems provide measurements at different frequencies with both horizontal and vertical polarization. A synergistic use of SAR with scatterometers, microwave emissivity, and surface resistance obtained from inverse expressions for latent heat transfer (equation [14]) may be a better basis for overcoming the shortcomings of individual spectral regions used in isolation.

Soil salinity

The development of soil and crop salinity indices should be based on multiple wavelengths in the visible, near-infrared, thermal-infrared, and microwave range. The new generation of satellite-borne, multiangle spectrometers that have high spectral resolution, such as MODIS on EOS-AM and PRISM on Envisat, can provide a wealth of new data in the visible and infrared spectral ranges. AVIRIS, TIMS, and ASAS, which are airborne prototypes of these sensors, have shown that new insights into soil salinity will soon be possible with systems on spacecraft.

Applied Research Needs

Some research topics that are well understood within the scientific community have never been applied or demanded by end users such as irrigation engineers. Applied research is therefore needed to make certain remote sensing methodologies and algorithms are well suited for the conditions encountered in irrigated areas—small fields, sparse canopies, and variable moisture in space and soil.

Thematic land classes

Although research on pattern recognition of thematic land classes is never-ending and generic solutions are hard to formulate, applied research related to object identification in small-scale irrigation practices remains necessary. The IRS images that have high spatial resolution should be further integrated with the spectrally attractive Thematic Mapper data; breakthroughs are expected after the arrival of MODIS data. The cloud penetration capabilities of radar images and the fine resolutions of ERS-SAR and Envisat-ASAR should be more thoroughly explored. Advances in the development of pattern recognition and classification of irrigated terrain can be achieved by making better use of fuzzy-set and neural network classifiers in association with hybrids of supervised and unsupervised statistical procedures. The added value of knowledge-based classifications using GIS (cadastral farm lots, tertiary unit boundaries, canal layout) are worth attention.

Intercomparison studies

The description of the effect of interferences caused by atmospheric water vapor, aerosols, ozone, and carbon dioxide on reflected and emitted spectral radiance is an important step in

the interpretation of signals registered from satellites. Atmospheric corrections with different degrees of complexity have been developed, tested, and widely described in the literature. It would be worthwhile to intercompare a short list of these procedures and algorithms. The ones compared should require a minimum of ground data (e.g., Moran et al. 1992; Perry and Moran 1994) and should be suitable for acquiring information on irrigation conditions without complex atmospheric measurements.

Abundant literature exists on the correlation between yield and vegetation indices for specific crops grown in various locations. An intercomparison of the regression curves found for identical crops grown under different physiographic and atmospheric conditions would be highly useful. Their general value can be appraised by merging data points from different experiments and analyzing the variances. Single and time-composited vegetation indices (NDVI, SAVI, TSARVI) should be incorporated in these intercomparison studies.

Semi-empirical models relating the difference between near-noon surface and air temperatures to daily evapotranspiration have been applied in several irrigation projects. A second option—more comprehensive descriptions that solve the energy balance instantaneously on the basis of surface albedo, surface temperature, and vegetation index—is being thoroughly tested in irrigation projects. An intercomparison study between the two approaches is recommended. Because both algorithms describe the sensible and latent heat fluxes explicitly, the evaporative fraction can be computed and compared with the CWSI, WDI, and SEBI crop-stress indicators. The data set should be taken from an irrigated landscape with multiple independent measurements of the surface energy balance to gain independent material for validation purposes.

Soil evaporation

If the partitioning of evapotranspiration into soil evaporation and crop transpiration can be made exact, then productivity per unit of water consumed by crops, i.e., water use efficiency, can be quantified at the regional scale. Partitioning of evapotranspiration provides a sound way to calculate water losses that occur between the diversion dam and the root zone. Ratios of actual evaporation to actual evapotranspiration may adequately indicate the potential water savings that would result from reducing evaporation losses from bare soil.

4.

Remote Sensing Costs

THE COST-EFFECTIVENESS of remotely sensed technologies is an important reason for shifting from classical field surveys to spaceborne identification of irrigated terrain and its conditions. Successful introduction of remote sensing does not depend solely on technical capabilities (discussed in chapters 2 and 3). Irrigation managers and policy makers will shift to advanced information technologies only if they get better results at equal or lower cost. The value of remote sensing data relies therefore on the balance of costs and benefits. The financial consequences of using remote sensing technologies becomes apparent only after investing in equipment, devices, and skilled labor necessary to process and interpret the images.

The first section of the chapter focuses on the investment required to make image analyses feasible, using experiences gained by a few governmental research institutes and private companies. Because not all users of remote sensing products are willing to invest in hardware and software, assistance from commercial consultants is indispensable. The second section, therefore, examines the market prospects for small enterprises that specialize in providing remote sensing analysis.

Investments

In a summary of a workshop devoted to remote sensing and irrigation, Vidal and Sagardoy (1995) attributed the limited application of satellite remote sensing to poor technology transfer and the large investments required, among other reasons. The costs of using satellite remote sensing are composed of image purchases, investments in hardware and software to make digital processing feasible, and the wages of skilled personnel who perform the analysis and field checks. Fortunately, hardware and software costs are falling rapidly, and image processing is becoming less expensive. Technological breakthroughs in digital imaging systems and high speed computers are making the purchase and processing of satellite images more affordable. Between 1994 and 1997, the cost of a work station, including image-processing software, fell from about US$100,000 to US$40,000.

Satellite data can be obtained from privately owned receiving stations (NOAA-AVHRR and Meteosat) or from commercial distributors who have access to ground reception facilities and sell high resolution Landsat, SPOT, and IRS images. The costs of installing an owner-operated dish antenna for receiving NOAA data, including image-processing software, is about US$25,000, which is a nonrecurrent cost. NOAA and the European Organisation for the Exploitation of Meteorological Satellites (a source of Meteosat images) charge so little for data retrieval that the service is virtually free.

The commercial price of AVHRR images is US$50 to $300. In contrast, the cost of a single Thematic Mapper scene is US$4,500 with a delivery time of 1 to 3 weeks. A guaranteed 7-day turn-around can be purchased for a 50 percent premium over the normal image cost, according to Moran (1994), or a 2-day turn-around can be purchased for a 200 percent premium over the normal price. The standard SPOT-XS image costs US$3,100.

Faced with foreign-exchange difficulties, many developing countries cannot afford to purchase images from commercial agencies outside their borders. Table 18 shows that the expense of preparing land-use maps varies from country to country, depending on labor costs and the type and number of images used. According to Thiruvengadachari and Sakthivadivel (1997), the per-hectare cost of monitoring waterlogging is about US$0.05 compared with US$0.02 to $0.10 for preparing crop inventories. Hence, the type of analysis plays a role as well.

Table 18. Costs of land-use mapping with remote sensing data.

Country	Image	Annual cost (US$/ha)	Source
Philippines	SPOT	0.08	Rajan 1991
Maldives	SPOT	0.03	Rajan 1991
Morocco	SPOT	0.20 to 0.80	Vidal and Baqri 1995
Indonesia	SPOT	0.08[a]	Lantieri 1995
Indonesia	SPOT	0.13[b]	Lantieri 1995
India	IRS	0.10[c]	Thiruvengadachari and Sakthivadivel 1997
India	IRS	0.03[d]	Thiruvengadachari and Sakthivadivel 1997

[a]National staff. [b]International staff. [c]Under 100,000 ha. [d]Over 250,000 ha.

Based on table 18, the average annual cost of land-use mapping is approximately US$0.16/ha. The expense of a remote sensing component for monitoring or improving irrigation management is a minor fraction of the total cost of irrigation schemes (construction: US$3,000/ha; annual operating and maintenance: US$50 to $200/ha). Remote sensing can only become cost effective if productivity of water or environmental sustainability improves due to the involvement of earth observation data. But experience with applying remote sensing to irrigation water management is not yet deep, so its overall cost effectiveness cannot be evaluated at this stage.

Menenti, Azzali, and D'Urso (1995) defined and compared cost indicators related to conducting remote sensing studies in government research in Egypt, India, Argentina, and the Netherlands. They surveyed the annual wages in both the private and public sector, procurement costs for computers, the price of a Thematic Mapper scene, and the unrestricted core funds of institutions. They concluded that the relative price levels were quite uneven for these countries. For instance, annual wages in the public sector in Egypt and India in 1991 were less than the price of a single TM scene, whereas in Argentina annual wages were double the price of a TM image. Costs related to the procurement of a personal computer also exceeded the annual wages in Egypt, which probably restrained research institutes from investing in

remote sensing technology. In the USA, the costs related to image processing to derive irrigation conditions equaled the price of a TM scene and the annual salary of a technician was about seven times as much. Hence, the data in table 18 are not universal, and cost ratios in remote sensing application studies affect the progress of the technology.

Commercialization

The pace of commercialization in remote sensing processing and interpretation will depend on the consumer's ability to make full use of the data purchased. Dialogue between remote sensing scientists and water managers and other members of the user community is vital because users need to be aware of the technical possibilities of remote sensing and the precision of the information deduced from it. Analysis of institutional research costs and farm economics will reveal whether investments in remote sensing applications for monitoring crop and water conditions are economically feasible. As water prices increase (US$0.03/m^3 in Arizona, USA), many farmers may decide to apply irrigation water only when the crop strictly demands it.

Commercial remote sensing has emerged in western USA with companies providing aircraft and helicopter-based reconnaissance services on request. This commercialization has accelerated the transfer of salient research findings into tools supporting operational irrigation management.

Moran (1994) reported the setup and results of a fascinating on-farm irrigation management study conducted at the 770-hectare Maricopa Agricultural Center in Arizona. An aircraft was deployed for low-altitude (100 m) multispectral measurements in essentially the same bands as Thematic Mapper. The aircraft made 36 flights to collect data for the computation of SAVI and CWSI. At the conclusion of the experiment in which US$100,000 had been invested in sensors, Moran (1994) calculated that low-altitude aircraft flights can be utilized for daily farm management at a cost of US$500 a day (plane rental and pilot salary). Although satellite remote sensing would provide less frequent acquisitions of data, it turned out in Moran's experiment to be more cost effective than other methods for surveying the same area (the net benefit from using the satellite was US$600,000 compared with US$130,000 from using aircraft). By applying remote sensing information on crop water status, farmers could use two fewer irrigation turns than standard irrigation guidelines call for.

As progress is made in real-time monitoring capability, observations from space can be substituted for field surveys of vast or remote areas. For instance, the annual Columbia Basin (USA) potato survey is executed commercially (Waddington and Lamb 1990). It was found that long data turn-around time was the principal impediment to using satellite data for identifying problems within fields and describing corrective action in a timely manner (delivery times are 4 days for SPOT, 2 weeks for MSS, and 3 weeks for TM).

In recent years, a promising technology in airborne multispectral radiometry has emerged (King 1995) that allows airplane surveys to supplement satellite data on partially cloudy days when satellite images are inadequate. An added advantage of airborne radiometry is that the data are available as soon as the plane lands.

5.

Conclusions and Recommendations

MORAN (1994) CITES Park, Colwell, and Meyers (1968) as being perhaps the first to recognize that scheduling irrigation and diagnosing irrigation efficiencies could be achieved best with spectral images from aircraft and satellites. Yet, 30 years later, the question is still being asked: Does the information from satellite remote sensing have potential for supporting the management of irrigated river basins?

The comprehensive review of chapter 2 demonstrates that satellite data can be utilized to diagnose irrigation processes. Table 19 summarizes the current state of technology and identifies possible applications and future needs for basic and applied research. Long bars in the applications column indicate which irrigation determinants are ready to be tested in demonstration projects. Further advances in basic research on remote sensing issues at international laboratories and universities are needed before applications that integrate remote sensing for irrigation are packaged. In table 19, the emphasis on potential evapotranspiration (suggested by the long bars in all three columns) is a consequence of the divergence in technically available solutions and the controversial perceptions held within the scientific community.

Information on composites pertinent to cartographic issues, such as the layout of an irrigation canal network, can be obtained from supervised classifications using very high resolution images (e.g., SPOT and IRS). Such images can also be applied for pattern recognition of mono-cropping systems. Irrigated area can be obtained from the temporal dynamics in vegetation indices such as SAVI (which is less sensitive to the interference of background soil reflectance than SR and NDVI).

Crop types do not have to be known in order to quantify biophysical properties of an irrigated area. SAVI values corrected for their minimum and maximum value can be used to compute the fractional vegetation cover. Leaf area index and other biophysical properties provide valuable information for estimating regional water and energy fluxes. The classical NDVI value is useful for determining photosynthetically active radiation and is therefore also a suitable predictor of crop yields as early as 2 months before harvest.

A thorough description of the irrigation conditions, such as water consumption of unstressed crops grown in the irrigation scheme, is essential for planning irrigation water deliveries. Crop coefficients can be spatially interpreted by means of SAVI. Research on the quantification of the land surface parameters for one-step versions (surface albedo, minimum surface resistance, surface roughness for momentum transport, surface roughness for heat transport, and displacement height) has been started, and this type of research needs further encouragement. The Penman-Monteith equation is the standard for calculation of crop water requirement in irrigated areas of the world. Methodologies for measuring the surface roughness for heat transport deserve ample attention because this is one of the most difficult parameters to quantify.

Table 19. State of research and applications in remote sensing for irrigation management (bar length indicates the attention the parameter should receive).

Parameter	Basic research	Applied research	Applications
		COMPOSITES	
Cartographic issues			
Irrigated area and irrigation intensity			
Mono-cropping systems			
Multiple-cropping systems			
Crop communities			
Land cover and use			
		BIOPHYSICAL PROPERTIES	
Fractional vegetation cover			
Leaf area index			
Transpiration coefficient			
		IRRIGATION CONDITIONS	
Potential evapotranspiration			
Potential transpiration			
Potential evaporation			
Actual evapotranspiration			
Actual transpiration			
Actual evaporation			
Field moisture deficit (ET_{act}/ET_{pot})			
Crop water stress (t_{act}/t_{pot})			
Surface soil moisture			
Deep soil moisture			
Soil salinity			
Crop yield			
Relative crop yield			

Monitoring of the irrigation processes can be done with the water deficit index. A more comprehensive, and thus more time-consuming, solution is the application of SEBAL, a term for crop water stress (evaporative fraction), which also provides the actual evapotranspiration. Data on regional evapotranspiration is the backbone for performance assessment and water accounting and is of paramount importance for verifying regional irrigation models and river basin models.

More attention should be dedicated to the classification of patchwork crop types. The partitioning of actual evapotranspiration into actual transpiration and bare-soil evaporation is an unresolved issue and deserves future attention. Research on assessing soil moisture with a full range spectrally different radiometers should be pursued. That might at the same time

accelerate progress in detecting soil salinity because the soil dielectric property is affected both by moisture and salts: wide-range spectral observations may help to alleviate the confusion of water and salt effects on backscattered and emitted microwave signals.

A standard package of technologies and software needs to be developed to make a better use of earth observations from space. Ideally, irrigation and river basin managers would routinely apply such a package with robustly tested analytical functions to transfer spectral radiances into information on irrigation processes. Irrigation determinants based on remote sensing should therefore rely less on ancillary field data and have positive cost-benefit ratios. These elements of robustness and cost-effectiveness can only be sorted out through demonstration projects (fig. 8).

Applications of remote sensing in irrigation management should be worked out through a two-way structure of demonstration and implementation (fig. 8). Demonstration projects must be jointly initiated by international organizations (such as FAO and the institutes of the Con-

Figure 8. Structure needed to transfer remote sensing technology from research to implementation by irrigation managers.

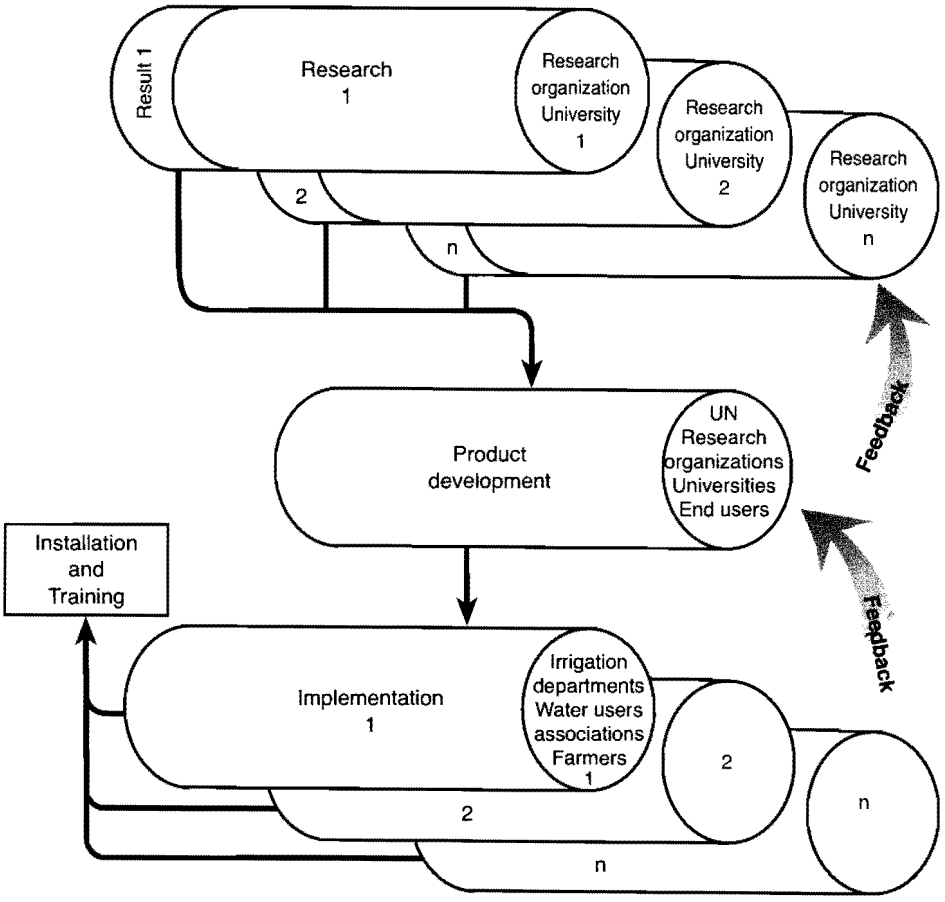

sultative Group on International Agriculture Research), the leading centers of scientific expertise (Annex 1), and end users. The aim should be to close the gap between the information remote sensing is technically capable of producing and the information needed for managing irrigation water and improving crop productivity. Research must focus on the unresolved gaps detected during such demonstration projects. Elements that are successfully evaluated in the demonstration phase should be transferred to implementation phases in close consultation with professionals in data communication. And training of technicians and researchers on water-related remote sensing issues needs attention.

Substantial scientific progress has been made during the last 15 years. The answer to the question of whether remote sensing techniques can be used to support the management of river basins and the irrigation schemes within basins is that the time is ripe for developing irrigation management products (information stemming from satellite measurements that irrigation managers can use in making decisions). Implementation is thus still a few years away.

Selected Major Centers of Expertise on Irrigation and Remote Sensing

Centro Regional Andino, Instituto Nacional de Ciencia y Técnicas Hídricas (INCYTH), Mendoza, Argentina

Colorado State University, Fort Collins, Colorado, USA

Commonwealth Scientific and Industrial Research Organisation (CSIRO), Griffith, Australia

DLO-Winand Staring Centre for Integrated Land, Soil, and Water Research (SC-DLO), Wageningen, Netherlands

Food and Agriculture Organization of the United Nations (FAO), Rome, Italy

French Institute of Agricultural and Environmental Engineering Research (CEMAGREF), Montpellier, France

International Institute for Aerospace Survey and Earth Sciences (ITC), Enschede, Netherlands

Indian Institute of Technology, Kanpur, India

Institute of Hydrology (IH), Wallingford, U.K.

International Water Management Institute (IWMI), Lahore, Pakistan, and Colombo, Sri Lanka

National Aeronautics and Space Administration, Goddard Space Flight Center, (NASA-GSFC), Greenbelt, Maryland, USA

National Remote Sensing Agency (NRSA), Hyderabad, India

National Agricultural Research Institute (INRA), Avignon, France

University of Arizona, Tucson, Arizona, USA

University of Bochum, Bochum, Germany

University of Copenhagen, Denmark

University of Orange Free State, South Africa

University of Tsukuba, Ibaraki, Japan

University of Valencia, Department of Thermodynamics, Burjassot, Valencia, Spain

United States Department of Agriculture (USDA), Phoenix, Arizona, Lubbock, Texas, and Beltsville, Maryland, USA

Utah State University, Logan, Utah, USA

ANNEX 2.

Current Fleet of Earth Resources Satellites (1 January 1998)[a]

Sensor	Satellite	Band no.	Spectral range	Spatial resolution	Swath width	Repeat cycle
LISS III	IRS-1C	1	0.52–0.59 μm	23.5 m	141 km	24 days
		2	0.62–0.68 μm	23.5 m	141 km	
		3	0.77–0.86 μm	23.5 m	141 km	
		4	1.55–1.75 μm	70.5 m	148 km	
PAN	IRS-1C	1	0.50–0.90 μm	5.8 m	70 km	5 days
WiFS	IRS-1C	1	0.62–0.68 μm	188 m	774 km	5 days
		2	0.77–0.86 μm	188 m	774 km	
RA	ERS-2	1	13.8 GHz (K band)	?	?	35 days
ATSR	ERS-2	1	1.6 μm	1 km	500 km	35 days
		2	3.7 μm	1 km	500 km	
		3	11 μm	1 km	500 km	
		4	12 μm	1 km	500 km	
		5	23.8 GHz	22 km	?	
		6	36.5 GHz	22 km	?	
AMI	ERS-2	1	SAR, 5.3 GHz	30 m	100 km	35 days
		2	Wave, 5.3 GHz	30 m	200 km	
		3	Wind, 5.3 GHz	50 km	500 km	
SAR	ERS-2	1	5.3 GHz (C band)	25 m	100 km	35 days
OPS	JERS	1	0.52-0.60	24 m	75 km	35 days
		2	0.63–0.69 μm	24 m	75 km	
		3	0.76–0.86 μm	24 m	75 km	
		4	1.60–1.71 μm	24 m	75 km	
		5	2.01–2.12 μm	24 m	75 km	
		6	2.13–2.25 μm	24 m	75 km	
		7	2.27–2.40 μm	24 m	75 km	
SAR	JERS	1	1.275 GHz (L-band)	18 m	75 km	44 days
		2	15 MHz	18 m	75 km	
SAR	Radarsat	1	5.3 GHz (C-band)	8 to 100 m	50 to 500 km	24 days
MSR	Meteosat	1	0.4–1.1 μm	2.3 km[b]	n.a.	Stationary
		2	5.7–7.1 μm	5.0 km[b]	n.a.	
		3	10.5–12.5 μm	5.0 km[b]	n.a.	
VISSR	GOES	1	0.55–0.7 μm	0.8 km[b]	n.a.	Stationary
		2	10.5–12.6 μm	8.9 km[b]	n.a.	
MSR	GMS	1	0.55–0.75 μm	1.3 km[b]	n.a.	Stationary
		2	10.5–12.5 μm	5.0 km[b]	n.a.	
VHRR	INSAT	1	0.55-0.75 μm	2.75 km[b]	n.a.	Stationary
		2	10.5-12.5 μm	11 km[b]	n.a.	

TM	Landsat-5	1	0.45–0.52 μm	30 m	185 km	16 days
		2	0.52–0.60 μm	30 m	185 km	
		3	0.63–0.69 μm	30 m	185 km	
		4	0.76–0.90 μm	30 m	185 km	
		5	1.55–1.75 μm	30 m	185 km	
		7	2.08–2.35 μm	30 m	185 km	
		6	10.4–12.5 μm	120 m	185 km	
MSS	Landsat-5	1	0.5–0.6 μm	79 m	185 km	16 days
		2	0.6–0.7 μm	79 m	185 km	
		3	0.7–0.8 μm	79 m	185 km	
		4	0.8–1.1 μm	79 m	185 km	
AVHRR	NOAA14	1	0.55–0.68 μm	1.1 km	2,800 km	0.5 day
		2	0.72–1.10 μm	1.1 km	2,800 km	
		3	3.55–3.93 μm	1.1 km	2,800 km	
		4	10.3–11.3 μm	1.1 km	2,800 km	
		5	11.4–12.4 μm	1.1 km	2,800 km	
TOVS	NOAA		27 optical and microwave bands		17 to 320 km	0.5 day
MUSK	RESURS-1	1	0.5–0.6 μm	170 m	600 km	4 days
		2	0.6–0.7 μm	170 m	600 km	
		3	0.7–0.8 μm	170 m	600 km	
		4	0.8–1.1 μm	170 m	600 km	
		5	10.4–12.6 μm	170 m	600 km	
MESSR	MOS	1	0.51–0.59 μm	50 m	100 km	17 days
		2	0.61–0.69 μm	50 m	100 km	
		3	0.73–0.80 μm	50 m	100 km	
		4	0.80–1.10 μm	50 m	100 km	
VTIR	MOS	1	0.5–0.7 μm	900 m	1,500 km	17 days
		2	6–7 μm	2.7 km	1,500 km	
		3	10.5–11.5 μm	2.7 km	1,500 km	
		4	11.5–12.5 μm	2.7 km	1,500 km	
MSR	MOS	1	23.8 GHz	32 km	317 km	17 days
		2	31.4 GHZ	23 km	317 km	
IFOV	MOS	1	visible	900 m	1,500 km	?
		2	infrared	2.7 km	?	
HRV	SPOT	1	0.51–0.59 μm	20 m	60 km	26 days
		2	0.61–0.68 μm	20 m	60 km	
		3	0.79–0.89 μm	20 m	60 km	
PAN	SPOT	1	0.51–0.73 μm	10 m	60 km	26 days

[a] ? = not found or available information contradictory; n.a. = not applicable.

[b] At equator.

Features of Planned Earth Resources Satellites

National Aeronautics and Space Administration (NASA)

EOS-ALT	Altimeter
EOS-ASTER	Onboard AM-1 (made in Japan). Across-track and along-track pointing, 500 to 900 nm (three channels, 15 m resolution), 1,600 to 2,500 nm (six channels, 30 m resolution), and 8 to 12 μm (five channels, 90 m resolution)
EOS-CERES	Earth radiation budget, onboard AM-1
EOS-CHEM	Chemistry mission for monitoring air pollution, troposphere, and ozone
EOS-ESTAR	Spaceborne L-band passive microwave radiometer
EOS-GLAS	Laser profiler for aerosols and PBL heights
EOS-LASA	Lidar
EOS-MIMR	Passive microwave radiometer, 6.8, 10.6, 18.7, 23.8, 36.5, and 89 GHz
EOS-MISR	15 bands programmable, 400 to 1,050 nm; spatial resolution: 250 m; revisit time: 2 to 9 days; onboard AM-1
EOS-MODIS	190 bands, 405 to 4,080 nm, and two thermal infrared bands; spatial resolution: 250 m to 1 km; revisit time: 1 to 2 days; onboard AM-1
EOS-MOPITT	Air pollution, onboard AM-1 (made in Canada)
EOS-SAR	SAR for land applications
EOS-SCATT	Scatterometer for sea applications
Landsat-7	Enhanced Thematic Mapper sensor with one new panchromatic band (15 m resolution) and one new thermal infrared band (60 m resolution), besides classical TM bands

European Space Agency (ESA)

Envisat-MERIS	15 narrow spectral bands, 400 to 1,025 nm; spatial resolution: 250 m and 1 km; revisit time: 3 days
Envisat-AATSR	15 bands programmable, 400 to 1,050 nm; three bands, 8 to 12.3 mm; spatial resolution: 1 km; revisit time: 1 day
Envisat-ASAR	C- and L-band SAR at 30, 100, and 1,000 m resolution; VV or HH mode; spatial resolution: 30 m
Envisat-GOMOS	Spectrometer in the ultraviolet to near-infrared spectral range for ozone and other trace gases from 20 to 100 km altitude
Envisat-MIMR	Passive microwaves, 89, 36.5, 23.8, 18.7, 10.65, and 6.8 GHz H+V

Envisat-MIPAS	Limb sounding instrument for emission spectra in the infrared region between 4.15 and 14.6 μm
Envisat-MWR	Passive microwaves, K band for atmospheric gases and cloud liquid content
Envisat-RA	Altimeter
Envisat-Sciamachy	Atmospheric gases and aerosol concentrations
Envisat-PRISM	15 bands programmable, 400 to 1,050 nm; along-track pointing; spatial resolution: 50 m; revisit time: 30 days

European Meteorological Satellite Program (Eumetsat)

METOP	Meteorological satellite for clouds and other atmospheric conditions
MSG	Meteosat second generation, 12 channels and 15 minutes temporal resolution

National Space Development Agency of Japan (NASDA)

AVNIR	Onboard ADEOS satellite; eight bands, 0.458 to 12.3 μm

Airborne Instruments

AIRSAR	NASA, Jet Propulsion Laboratory; 5.3 GHz (C-band), 1.25 GHz (L-band), 0.43 GHz (P-band); radar horizontal/vertical polarization
ASAS	NASA, Goddard Space Flight Center; 62 bands from 0.4 to 1.1 μm; multiple observation angles with 15 degree increments
AVIRIS	NASA, Jet Propulsion Laboratory; 32 bands from 0.38–0.69 μm, 64 bands from 0.67–1.27 μm, 64 bands from 1.26–1.88 μm, 64 bands from 1.88–2.5 μm
CAESAR	Nederlandse Lucht en Ruimtevaart; bands from 0.4 to 1.02 μm
DAIS	Deutsche Luft und Raumtefahrt; 32 bands from 0.4 to 1.01 μm, eight bands from 1.5 to 1.788 μm, 32 bands from 1.97 to 2.45 μm, six bands from 8.7 to 12.7 μm
LASALT	Altimeter transmitting and receiving 4,000 pulses per second at 0.904 μm
PBMR	Microwave radiometer, 1.413 GHz (L-band)
PORTOS	Passive microwave radiometer at 90, 36.5, 23.8, 10.7, and 7.6 GHz
TIMS	NASA, Jet Propulsion Laboratory; six bands (8.2 to 12.2 μm).

Miscellaneous

POLDER	Nine bands from 443 to 910 nm; spatial resolution: 6 to 7 km; revisit time: 4 days
SCANSAR	300 to 500 km swath width, 250 m spatial resolution
SSM/I	19 GHz passive microwave radiometer, 50 km spatial resolution

TRMM	Precipitation radar; 13.8 GHz; spatial resolution: 4.3 km, swath width: 220 km
TOPEX/Poseidon	Detects sea level changes
TMI	Microwave imager (10–86 GHz; spatial resolution: 5 to 45 km; swath width: 760 km)
VIRS	Visible and infrared sensor (0.63–12.0 mm; spatial resolution: 2.2 km, swath width: 720 km)
MIR-Priroda	Multifrequency microwave radiometer
LCCD	CBERS Landsat-like satellite plus 20 m panchromatic band (made in China and Brazil)
Resource	Developed by Boeing and agribusiness firms for crop conditions; four channels in visible and near-infrared, onboard Ikonos; spatial resolution: 10 m
Quick Bird	Earth Watch, very high resolution (few meters)
Ikonos	Eosat, very high resolution (4 m multispectral, 1 m panchromatic)
Orbview	Onboard Orbimage, very high resolution satellite (few meters)
SPIN	Russian very high resolution satellite (few meters)
GEROS	Medium spatial resolution (tens of meters)
Cibstat	Kodak Company; medium spatial resolution (tens of meters)
Early Bird	Earth Watch, three bands from 0.49 to 0.875 μm with 15 meter resolution; one band from 0.445 to 0.650 μm with 3 meter resolution
XSTAR	Matra Maroconi, medium spatial resolution applications (tens of meters)
MOMS	Onboard PRIRODA (Germany/Russia)

Formulation of Vegetation Indices

1. The Intrinsic Indices

Simple Ratio (SR)

$$SR = \frac{NIR}{R}$$

Normalized Difference (NDVI)

$$NDVI = \frac{NIR - R}{NIR + R}$$

Normalized Difference Wetness Index (NDWI)

$$NDWI = \frac{SWIR - MIR}{SWIR + MIR}$$

Green Vegetation Index (GVI)

$$GVI = \frac{NIR + SWIR}{R + MIR}$$

2. The Soil-Line Related Indices

Perpendicular VI (PVI)

$$NIR_{soil} = a\ R_{soil} + b$$

$$PVI = \frac{NIR - aR - b}{\sqrt{1 + a^2}}$$

Weighted Difference VI (WDVI)

$$a = NIR_{soil} / R_{soil}$$

$$WDVI = NIR - a\ R$$

Soil Adjusted VI (SAVI)

$$L = 0.5$$

$$SAVI = \frac{(1 + L)(NIR - R)}{NIR + R + L}$$

Optimized Soil Adjusted VI (OSAVI)

$$L = 0.16$$

$$OSAVI = \frac{(NIR - R)}{NIR + R + 0.16}$$

Transformed Soil Adjusted VI (TSAVI)

$$NIRsoil = a\ Rsoil + b$$

$$TSAVI = \frac{a(NIR - aR - b)}{R + a(NIR - b) + 0.08\ (1 + a^2)}$$

Modified Soil Adjusted VI (MSAVI)

$$L = 1 - 2a.NDVI.WDVI$$

$$MSAVI = \frac{a(NIR - aR - b)}{NIR + R + L}$$

$$MSAVI = \frac{1}{2}\left[2NIR + 1 - \sqrt{(2NIR + 1)^2 - 8(NIR - R)} \right]$$

Two-axis VI (TWVI)

$$D = \frac{NIRsoil - aRsoil - b}{(1 + a^2)^{0.5}}$$

$$\Delta = (2 \exp(-k\ LAI)\ D)^{0.5}$$

$$TWVI = (1 + L)\frac{NIR - R - \Delta}{NIR + R + L}$$

3. *Atmospherically Corrected Indices:*

Atmospherically Resistant VI (ARVI)

$$RB = R - \gamma (B - R)$$

where γ depends on the aerosol type

$$ARVI = \frac{NIR - RB}{NIR + RB}$$

Soil Adjusted and Atmospherically Resistant VI (SARVI)

$$L = 0.5$$

$$SARVI = (1 + L)\frac{NIR - RB}{NIR + RB + L}$$

Transformed Soil Adjusted and Atmospherically Resistant VI (TSARVI)

$$NIRsoil = a\ RBsoil + b$$

$$TSARVI = \frac{a(NIR - aRB - b)}{RB + a(NIR - b) + 0.08(1 + a^2)}$$

Global Environment Monitoring Index (GEMI)

$$\eta = \frac{2(NIR^2 - R^2) + 1.5NIR + 0.5R}{NIR + R + 0.5}$$

$$GEMI = \eta(1 - 0.25\eta)\frac{R - 0.125}{1 - R}$$

Remote Sensing Abbreviations and Acronyms

AATSR	Advanced Along-Track Scanning Radiometer
ADEOS	Advanced Earth Observing Satellite
AIRSAR	Airborne SAR
ALT	Altimeter
AM-1	After Midnight 1
amw	Active microwave
ARVI	Atmospherically resistant vegetation index
ASAR	Advanced synthetic aperture radar
ASAS	Advanced Solid-State Array Spectrometer
ASTER	Advanced Spaceborne Thermal Emission and Reflection Radiometer
ATLID	Atmospheric lidar
ATSR	Along-Track Scanning Radiometer
AVHRR	Advanced Very High Resolution Radiometer
AVIRIS	Advanced Visible and Infrared Imaging Spectrometer
AVNIR	Advanced Visible and Near Infrared Radiometer
CAESAR	CCD Airborne Experimental Scanner for Application in Remote Sensing
CBERS	Chinese Brazilian Earth Resources Satellite
CCD	Cold cloud duration; or charge-coupled device (solid state detector type)
CERES	Clouds and the Earth's Radiant Energy System
CHEM	Chemical
CORINE	Coordination of Information on the Environment
CWSI	Crop water stress index
DAIS	Digital Airborne Imaging Spectrometer
Envisat	Environmental Satellite
EOS	Earth Observing System
ERBE	Earth Radiation Budget Experiment
ERS	European Remote Sensing Satellite
ESTAR	Electronically Scanned Thinned Array Radiometer
fPAR	Fraction of photosynthetically active radiation absorbed by the vegetation canopy
GAC	Global area coverage
GEMI	Global environment monitoring index
GIS	Geographic information system
GLAS	Geoscience Laser Altimeter System
GMS	Geostationary Meteorological Satellite
GOES	Geostationary Operational Environmental Satellite

GOMOS	Global Ozone Monitoring by Occultation of Stars
GVI	Green vegetation index
HIRS	High Resolution Infrared Radiation Sounder
IRS	Indian Remote Sensing Satellite
ISCCP	International Satellite Cloud Climatology Project
ISLSCP	International Satellite Land-Surface Climatology Project
JERS	Japanese Earth Resources Satellite
LAI	Leaf area index
Landsat	Land Satellite
LASA	Laser Atmospheric Sounder and Altimeter
LASALT	Laser Altimeter
LISS	Linear Imaging Self-Scanned Sensor
MERIS	Medium Resolution Imaging Spectrometer
Meteosat	Meteorological Satellite
METOP	Meteorological Operational Program
MIMR	Multifrequency Imaging Microwave Radiometer
MIPAS	Michelson Interferometer for Passive Atmospheric Sounding
MIR	Millimeter wave Imaging Radiometer
MISR	Multiangle Imaging Spectroradiometer
MODIS	Moderate Resolution Imaging Spectrometer
MOMS	Modular Opto-electronic Multispectral Scanner
MOPITT	Measurements of Pollution in the Troposphere
MOS	Marine Observation Satellite
MSARVI	Modified soil-adjusted atmospherically resistant vegetation index
MSAVI	Modified soil-adjusted vegetation index
MSG	Meteosat second generation
MSR	Microwave Scanning Radiometer
MSS	Multispectral Scanner
MWR	Microwave Radiometer
NDVI	Normalized difference vegetation index
NDWI	Normalized difference wetness index
nir	Near infrared
NOAA	National Oceanic and Atmospheric Administration Satellite
OSAVI	Optimized soil-adjusted vegetation index
PAR	Photosynthetically active radiation
PBL	Planetary boundary layer
PBMR	Push Broom Microwave Radiometer
pmw	Passive microwave
POLDER	Polarization and Directionality of the Earth's Reflectances
PORTOS	Passive microwave radiometer (in French)
PRISM	Panchromatic Remote Sensing Instrument for Stereo Mapping
Priroda	Nature (in Russian)

PVI	Perpendicular vegetation index
RA	Radar Altimeter
SAR	Synthetic aperture radar
SARVI	Soil-adjusted atmosphericalIy resistant vegetation index
SAVI	Soil-adjusted vegetation index
SCANSAR	Scanning SAR
SCATT	Scatterometer
Sciamachy	Scanning Imaging Absorption Spectrometer for Atmospheric Cartography
SEBAL	Surface energy balance algorithm for land
SEBI	Surface energy-balance index
SMMR	Scanning Multichannel Microwave Radiometer
SPOT	Satellite pour l'Observation de la Terre
SR	Simple ratio
SSM/I	Special Sensor Microwave/Imager
SVAT	Soil-vegetation-atmosphere transfer
TCVI	Time-composited vegetation index
TIMS	Thermal Infrared Multispectral Scanner
tir	Thermal infrared
TM	Thematic Mapper
TMI	TRMM Microwave Imager
TOPEX	The Ocean Topography Experiment
TOVS	TIROS Operational Vertical Sounder
TRMM	Tropical Rainfall Measuring Mission
TSARVI	Transformed soil-adjusted atmospheric resistant vegetation index
TSAVI	Transformed soil-adjusted vegetation index
TVI	Transformed vegetation index
TWVI	Two-axis vegetation index
VIRS	Visible and Infrared Scanner
vis	Visible
VISSR	Visible Infrared Spin Scan Radiometer
WCRP	World Climate Research Program
WDI	Water deficit index
WDVI	Weighted difference vegetation index
WiFS	Wide Field Sensor
XS	Multispectral

Literature Cited

Abbott, M. B., J. C. Bathurst, J. A. Cunge, P. E. O'Connell, and J. Rasmussen. 1986. An introduction to the European Hydrological System—Système Hydrologique Européen, SHE: 1. History and philosophy of a physically-based, distributed modelling system. *Journal of Hydrology* 87:45–59.

Abdellaoui, A., F. Becker, and E. Olory-Hechninger. 1986. Use of Meteosat for mapping thermal inertia and evapotranspiration over a limited region of Mali. *Journal of Climate and Applied Meteorology* 25:1,489–1,506.

Agbu, P. A., D. J. Fehrenbacher, and I. J. Jansen. 1990. Soil property relationships with SPOT satellite digital data in East Central Illinois. *Soil Science Society of America Journal* 54:807–812.

Ahmad, M. D., J. Jamieson, S. Asif, and P. Strosser. 1996. Use of satellite imagery for land use mapping and crop identification in irrigation systems in Pakistan. Paper A-2 in *Proceedings of the 17th Asian Conference on Remote Sensing.* Colombo: Survey Department. 9 p.

Ahmed, R. H., and C. M. U. Neale. 1996. Mapping field crop evapotranspiration using airborne multispectral imagery. In *IGARSS '96: 1996 International Geoscience and Remote Sensing Symposium*, ed. T. 1. Stein, 2,369–2,371. New York: Institute of Electrical and Electronics Engineers.

Akiyama, T., Y. Inoue, M. Shibayama, Y. Awaya, and N. Tanaka. 1996. Monitoring and predicting crop growth and analysing agricultural ecosystems by remote sensing. *Agricultural and Food Science in Finland* 5:367–376.

Al-Kaisi, M., L. J. Brun, and J. W. Enz. 1989. Transpiration and evapotranspiration from maize as related to leaf area index. *Agricultural and Forest Meteorology* 48:111–116.

Allen, R. G., M. Smith, A. Perrier, and L. S. Perreira. 1995. An update for the definition of reference evapotranspiration. *ICID* (International Commission on Irrigation and Drainage) *Bulletin* 43(2): 1–92.

Arino, O., G. Dedieu, and P. Y. Deschamps. 1991. Accuracy of satellite land surface reflectance determination. *Journal of Applied Meteorology* 30:960–972.

Arino, O., G. Dedieu, and P. Y. Deschamps. 1992. Determination of land surface spectral reflectances using Meteosat and NOAA/AVHRR shortwave channel data. *International Journal of Remote Sensing* 13(12): 2,263–2,287.

Arnold, J. G., and J. R. Williams. 1987. Validation of SWRRB simulator for water resources in rural basins. *Journal of Water Research Planning and Management* 113(2): 243–256.

Ashcroft, P. M., J. A. Catt, P. J. Curran, J. Munden, and R. Webster. 1990. The relation between reflected radiation and yield on the Broadbalk winter wheat experiment. *International Journal of Remote Sensing* 11(10): 1,821–1,836.

Asrar, G., ed. 1989. *Theory and applications of optical remote sensing.* New York: John Wiley.

Asrar, G., R. B. Myneni, and B. J. Choudhury. 1992. Spatial heterogeneity in vegetation canopies and remote sensing of absorbed photosynthetically active radiation: A modelling study. *Remote Sensing of Environment* 41:85–103.

Attia, B., M., Andjelic, and W. Klohn. 1995. River Nile monitoring, forecasting and simulation project. In *Use of remote sensing techniques in irrigation and drainage,* ed. A. Vidal and J. A. Sagardoy, 17–26. Water Reports 4. Rome: FAO.

Azzali, S., and M. Menenti, eds. 1996. *Fourier analysis of temporal NDVI in the Southern African and American continents.* Report 108. Wageningen, Netherlands: DLO-Winand Staring Centre. 149 p.

Azzali, S., W. G. M. Bastiaanssen, M. Menenti, H. de Brouwer, A. M. J. Meijerink, J. Maza, and A. W. Zevenbergen. 1991. *Remote sensing and watershed modelling.* Report 48. Wageningen, Netherlands: DLO-Winand Staring Centre. 123 p.

Azzali, S., M. Menenti, I. J. M. Meeuwissen, and T. N. M. Visser. 1991. Application of remote sensing techniques to map crop coefficients in an Argentinean irrigation scheme. In *Advances in water resources technology,* ed. G. Tsakiris, 637–643. Rotterdam: Balkema.

Badhwar, G. D., C. E. Gargatini, and F. V. Redondo. 1987. Landsat classification of Argentina summer crops. *Remote Sensing of Environment* 21:111-117.

Baily, J. O. 1990. The potential value of remotely sensed data in the assessment of evapotranspiration and evaporation. *Remote Sensing Reviews* 4(2): 349–377.

Baker, F. A., D. L. Verbyla, and C. S. Hodges. 1993. Classification and regression tree analysis for assessing hazard of pine mortality caused by *Heterobasidion annosum. Plant Disease* 77(2): 136–139.

Baret, F., and G. Guyot. 1991. Potentials and limits of vegetation indices for LAI and APAR assessment. *Remote Sensing of Environment* 35:161–173.

Barkstrom, B., E. F. Harrison, G. L. Smith, R. N. Green, J. Kibler, and R. D. Cress. 1989. Earth Radiation Budget Experiment (ERBE) archival and April 1985 results. *Bulletin of the American Meteorological Society* 70:1,254–1,256.

Barnett, T. L., and D. R. Thompson. 1983. Large area relation of Landsat MSS and NOAA 6 AVHRR spectral data to wheat yield. *Remote Sensing of Environment* 13:277–290.

Barrett, E. C., M. Beaumont, and R. Herschy. 1990. Satellite remote sensing of operational hydrology. *Remote Sensing Reviews* 4(2): 223–472.

Bastiaanssen, W. G. M., D. H. Hoekman, and R. A. Roebeling. 1994. *A methodology for the assessment of surface resistance and soil water storage variability at mesoscale based on remote sensing measurements.* IAHS Special Publications 2. Wallingford, U.K.: Institute of Hydrology. 66 p.

Bastiaanssen, W. G. M., M. Menenti, A. J. Dolman, R. A. Feddes, and H. Pelgrum. 1996. Remote sensing parameterization of meso-scale land surface evaporation. In *Radiation and water in the climate system: Remote measurements,* ed. E. Raschke, 401–429. Berlin: Springer-Verlag.

Bastiaanssen, W. G. M., M. Menenti, R. A. Feddes, and A. A. M. Holtslag. Forthcoming. A remote sensing surface energy balance algorithm for land (SEBAL). Part 1: Formulation. *Journal of Hydrology.*

Bastiaanssen, W. G. M., H. Pelgrum, P. Droogers, H. A. R. de Bruin, and M. Menenti. 1997. Area-average estimates of evaporation, wetness indicators and top soil moisture during two golden days in EFEDA. *Agricultural and Forest Meteorology* 87:119–137.

Bastiaanssen, W. G. M., H. Pelgrum, J. Wang, Y. Ma, J. F. Moreno, G. J. Roerink, R. A. Roebeling, and T. van der Wal. Forthcoming. A remote sensing surface energy balance algorithm for land (SEBAL). Part 2: Validation. *Journal of Hydrology.*

Bastiaanssen, W. G. M., T. van der Wal, and T. N. M. Visser. 1996. Diagnosis of regional evaporation by remote sensing to support irrigation performance assessment. *Irrigation and Drainage Systems* 10:1–23.

Batchily, A. K., A. R. Huete, M. S. Moran, and H. Liu. 1994. Variation of vegetation indices derived from multi-temporal TM images. In *Pecora 12: Land information from space-based systems: Proceedings of the 12th Pecora Symposium, 24–26 August 1993, Sioux Falls South Dakota,* 451–457. Bethesda, Maryland, USA: American Society for Photogrammetry and Remote Sensing.

Batista, G. T., M. M. Hixson, and M. E. Bauer. 1985. Landsat MSS crop classification performance as a function of scene characteristics. *International Journal of Remote Sensing* 6:1,521–1,533.

Bauer, M. E., J. E. Cipra, P. E. Anuta, and J. B. Etheridge. 1979. Identification and area estimation of agricultural crops by computer classification of Landsat MSS data. *Remote Sensing of Environment* 8:72–92.

Bausch, W. C. 1993. Soil background effects on reflectance-based crop coefficients for corn. *Remote Sensing of Environment* 46:213–222.

Bausch, W. C. 1995. Remote sensing of crop coefficients for improving the irrigation scheduling of corn. *Agricultural Water Management* 27(1): 55–68.

Bausch, W. C., and C. M. U. Neale. 1987. Crop coefficients derived from reflected canopy radiation: A concept. *Transactions of the American Society of Agricultural Engineering* 30(3): 703–709.

Becker, F. 1987. The impact of spectral emissivity on the measurement of land surface temperature from a satellite. *International Journal of Remote Sensing* 8(10): 1,509–1,522.

Becker, F., and Z. L. Li. 1990a. Temperature-independent spectral indices in thermal infrared bands. *Remote Sensing of Environment* 32:17–33.

Becker, F., and Z. L. Li. 1990b. Towards a local split window method over land surfaces. *International Journal of Remote Sensing* 11:369–393.

Beljaars, A. C. M., and A. A. M. Holtslag. 1991. Flux parameterization over land surfaces for atmospheric models. *Journal of Applied Meteorology* 30(3): 327–341.

Benediktsson, J. A., P. H. Swain, and O. K. Ersoy. 1990. Neural network approaches versus statistical methods in classification of multisource remote sensing data. *IEEE Transactions on Geoscience and Remote Sensing* 28:540–551.

Benedetti, R., and P. Rossini. 1993. On the use of NDVI profiles as a tool for agricultural statistics: The case study of wheat yield estimate and forecast in Emilia Romagna. *Remote Sensing of Environment* 45:311–326.

Bernard, R., P. Martin, J. L. Thony, M. Vauclin, and D. Vidal-Madjar. 1982. C-band radar for determining surface soil moisture. *Remote Sensing of Environment* 12:189–200.

Beven, K. J., and J. Fischer. 1996. Remote sensing and scaling in hydrology. In *Scaling up in hydrology using remote sensing,* ed. J. B. Stewart, T. Engman, R. A. Feddes, and Y. Kerr, 1–18. New York: John Wiley.

Beven, K. J., E. F. Wood, and M. Sivapalan. 1988. On hydrological heterogeneity: Catchment morphology and catchment response. *Journal of Hydrology* 100:353–375.

Bouchet, R. J. 1963. Evapotranspiration réelle et potentielle: Signification climatique. In *Evaporation,* 134–142. International Association of Hydrological Sciences Publication 62. Gentbrugge, Belgium: General Assembly of Berkeley, Committee for Evaporation.

Bouman, B. A. M. 1992. Linking physical remote sensing models with crop growth simulation models applied for sugarbeet. *International Journal of Remote Sensing* 14:2,565–2,581.

Bouman, B. A. M., and D. Uenk. 1992. Crop classification possibilities with radar in ERS-1 and JERS-1 configuration. *Remote Sensing of Environment* 40:1–13.

Braden, H., and Th. Blanke. 1993. About the use of remotely sensed surface temperatures for controlling estimates of evapotranspiration. *Modeling Geo-Biosphere Processes* 2:53–66.

Brena, J., H. Sanvicente, and L. Pulido. 1995. Salinity assessment in Mexico. In *Use of remote sensing techniques in irrigation and drainage,* ed. A. Vidal and J. A. Sagardoy, 173–178. Water Reports 4. Rome: FAO.

Brisco, B., R. J. Brown, and M. J. Manore. 1989. Early season crop discrimination with combined SAR and TM data. *Canadian Journal of Remote Sensing* 15(1): 44–54.

Bruin, H. A. R. de. 1989. Physical aspects of the planetary boundary layer with special reference to regional evapotranspiration. In *Estimation of areal evapotranspiration,* ed. T. A. Black, D. L. Spittlehouse, M. D. Novak, and D. T. Price, 117–132. International Association of Hydrological Sciences Publication 177. Wallingford, U.K.: Institute of Hydrology.

Buettner, K. J. K., and C. D. Kern. 1965. The determination of emissivities of terrestrial surfaces. *Journal of Geophysical Research* 70(6): 1,329–1,337.

Bussières, N., and K. Goita. 1997. Evaluation of strategies to deal with cloudy situations in satellite evapotranspiration algorithms. In *Applications of remote sensing in hydrology: Proceedings of the Third International Workshop, 16–18 October 1996, NASA, Goodard Space Flight Center, Greenbelt, Maryland, USA,* ed. G. W. Kite, A. Pietroniro, and T. J. Pultz, 33–44. NHRI Symposium 17. Saskatoon, Saskatchewan, Canada: National Hydrology Research Institute.

Buttner, G., and F. Csillag. 1989. Comparative study of crop and soil mapping using multitemporal and multispectral SPOT and Landsat Thematic Mapper data. *Remote Sensing of Environment* 29:241–249.

Carbone, G. J., S. Narumalani, and M. King. 1996. Application of remote sensing and GIS technologies with physiological crop models. *Photogrammetric Engineering and Remote Sensing* 62(2): 171–179.

Carlson, T. N. 1986. Regional scale estimates of surface moisture availability and thermal inertia. *Remote Sensing Review* 1:197–247.

Carlson, T. N., R. R. Gillies, and E. M. Perry. 1994. A method to make use of thermal infrared temperature and NDVI measurements to infer soil water content and fractional vegetation cover. *Remote Sensing Reviews* 52:45–59.

Carlson, T. N., E. M. Perry, and T. J. Schmugge. 1990. Remote sensing of soil moisture availability and fractional vegetation cover for agricultural fields. *Agricultural and Forest Meteorology* 52:45–69.

Carlson, T. N., O. Taconet, A. Vidal, R. R. Gillies, A. Olioso, and K. Humes. 1995. An overview of the workshop on thermal remote sensing held at La Londe les Maures, France, September 20–24, 1993. *Agricultural and Forest Meteorology* 77:141–151.

Casas, S. 1995. Salinity assessment based on combined use of remote sensing and GIS. In *Use of remote sensing techniques in irrigation and drainage,* ed. A. Vidal and J. A. Sagardoy, 185–197. Water Reports 4. Rome: FAO.

Caselles, V., and J. Delegido. 1987. A simple model to estimate the daily value of the maximum evapotranspiration from satellite temperature and albedo images. *International Journal of Remote Sensing* 8:1,151–1,162.

Caselles, V., C. Coll, E. Valor, and E. Rubio. 1995. Mapping land surface emissivity using AVHRR data application to La Mancha, Spain. *Remote Sensing Reviews* 12:311–333.

Caselles, V., J. A. Sobrino, and F. Becker. 1988. Determination of the effective emissivity and temperature under vertical observation of a citrus orchard. Application to frost snow casting. *International Journal of Remote Sensing* 9:715–727.

Chanzy, A., T. J. Schmugge, J.-C. Calvet, Y. Kerr, P. van Oevelen, O. Grosjean, and J. R. Wang. 1997. Airborne microwave radiometry on a semi-arid area during HAPEX-Sahel. *Journal of Hydrology* 188-189:285–309.

Chaturvedi, L., K. R. Carver, J. C. Harlan, G. D. Hancock, F. V. Small, and K. J. Dalstead. 1983. Multispectral remote sensing of saline seeps. *IEEE Transactions on Geoscience and Remote Sensing* 21(3): 239–250.

Chen, E., L. H. Allen, J. F. Bartholic, and J. F. Gerber. 1983. Comparison of winter nocturnal geostationary satellite infrared-surface temperature with shelter-height temperature in Florida. *Remote Sensing of Environment* 13:313–327.

Chen, T. S., and G. Ohring. 1984. On the relationship between clear sky planetary and surface albedos. *Journal of Atmospheric Science* 41:156–158.

Choudhury, B. J. 1989. Estimating evaporation and carbon assimilation using infrared temperature data: Vistas in modeling. In *Theory and applications of optical remote sensing*, ed. G. Asrar, 628–690. New York: John Wiley.

Choudhury, B. J. 1991. Multispectral satellite data in the context of land surface heat balance. *Review of Geophysics* 29:217–236.

Choudhury, B. J. 1994. Synergism of multispectral satellite observations for estimating regional land surface evaporation. *Remote Sensing of Environment* 49:264–274.

Choudhury, B. J., and R. E. Golus. 1988. Estimating soil wetness using satellite data. *International Journal of Remote Sensing* 9:1,251–1,257.

Choudhury, B. J., N. U. Ahmed, S. B. Idso, R. J. Reginato, and C. S. T. Daughtry. 1994. Relations between evaporation coefficients and vegetation indices studied by model simulations. *Remote Sensing of Environment* 50:1–17.

Choudhury, B. J., S. B. Idso, and R. J. Reginato. 1987. Analysis of an empirical model for soil heat flux under a growing wheat crop for estimating evaporation by an infra-red temperature based energy balance equation. *Agricultural and Forest Meteorology* 39:283–297.

Choudhury, B. J., Y. H. Kerr, E. G. Njoku, and P. Pampaloni. 1995. *Passive microwave remote sensing of land-atmosphere interactions.* Utrecht, Netherlands: VSP Publishing.

Choudhury, B. J., J. R. Wang, A. Y. Hsu, and Y. L. Chien. 1990. Simulated and observed 37 GHz emission over Africa. *International Journal of Remote Sensing* 11:1,837–1,868.

Cialella, A. T., R. Dubayah, W. Lawrence, and E. Levine. 1997. Predicting soil drainage class using remotely sensed and digital elevation data. *Photogrammetric Engineering and Remote Sensing* 63(2): 171–178.

Cihlar, J., L. St-Laurent, and J. A. Dyer. 1991. Relation between the normalized difference vegetation index and ecological variables. *Remote Sensing of Environment* 35:279–298.

Clevers, J. G. P. W. 1988. The derivation of a simplified reflectance model for the estimation of leaf area index. *Remote Sensing of Environment* 25:53–69.

Clevers, J. G. P. W. 1989. The application of a weighted infra-red vegetation index for estimating leaf area index by correcting for soil moisture. *Remote Sensing of Environment* 29:25–37.

Clothier, B. E., K. L. Clawson, P. J. Pinter, M. S. Moran, R. J. Reginato, and R. D. Jackson. 1986. Estimation of soil heat flux from net radiation during the growth of alfalfa. *Agricultural and Forest Meteorology* 37:319–329.

Cognard, A. L., C. Loumagne, M. Normand, Ph. Oliver, C. Ottle, D. Vidal-Madjar, S. Louahala, and A. Vidal. 1995. Evaluation of the ERS1/synthetic aperture radar capacity to estimate surface soil moisture: Two years' results over the Naizin watershed. *Water Resources Research* 31:975–982.

Coll, C., V. Caselles, and T. J. Schmugge. 1994. Estimation of land surface emissivity differences in the split-window channels of AVHRR. *Remote Sensing of Environment* 48:127–134.

Congalton, G. R. 1991. A review of assessing the accuracy of classifications of remotely sensed data. *Remote Sensing of Environment* 37:35–46.

Courault, D., J. P. Lagouarde, and B. Aloui. 1996. Evaporation for maritime catchment combining a meteorological model with vegetation information and airborne surface temperatures. *Agricultural and Forest Meteorology* 82:93–117.

Cruickshank, M. M., and R. W. Tomlinson. 1996. Application of CORINE land cover methodology to the UK: Some issues raised from Northern Ireland. *Global Ecology and Biogeography* 5:235–248.

Csillag, F. 1986. Comparison of some classification methods on a test-site (Kiskore, Hungary): Separability as a measure of accuracy. *International Journal of Remote Sensing* 7:1,705–1,714.

Curran, P. J. 1985. *Principles of remote sensing.* London: Longman. 282 p.

Curran, P. J. 1987. Remote sensing in agriculture: An introductory review. *Journal of Geography* 86:147–156.

D'Urso, G., and M. Menenti. 1996. Performance indicators for the statistical evaluation of digital image classifications. *ISPRS Journal of Photogrammetry and Remote Sensing* 51:78–90.

D'Urso, G., and A. Santini. 1996. A remote sensing and modelling integrated approach for the management of irrigation distribution systems. In *Evapotranspiration and irrigation scheduling: Proceedings of the International Conference, November 3–6, 1996, San Antonio, Texas, USA,* ed. C. R. Camp, E. J. Sadler, and R. E. Yoder, 435–441. St. Joseph, Michigan, USA: American Society of Agricultural Engineers.

Darnell, W. L., W. F. Staylor, S. K. Gupta, and F. M. Denn. 1988. Estimation of surface insulation using sun-synchronous satellite data. *Journal of Climate* 1:820–835.

Darnell, W. L., W. F. Staylor, S. K. Gupta, N. A. Ritchey, and A. C. Wilber. 1992. Seasonal variation of surface radiation budget derived from International Satellite Cloud Climatology Project C1 data. *Journal of Geophysical Research* 97(D14): 15,741–15,760.

Daughtry, C. S. T., K. P. Gallo, S. N. Goward, S. D. Prince, and W. P. Kustas. 1992. Spectral estimates of absorbed radiation and phytomass production in corn and soybean canopies. *Remote Sensing of Environment* 39:141–152.

Daughtry, C. S. T., W. P. Kustas, M. S. Moran, P. J. Pinter, R. D. Jackson, P. W. Brown, W. D. Nichols, and L. W. Gay. 1990. Spectral estimates of net radiation and soil heat flux. *Remote Sensing of Environment* 32:111–124.

Davis, F. W., and J. Dozier. 1990. Information analysis of a spatial database for ecological land classification. *Photogrammetric Engineering and Remote Sensing* 56(5): 605–613.

Deblonde, G., and J. Cihlar. 1993. A multiyear analysis of the relationship between surface environmental variables and NDVI over the Canadian landmass. *Remote Sensing Reviews* 7:151–177.

Dedieu, G., P. Y. Deschamps, and Y. Kerr. 1987. Satellite estimation of solar irradiance at the surface of the earth and of surface albedo using a physical model applied to Meteosat data. *Journal of Climate and Applied Meteorology* 26:79–87.

Defries, R. S., and R. G. Townshend. 1994. NDVI-derived land cover classification at a global scale. *International Journal of Remote Sensing* 15:3,567–3,586.

Della Mana, S., and R. Gombeer. 1990. Evaluation of the land resources and the irrigation potential of the Tocantins river valley-Brazil using Landsat-5 TM data. In *Remote sensing in evaluation and management of irrigation,* ed. M. Menenti, 311–322. Mendoza, Argentina: Instituto Nacional de Ciencia y Técnicas Hídricas.

Diak, G. R. 1990. Evaluation of heat flux, moisture flux and aerodynamic roughness at the land surface from knowledge of the PBL height and satellite-derived skin temperatures. *Agricultural and Forest Meteorology* 52:181–198.

Diak, G., and C. Gautier. 1983. Improvements to a simple model for estimating insolation from GOES data. *Journal of Climate and Applied Meteorology* 22:505–508.

Diak, G. R., W. L. Bland, and J. Mecikalski. 1996. A note on first estimates of surface insolation from GOES-8 visible satellite data. *Agricultural and Forest Meteorology* 82:219–226.

Dickinson, R. E. 1995. Land processes in climate models. *Remote Sensing of Environment* 51:27–38.

Dijk, R., and D. van Eick. 1987. *Remote sensing: Een vergelijking van Landsat MSS en TM beelden van Mendoza met behulp van textuuranalyse en classificatie.* ICW Nota 1816. Wageningen, Netherlands: ICW (Instituut voor Cultuurtechnick en Waterhuishouding). 30 p.

Doorenbos, J., and A. H. Kassam, 1979. *Yield response to water.* Irrigation and Drainage Paper 33. Rome: FAO. 193 pp.

Doorenbos, J., and W. O. Pruitt. 1977. Guidelines for predicting crop water requirements, Irrigation and Drainage Paper 24. Rome: FAO. 156 p.

Dubey, R. P., N. Ajwani, M. H. Kalubarme, V. N. Sridhar, and R. R. Navalgund. 1994. Pre-harvest wheat yield and production estimation for the Punjab, India. *International Journal of Remote Sensing* 15(10): 2,137–2,144.

Dubois, P. C., J. van Zyl, and E. T. Engman. 1995. Measuring soil moisture with imaging radars. *IEEE Transactions on Geoscience and Remote Sensing* 30:915–926.

Dugas, W. A., L. J. Fritschen, L. W. Gay, A. A. Held, A. D. Matthias, D. C. Reicosky, P. Steduto, and J. L. Steiner. 1991. Bowen ratio, eddy correlation and portable chamber measurements of sensible and latent heat flux over irrigated spring wheat. *Agricultural and Forest Meteorology* 56:1–20.

Dugdale, G., and J. R. Milford. 1986. Rainfall estimation over the Sahel using Meteosat thermal infrared data. In *ISLSCP. Parameterisation of land-surface characteristics: Use of satellite data in climate studies,* ed., E. Rolfe and B. Battrick, 315–319. Paris: European Space Agency.

Dwivedi, R. S. 1996. Monitoring of salt-affected soils of the Indo-Gangetic alluvial plains using principal component analysis. *International Journal of Remote Sensing* 17(10): 1,907–1,914.

Ehrlich, D., J. E. Estes, J. Scepan, and K. C. McGwire. 1994. Crop area monitoring within an advanced agricultural information system. *Geocarto International* 9(4): 31–42.

El-Kady, M., and C. B. Mack. 1997. Crop inventory in Egypt using remote sensing. Ministry of Public Works and Water Resources, Cairo. Duplicated.

Ellingson, R. G. 1995. Surface longwave fluxes from satellite observations: A critical review. *Remote Sensing of Environment* 51:89–97.

Elvidge, C. D. 1988. Thermal infrared reflectance of dry plant materials: 2.5–20 mm. *Remote Sensing of Environment* 26:265–285.

Engman, E. T., and N. Chauhan. 1995. Status of microwave soil moisture measurements with remote sensing. *Remote Sensing of Environment* 51:189–198.

Engman, E. T., and R. J. Gurney. 1991. *Remote sensing in hydrology.* London: Chapman and Hall. 225 p.

Epema, G. F. 1990. Effect of moisture content on spectral reflectance in a playa area in southern Tunisia. *International Symposium on Remote Sensing and Water Resources: Proceedings,* 301–308. Enschede, Netherlands: International Association of Hydrogeologists.

Everitt, J. H., D. E. Escobar, A. H. Gerbermann, and M. A. Alaniz. 1988. Detecting saline soils with video imagery. *Photogrammetric Engineering and Remote Sensing* 54:1,283–1,287.

Feddes, R. A. 1987. Simulating water management and crop production with the SWACROP model. Paper presented at the Third International Workshop on Land Drainage, Ohio State University, Department of Agricultural Engineering, Columbus, Ohio, USA, 7–11 December 1987. 14 p.

Fitzgerald, R. W., and B. G. Lees. 1994. Assessing the classification accuracy of multisource remote sensing data. *Remote Sensing of Environment* 47:362–368.

Franklin, S. E., and B. A. Wilson. 1991. Spatial and spectral classification of remote sensing imagery. *Computers and Geoscience* 17(8): 1,151–1,172.

Friedl, M. A., and F. W. Davis. 1994. Sources of variation in radiative surface temperature over a tall grass prairie. *Remote Sensing of Environment* 48:1–17.

Frouin, R., and R. T. Pinker. 1995. Estimating photosynthetically active radiation (PAR) at the earth's surface from satellite observations. *Remote Sensing of Environment* 51:98–107.

Frouin, R., C. Gautier, and J. J. Morcrette. 1990. Downward longwave irradiance at the ocean surface from satellite data: Methodology and in situ validation. *Journal of Geophysical Research* 93(C1): 597–619.

Fuchs, M., and C. B. Tanner. 1966. Infrared thermometry of vegetation, *Agronomy Journal* 58:597–601.

Fuller, R., and N. Brown. 1996. A CORINE map of Great Britain by automated means: Techniques for automatic generalization of the land cover map of Great Britain. *International Journal of Geographical Information Systems* 10(8): 937–953.

Gautier, C., C. Diak, and S. Masse. 1980. A simple physical model to estimate incident solar radiation at the surface from GOES satellite data. *Journal of Applied Meteorology* 19:1,005–1,012.

Gong, P., and P. J. Howarth. 1992. Land-use classification of SPOT-HRV data using a cover-frequency method. *International Journal of Remote Sensing* 13(8): 1,459–1,471.

Goossens, R. E. A., M. El Badawi, T. K. Ghabour, and M. de Dapper. 1993. A simulation model to monitor the soil salinity in irrigated arable land in arid areas based upon remote sensing and GIS. *EARSeL Advances in Remote Sensing* 2(3): 165–171.

Goossens, E. M. C., R. E. A. Goossens, Th. K. Ghabour, and A. G. Gad. 1993. Detailed assessment of degradation processes in the agricultural land of a newly reclaimed area in Egypt, using multitemporal high resolution satellite data. *EARSeL Advances in Remote Sensing* 2(3): 91–101.

Goward, S. N., and A. S. Hope. 1989. Evaporation from combined reflected solar and emitted terrestrial radiation: Preliminary FIFE results from AVHRR data. *Advances in Space Research* 9:239–249.

Goward, S. N., and K. F. Huemmrich. 1992. Vegetation canopy PAR absorptance and the normalized difference vegetation index: An assessment using the SAIL model. *Remote Sensing of Environment* 39:110–114.

Goward, S. N., C. J. Tucker, and D. G. Dye. 1985. North American vegetation patterns observed with the NOAA-7 Advanced Very High Resolution Radiometer. *Vegetatio* 64:3–14.

Granger, R. J. 1997. Comparison of surface and satellite-derived estimates of evapotranspiration using a feedback algorithm. In *Applications of remote sensing in hydrology: Proceedings of the Third International Workshop, 16–18 October 1996, NASA, Goodard Space Flight Center, Greenbelt, Maryland, USA*, ed. G. W. Kite, A. Pietroniro, and T. J. Pultz, 71–81. NHRI Symposium 17. Saskatoon, Saskatchewan, Canada: National Hydrology Research Institute.

Griffith, C. G., W. L. Woodley, P. G. Grube, D. W. Martin, J. Stout, and D. N. Skidar. 1978. Rain estimation from geosynchronous satellite imagery-visible and infrared studies. *Monthly Weather Review* 106:1,153–1,171.

Griggs, M. 1968. Emissivities of natural surfaces in the 8 to 14 micron spectral region. *Journal of Geophysical Research* 73(24):7,545–7,551.

Gupta, S. K., 1989. A parameterization for longwave surface radiation from sun-synchronous satellite data. *Journal of Climate* 2:305–320.

Gutman, G. G. 1991. Vegetation indices for AVHRR: An update and future prospects. *Remote Sensing of Environment* 35:121–136.

Gutman, G. G., G. Ohring, D. Tarpley, and R. Ambroziak. 1989. Albedo of the US Great Plains as determined from NOAA-9 AVHRR data. *Journal of Climate* 2:608–617.

Hall, F. G, K. F. Huemmrich, and S. N. Goward. 1990. Use of narrow-band spectra to estimate the fraction of absorbed photosynthetically active radiation. *Remote Sensing of Environment* 28:47–54.

Hall, F. G., J. R. Townshend, and E. T. Engman. 1995. Status of remote sensing algorithms for estimation of land surface state parameters. *Remote Sensing of Environment* 51:138–156.

Hall, F. G., K. F. Huemmrich, S. J. Goetz, P. J. Sellers, and J. E. Nickeson. 1992. Satellite remote sensing of surface energy balance: Success, failures and unresolved issue in FIFE. *Journal of Geophysical Research* 97(D17): 19,061–19,089.

Hall-Konyves, K. 1990. Crop monitoring in Sweden. *International Journal of Remote Sensing* 11(3): 461–484.

Hanks, R. J. 1974. Model for predicting plant growth as influenced by evapotranspiration and soil water-use relationship: An overview. In *Limitations to efficient water use in crop production*, ed. H. M. Taylor, W. R. Jordan, and T. R. Sinclair, 393–411. Madison, Wisconsin USA: American Society of Agronomy.

Hardisky, M. A., V. Klemas, and F. C. Daiber. 1983. Remote sensing salt marsh biomass and stress detection. *Advances in Space Research* 2:219–229.

Hargreaves, G. H., and Z. A. Samani. 1985. Reference crop evapotranspiration from temperature. *Applied Engineering in Agriculture* 1(2): 96–99.

Hatfield, J. L. 1983. Remote sensing estimators of potential and actual crop yield. *Remote Sensing of Environment* 13(4): 301–311.

Hatfield, J. L. 1989. Aerodynamic properties of partial canopies. *Agricultural and Forest Meteorology* 46:15–22.

Hatfield, J. L., R. J. Reginato and S. B. Idso. 1984. Evaluation of canopy temperature-evapotranspiration models over various surfaces. *Agricultural and Forest Meteorology* 32:41–53.

Hatton, T. J., L. L. Pierce, and J. Walker. 1993. Ecohydrological changes in the Murray-Darling Basin: II. Development and tests of a water balance model. *Journal of Applied Ecology* 30:274–282.

Hawkins, R. H., A. T. Hjemfelt, and A. W. Zevenbergen. 1985. Runoff probability, storm depth and curve numbers. *Journal of the Irrigation and Drainage Division, ASCE* 111:330–340.

Heilman, J. L., and D. G. Moore. 1980. Thermography for estimating near-surface soil moisture under developing crop canopies. *Journal of Applied Meteorology* 19:324–328.

Heilman, J. L., W. E. Heilman, and D. G. Moore. 1982. Evaluating the crop coefficient using spectral reflectance. *Agronomy Journal* 74:967–971.

Hepner, G. F., T. Logan, N. Ritter, and N. Bryant. 1990. Artificial neural network classification using a minimal training set: Comparison to a conventional supervised classification. *Photogrammetric Engineering and Remote Sensing* 56(4): 469–473.

Hiler, E. A., and R. N. Clark. 1971. Stress day index to characterize effects of water stress on crop yields. *Transactions of the ASAE* 14:757–761.

Hipps, L. E. 1989. The infrared emissivities of soil and *Artemisia tridentata* and subsequent temperature corrections in a shrub-steppe ecosystem. *Remote Sensing of Environment* 27:337–342.

Hobbs, R. J., and H. A. Mooney. 1990. *Remote sensing of biosphere functioning.* New York: Springer-Verlag.

Hoogeboom, P. 1983. Classification of agricultural crops in radar images. *IEEE Transactions on Geoscience and Remote Sensing* 21(3): 329–336.

Hope, A. S., D. E. Petzold, S. N. Goward, and R. M. Ragan. 1986. Simulated relationships between spectral reflectance, thermal emissions and evapotranspiration of a soybean canopy. *Water Resources Bulletin* 22:1,011–1,019.

Hsu, K., X. Gao, S. Sorooshian, and H. V. Gupta. 1997. A neural network suitable for estimation of physical variables from satellite remotely sensed data. Duplicated.

Huete, A. R. 1988. A soil-adjusted vegetation index (SAVI). *Remote Sensing of Environment* 25:89–105.

Huete, A. R., R. D. Jackson, and D. F. Post. 1985. Spectral response of a plant canopy with different soil backgrounds. *Remote Sensing of Environment* 17:37–53.

Huising, E. J. 1993. Land use zones and land use patterns in the Atlantic Zone of Costa Rica. Ph.D. diss., Agricultural University, Wageningen, Netherlands. 222 p.

Hunt, G. R. 1977. Spectral signatures of particular minerals in the visible and near-infrared. *Geophysics* 42:501–513.

Hurtado, E., M. M. Artigao, and V. Caselles. 1994. Estimating maize (*Zea mays*) evapotranspiration from NOAA-AVHRR thermal data in the Albacete area, Spain. *International Journal of Remote Sensing* 15(10): 2,023–2,037.

Hussin, Y. A., and S. R. Shaker. 1996. Optical and radar satellite image fusion techniques and their applications in monitoring natural resources and land use changes. *AEU* (Archiv für Elektronik und Übertragunstech*) 50(2): 169-176.*

Huurneman, G., and L. Broekema. 1996. Classification of multi-sensor data using a combination of image analysis techniques. Paper E-2 in *Proceedings of the 17th Asian Conference on Remote Sensing*. Colombo: Survey Department. 6 p.

Huygen, J., 1989. *Estimation of rainfall in Zambia using Meteosat-TIR data: Monitoring agro-ecological resources with remote sensing and simulation.* ARS Report 12. Wageningen, The Netherlands: DLO-Winand Staring Centre. 71 pp.

IAH (International Association of Hydrogeologists). 1990. *International Symposium on Remote Sensing and Water Resources: Proceedings.* Enschede, Netherlands.

Idso, S. B., R. D. Jackson, W. L. Ehrler, and S. T. Mitchell. 1969. A method for determination of infrared emittance of leaves. *Ecology* 50:899–902.

Idso, S. B., R. D. Jackson, P. J. Pinter, R. J. Reginato, and J. L. Hatfield. 1981. Normalizing the stress-degree-day parameter for environmental variability. *Agricultural Meteorology* 24:45–55.

Idso, S. B., R. J. Reginato, R. D. Jackson, and P. J. Pinter. 1981. Measuring yield-reducing plant water potential depressions in wheat by infrared thermometry. *Irrigation Science* 2:205–212.

Idso, S. B., T. J. Schmugge, R. D. Jackson, and R. J. Reginato. 1975. The utility of surface temperature measurements for remote sensing of soil water studies. *Journal of Geophysical Research* 80(21): 3,044–3,049.

Imhoff, M. L., C. Vermillion, M. H. Story, A. M. Choudhury, A. Gafoor, and F. Polycon. 1987. Monsoon flood boundary delineation and damage assessment using space borne imaging radar and Landsat data. *Photogrammetric Engineering and Remote Sensing* 53:405–413.

Jackson, R. D. 1984. Total reflected solar radiation calculated from multi-band sensor data. *Agricultural and Forest Meteorology* 33:163–175.

Jackson, R. D., S. B. Idso, R. J. Reginato, and P. J. Pinter. 1980. Remotely sensed crop temperatures and reflectances as inputs to irrigation scheduling. In *Proceedings: American Society of Civil Engineers, Irrigation and Drainage Division, Specialty Conference, Boise, Idaho, 1980,* 390–397. New York: American Society of Civil Engineering.

Jackson, R. D., S. B. Idso, R. J. Reginato, and P. J. Pinter. 1981. Canopy temperature as a crop water stress indicator. *Water Resources Research* 17:1,133–1,138.

Jackson, R. D., W. P. Kustas, and B. J. Choudhury. 1988. A reexamination of the crop water stress index. *Irrigation Science* 9:309–317.

Jackson, R. D., P. J. Pinter, and R. J. Reginato. 1985. Net radiation calculated from remote multispectral and ground station meteorological data. *Agricultural and Forest Meteorology* 35:153–164.

Jackson, R. D., R. J. Reginato, and S. B. Idso. 1977. Wheat canopy temperatures: A practical tool for evaluating water requirements. *Water Resources Research* 13:651–656.

Jackson, R. D., T. J. Schmugge, and P. E. O'Neill. 1984. Passive microwave remote sensing of soil moisture from an aircraft platform. *Remote Sensing of Environment* 14:135–151.

Jackson, T. J., E. T. Engman, D. Le Vine, T. J. Schmugge, R. Lang, E. Wood, and W. Teng. 1994. Multitemporal passive microwave mapping in Machydro'90. *IEEE Transactions on Geoscience and Remote Sensing* 32(1): 201–206.

Janssen, L. L. F., and H. Middelkoop. 1992. Knowledge–based crop classification of a Landsat TM image. *International Journal of Remote Sensing* 13(15): 2,827–2,837.

Janssen, L. F., and M. Molenaar. 1995. Terrain objects, their dynamics and their monitoring by the integration of GIS and remote sensing. *IEEE Transactions on Geoscience and Remote Sensing* 33(3): 749–758.

Jarvis, P. G. 1976. The interpretation of the variations in leaf water potential and stomatal conductance found in canopies in the field. *Philosophical Transactions of the Royal Society of London* B273:593–610.

Jayasekera, A. A., and W. R. Walker. 1990. Remotely sensed data and geographic information systems: For management and appraisal of large scale irrigation projects in the developing countries. In *Advances in planning, design, and management of irrigation systems as relate to sustainable land use*, ed. J. Feyen, E. Mwendera, and M. Badji, 453-461. Leuven, Belgium: Center for Irrigation Engineering.

Jensen, J. R. 1986. *Introductory digital image processing: A remote sensing perspective.* Englewood Cliffs, New Jersey, USA: Prentice-Hall. 373 p.

Jewell, N. 1989. An evaluation of multi-date SPOT data for agriculture and land use mapping in the United Kingdom. *International Journal of Remote Sensing* 10:939–951.

Johnstone, R. M., and M. M. Barson. 1990. *An assessment of the use of remote sensing techniques in land degradation studies.* Bulletin 5. Canberra, Australia: Australian Department of Primary Industries and Energy, Bureau of Rural Resources. 64 p.

Jordan, C. F. 1969. Derivation of leaf area index from quality of light on the forest floor. *Ecology* 50:663–666.

Joseph, G. 1997. Role of remote sensing in resource management for arid regions with special reference to western Rajasthan. *Current Science* 72(10): 47–54.

Joshi, M. D., and B. Sahai. 1993. Mapping of salt-affected land in Saurashtra coast using Landsat satellite data. *International Journal of Remote Sensing* 14(10): 1,919–1,929.

Kahle, A. B. 1987. Surface emittance, temperature and thermal inertia derived from Thermal Infrared Multispectral Scanner (TIMS) data for Death Valley, California. *Geophysics* 52(7): 858–874.

Kahle, A. B., and R. E. Alley. 1992. Separation of temperature and emittance in remotely sensed radiance measurements. *Remote Sensing of Environment* 42:107–111.

Kaufman, Y. J., and D. Tanre. 1992. Atmospherically resistant vegetation index (ARVI) for EOS-MODIS. *IEEE Transactions on Geoscience and Remote Sensing* 30:261–270.

Kauth, R. J., and G. S. Thomas. 1976. The tasseled cap: A graphic description of spectral-temporal development of agricultural crops as seen by Landsat. In *Symposium on machine processing of remotely sensed data*, 41–51. New York: Institute of Electrical and Electronics Engineers.

Kealy, P. S., and S. J. Hook. 1993. Separating temperature and emissivity in thermal infrared multispectral scanner data: Implications for recovering land surface temperatures. *IEEE Transactions on Geoscience and Remote Sensing* 31:1155–1164.

Kerdiles, H., G. Magrin, C. M. Rebella, and B. Seguin. 1995. Vegetation monitoring and yield prediction from NOAA-AVHRR GAC data in the Argentinean Pampa. In *Multispectral and microwave sensing of forestry, hydrology and national resources*, ed., E. Mougin, K. J. Ranson, J. A. Smith, 151-162. Proceedings of SPIE, vol. 2,314. Bellingham, Washington, USA: International Society for Optical Engineering.

Kerr, Y. H., J. Imbernon, G. Dedieu, O. Hautecoeur, J. P. Lagouarde, and B. Seguin. 1989. NOAA AVHRR and its uses for rainfall and evapotranspiration monitoring. *International Journal of Remote Sensing* 10:847–854.

Kerr, Y. H., J. P. Lagouarde, and J. Imbernon. 1992. Accurate land surface retrieval from AVHRR data with use of an improved split window algorithm. *Remote Sensing of Environment* 41:197–209.

King, D. J. 1995. Airborne multispectral digital camera and video sensors: A critical review of system designs and applications. *Canadian Journal of Remote Sensing* 21(3): 245-273.

Kite, G. W. 1995. Use of remotely sensed data in the hydrological modelling of the upper Columbia watershed *Canadian Journal of Remote Sensing* 22(1): 14–22.

Kite, G. W., and N. Kouwen. 1992. Watershed modeling using land classifications. *Water Resources Research* 28(12): 3,193–3,200.

Kite, G. W., A. Dalton, and K. Dion. 1994. Simulation of streamflow in a macroscale watershed using general circulation model data. *Water Resources Research* 30(5): 1,547–1,559.

Kite, G. W., A. Pietroniro, and T. J. Pultz, eds. 1997. *Applications of remote sensing in hydrology: Proceedings of the Third International Workshop, 16–18 October 1996, NASA, Goodard Space Flight Center, Greenbelt, Maryland, USA*. NHRI Symposium 17. Saskatoon, Saskatchewan, Canada: National Hydrology Research Institute. 350 p.

Kiyonary, F., H. Shimoda, Y. Matumae, R. Yamaguchi, and T. Sakata. 1988. Evaluation of unsupervised methods for land cover/use classification of Landsat-TM data. *Geocarto International* 2:37–44.

Koblinsky, C. J., R. T. Clarke, A. C. Brenner, and H. Frey. 1993. The measurement of river levels with satellite altimetry. *Water Resources Research* 29:1,839–1,848.

Koepke, P. 1989. Removal of atmospheric effects from AVHRR albedos. *Journal of Applied Meteorology* 28(6): 1,341–1,348.

Koepke, P., K. T. Kriebel, and B. Dietrich. 1985. The effect of surface reflection and of atmospheric parameters on the shortwave radiation budget. *Advances in Space Research* 5:351–354.

Kontoes, C., G. G. Wilkinson, A. Burril, S. Goffredo, and J. Megier. 1993. An experimental system for the integration of GIS data in knowledge-based image analysis for remote sensing of agriculture. *International Journal of Geographical Information Systems* 7(3): 247–262.

Kornfield, J., and J. Susskind. 1977. On the effect of surface emissivity on temperature retrievals. *Monthly Weather Review* 105:1,605–1,608.

Kustas, W. P., and C. S. T. Daughtry. 1990. Estimation of the soil heat flux/net radiation ratio from spectral data. *Agricultural and Forest Meteorology* 49:205–223.

Kustas, W. P., and J. M. Norman. 1996. Use of remote sensing for evapotranspiration monitoring over land surfaces. *IAHS Hydrological Sciences Journal* 41(4): 495–516.

Kustas, W. P., M. S. Moran, K. S. Humes, D. I. Stannard, P. J. Pinter, L. E. Hipps, E. Swiatek, and D. C. Goodrich. 1994. Surface energy balance estimates at local and regional scales using optical remote sensing from aircraft platform and atmospheric data collected over semiarid rangelands. *Water Resources Research* 30(5): 1,241–1,259.

Labed, J., and M. P. Stoll. 1991. Spatial variability of land surface emissivity in the thermal infrared band: Spectral signature and effective surface temperature. *Remote Sensing of Environment* 38:1–17.

Laguette, S., A. Vidal, and P. Vossen. 1995. Monitoring of yield indicators in Europe by combined use of NOAA-AVHRR and an agrometeorological model. In *International Colloquium on Photosynthesis and Remote Sensing, Montpellier, France 28–30 August 1995*, 323–326. Paris: European Association of Remote Sensing Laboratories.

Lambin, E. F., and D. Ehrlich. 1996. The surface temperature-vegetation index space for land cover and land-cover change analysis. *International Journal of Remote Sensing* 17(3): 463–487.

Lantieri, D. 1995. Use of high-resolution satellite data for irrigation management and monitoring: Pilot study in Indonesia. In *Use of remote sensing techniques in irrigation and drainage*, ed. A. Vidal and J. A. Sagardoy, 75–79. Water Reports 4. Rome: FAO.

Lathrop, R. G., and T. M. Lillesand. 1987. Calibration of Thematic Mapper thermal data for water surface temperature mapping: A case study of the Great Lakes. *Remote Sensing of Environment* 22:297–307.

Leguizamon, S., H. Pelgrum, S. Azzali, and M. Menenti. 1996. Unsupervised classification of remotely sensed data by means of the Fuzzy C-means approach. In *Fourier analysis of temporal NDVI in the Southern African and American continents*, ed. S. Azzali and M. Menenti, 25–36. Report 108. Wageningen, Netherlands: DLO-Winand Staring Centre.

Li, Z., and H. G. Leighton. 1993. Global climatologies of solar radiation budgets at the surface and in the atmosphere for 5 years of ERBE data. *Journal of Geophysical Research* 98(D3): 4,919–4,930.

Lillesand, T. M., and R. W. Kiefer. 1987. *Remote sensing and image interpretation.* New York: John Wiley and Sons. 721 p.

Lloyd, D. 1989. A phenological description of Iberian vegetation using short wave vegetation index image. *International Journal of Remote Sensing* 10:827–833.

Lo, T. H. C., F. L. Scarpace, and T. M. Lillesand. 1986. Use of multitemporal spectral profiles in agricultural land cover classification. *Photogrammetric Engineering and Remote Sensing* 52:535–544.

Lourens, U. 1990. Using Landsat TM to monitor irrigated land at the individual farm level. In *Remote sensing in evaluation and management of irrigation*, ed. M. Menenti, 231–235. Mendoza, Argentina: Instituto Nacional de Ciencia y Técnicas Hídricas.

Lourens, U. W., C. M. van Sandwyk, J. M. de Jager, and W. J. van den Berg. 1995. Accuracy of an empirical model for estimating daily irradiance in South Africa from METEOSAT weather satellite imagery. *Agricultural and Forest Meteorology* 71(1-2): 75–86.

Luvall, J. C., and H. R. Holbo. 1989. Measurements of short-term thermal response of coniferous forest canopies using thermal scanner data. *Remote Sensing of Environment* 27: 1–10.

Maas, S. J. 1991. Use of remotely sensed information in agricultural crop yield. *Agronomy Journal* 80:655–662.

Makkink, G. F. 1957. Testing the Penman formula by means of lysimeters. *Journal of International Water Engineering* 11:277–288.

Maselli, F., L. Petkov, G. Maracchi, and C. Conese. 1996. Eco-climatic classification of Tuscany through NOAA-AVHRR data. *International Journal of Remote Sensing* 17(12): 2,369–2,384.

Massoud, F. I. 1977. The use of satellite imagery in detecting and delineating salt affected soils. In *1er colloque pedologie et teledection*, 77–84. Rome: Association Internationale de la Science du Sol.

McNaughton, K. G., and B. J. J. M. van den Hurk. 1995. A "Lagrangian" revision of the resistors in the two-layer model for calculating the energy budget of a plant canopy. *Boundary Layer Meteorology* 74:262–288.

Meeuwissen, I. J. M. 1989. *Mapping of vegetation and evapotranspiration in the Rio Tunuyan irrigation scheme, Mendoza, Argentina using a satellite image.* ICW Note 1965. Wageningen, Netherlands: DLO-Winand Staring Centre. 42 p.

Menenti, M. 1984. Physical aspects and determination of evaporation in deserts applying remote sensing techniques. Ph.D. thesis, DLO-Winand Staring Centre, Wageningen, Netherlands. 202 p.

Menenti, M., ed. 1990. *Remote sensing in evaluation and management of irrigation.* Mendoza, Argentina: Instituto Nacional de Ciencia y Técnicas Hídricas. 337 p.

Menenti, M. 1993. Understanding land surface evapotranspiration with satellite multispectral measurements. *Advances in Space Research* 13(5): 89–100.

Menenti, M., and B. J. Choudhury. 1993. Parameterization of land surface evaporation by means of location dependent potential evaporation and surface temperature range. In *Exchange processes at the land surface for a range of space and time scales,* ed. H.-J. Bolle, R. A. Feddes, and J. D. Kalma, 561–568 International Association of Hydrological Sciences Publication 212. Wallingford, U.K.: Institute of Hydrology.

Menenti, M., and J. C. Ritchie. 1994. Estimation of effective aerodynamic roughness of Walnut Gulch watershed with laser altimeter measurements. *Water Resources Research* 30(5): 1,329–1,337.

Menenti, M., S. Azzali, and G. D'Urso. 1995. Management of irrigation schemes in arid countries. In *Use of remote sensing techniques in irrigation and drainage,* ed. A. Vidal and J. A. Sagardoy, 81–89. Water Reports 4. Rome: FAO.

Menenti, M., S. Azzali, D. A. Collado, and S. Leguizamon. 1986. Multitemporal analysis of Landsat multispectral scanner (MSS) and Thematic Mapper ™ data to map crops in the Po valley (Italy) and in Mendoza (Argentina). In *Remote sensing for resources development and environmental management,* ed. M. C. J. Damen, G. Sicco Smit, and H. Th. Verstappen, 293–299. Rotterdam: Balkema.

Menenti, M., S. Azzali, W. Verhoef, and R. van Swol. 1993. Mapping agro-ecological zones and time lag in vegetation growth by means of Fourier analysis of time series of NDVI images. *Advances in Space Research* 13:233–237.

Menenti, M., W. G. M. Bastiaanssen, and D. van Eick. 1989. Determination of surface hemispherical reflectance with Thematic Mapper data. *Remote Sensing of Environment* 28:327–337.

Menenti, M., W. G. M. Bastiaanssen, D. van Eick, and M. A. Abd el Karim. 1989. Linear relationships between surface reflectance and temperature and their application to map actual evaporation of groundwater. *Advances in Space Research* 9(1): 165–176.

Menenti, M., A. Lorkeers, and M. Vissers. 1986. An application of Thematic Mapper data in Tunisia. *ITC Journal* no. 1:35–42.

Mirabile, C., R. Hudson, G. Ibanez, and H. Masotta. 1995. Detection, delimitation, and dynamic control of saline areas in irrigated soils through the use of Landsat TM satellite images. In *Use of remote sensing techniques in irrigation and drainage,* ed. A. Vidal and J. A. Sagardoy, 179–184. Water Reports 4. Rome: FAO.

Mogensen, V. O., C. R. Jensen, G. Mortensen, J. H. Thage, J. Koribidis, and A. Ahmed. 1996. Spectral reflectance index as an indicator of drought of field grown oilseed rape (*Brassica napus* L.). *European Journal of Agronomy* 5:125–135.

Molden, D. J. 1997. Conceptual framework for water accounting. International Irrigation Management Institute, Colombo. Duplicated.

Monteith, J. L. Evaporation and the environment. In *The state and movement of water in living organisms,* ed. G. E. Fogg, 205–234. London: Cambridge University Press.

Monteith, J. L., and M. H. Unsworth. 1990. *Principles of environmental physics.* London: Edward Arnold. 291 p.

Moran, M. S. 1994. Irrigation management in Arizona using satellites and airplanes. *Irrigation Science* 15:35–44.

Moran, M. S., and R. D. Jackson. 1991. Assessing the spatial distribution of evapotranspiration using remotely sensed inputs. *Journal of Environmental Quality* 20:725–737.

Moran, M. S., T. R. Clarke, Y. Inoue, and A. Vidal. 1994. Estimating crop water deficit using the relation between surface-air temperature and spectral vegetation index. *Remote Sensing of Environment* 49(2): 246–263.

Moran, M. S., R. D. Jackson, L. H. Raymond, L. W. Gay, and P. N. Slater. 1989. Mapping surface energy balance components by combining Landsat Thematic Mapper, and ground-based meteorological data. *Remote Sensing of Environment* 30:77–87.

Moran, M. S., R. D. Jackson, P. N. Slater, and P. M. Teillet. 1992. Evaluation of simplified procedures for retrieval of land surface reflectance factors from satellite sensor output. *Remote Sensing of Environment* 41:169–184.

Moran, M. S., S. J. Maas, and P. J. Pinter. 1995. Combining remote sensing and modeling for estimating surface evaporation and biomass production. *Remote Sensing Reviews* 12:335–353.

Morton, F. I. 1983. Operational estimates of areal evapotranspiration and their significance to the science and practice of hydrology. *Journal of Hydrology* 66:1–76.

Moser, W., and E. Raschke. 1984. Incident solar radiation over Europe estimated from Meteosat data. *Journal of Climate and Applied Meteorology* 24:389–401.

Mougenot, B. M. Pouget, and G. F. Epema. 1993. Remote sensing of salt affected soils. *Remote Sensing Reviews* 7:241–259.

Mubekti, K., K. Miyama, and S. Ogawas. 1991. Study on rice yield distribution by using Landsat TM data: The Hokkaido National Agricultural Experiment Station. *Rural Development Research* 5:101–113.

Mulders, M. A. 1987. *Remote sensing in soil science.* Developments in Soil Science 15. Amsterdam: Elsevier.

Mulders, M. A., and G. F. Epema. 1986. The Thematic Mapper: A new tool for soil mapping in arid areas. *ITC Journal* no. 1: 24–29.

Murthy, C. S., S. Thiruvengadachari, P. V. Raju, and S. Jonna. 1996. Improved ground sampling and crop yield estimation using satellite data. *International Journal of Remote Sensing* 17(5): 945–956.

Musiake, K., T. Oki, T. Nakaegawa, and K. Wakasa. 1995. Verification experiment of extraction of soil moisture information using SAR mounted on JERS-1/ERS-1. In Vol. 2 of *Final report of JERS-1/ERS-1 systems verification program*, 617–624. Tokyo: Ministry of International Trade and Industry and National Space Development Agency.

Myneni, R. B., and D. L. Williams. 1994. On the relationship between FAPAR and NDVI. *Remote Sensing of Environment* 49(3): 200–211.

Nacke, G. 1991. Surface albedo derived from Meteosat imagery with an application to Africa. *Journal of Geophysical Research* 96(D10): 18,581–18,601.

Nageswara Rao, P. P., and A. Mohankumar. 1994. Cropland inventory in the command area of Krishnarajasagar project using satellite data. *International Journal of Remote Sensing* 15(6): 1,295–1,305.

Neale, C. M. U., R. H. Ahmed, M. S. Moran, P. J. Pinter, J. Qi, and T. R. Clarke. 1996. Estimating seasonal cotton evapotranspiration using canopy reflectance. In *Evapotranspiration and irrigation scheduling: Proceedings of the International Conference, November 3 to 6, 1996, San Antonio, Texas, USA*, ed. C. R. Camp, E. J. Sadler, and R. E. Yoder, 173–181. St. Joseph, Michigan, USA: American Society of Agricultural Engineers.

Neale, C. M. U., W. C. Bausch, and D. F. Heeremann. 1989. Development of reflectance-based crop coefficients for corn. *Transactions of the ASAE* 32(6): 1,891–1,899.

Negri, A. J., R. F. Adler, R. A. Maddox, K. W. Howard, and P. R. Keehn. 1993. A regional rainfall climatology over Mexico and southwest United States derived from passive microwave and geosynchronous infrared data. *Journal of Climate* 6:2,144–2,161.

Nemani, R. R., and S. W. Running. 1989. Estimation of regional surface resistance to evapotranspiration from NDVI and thermal-IR AVHRR data. *Journal of Applied Meteorology* 28:276–284.

Nemani, R. R., L. Pierce, S. W. Running, and S. Goward. 1993. Developing satellite-derived estimates of surface moisture stress. *Journal of Applied Meteorology* 32:548–557.

Nerry, F., J. Labed, and M. P. Stoll. 1990. Spectral properties of land surfaces in the thermal infrared. 1. Laboratory measurements of absolute spectral emissivity signatures. *Journal of Geophysical Research* 95(B5): 7,027–7,044.

Newell, N. 1989. An evaluation of multi-date SPOT data for agriculture and land use mapping in the United Kingdom. *International Journal of Remote Sensing* 10:939–951.

Nieuwenhuis, G. J. A., A. J. W. de Wit, T. van der Wal, C. A. Mucher, and H. J. C. van Leeuwen. 1996. *Integrated use of high and low resolution satellite data and crop growth models*. Wageningen, Netherlands: DLO-Winand Staring Centre. 129 p.

Nieuwenhuis, G. J. A., E. M. Smidt, and H. A. M. Thunnissen. 1985. Estimation of regional evapotranspiration of arable crops from thermal infrared images. *International Journal of Remote Sensing* 6(8): 1,319–1,334.

Njoku, E. G., and D. Entekhabi. 1996. Passive microwave remote sensing to soil moisture. *Journal of Hydrology* 184:101–129.

Norman, J. M., and F. Becker. 1995. Terminology in thermal infrared remote sensing of natural surfaces. *Agricultural and Forest Meteorology* 77:153–166.

Norman, J. M., M. Divakarla, and N. S. Goel. 1995. Algorithms for extracting information from remote thermal-IR observations of the earth's surface. *Remote Sensing of Environment* 51:157–168.

Norman, J. M., W. P. Kustas, and K. S. Humes. 1995. Source approach for estimating soil and vegetation energy fluxes in observations of directional radiometric surface temperature. *Agricultural and Forest Meteorology* 77:263–293.

Nunez, M., T. L. Hart, and J. D. Kalma. 1984. Estimating solar radiation in a tropical environment using satellite data. *Journal of Climatology* 4:573–585.

Nunez, M., W. J. Skirving, and N. R. Viney. 1987. A technique for estimating regional surface albedos using geostationary satellite data. *Journal of Climatology* 7:1–11.

Ormsby, J. P., B. J. Choudhury, and M. Owe. 1987. Vegetation spatial variability and its effect on vegetation indices. *International Journal of Remote Sensing* 8:1,301–1,306.

Ottle, C., D. Vidal-Madjar, A. L. Cognard, C. Loumagne, and M. Normand. 1996. Radar and optical remote sensing to infer evapotranspiration and soil moisture. In *Scaling up in hydrology using remote sensing*, ed. J. B. Stewart, T. Engman, R. A. Feddes, and Y. Kerr, 221–233. New York: John Wiley.

Owe, M., A. T. C. Chang, and A. A. van de Griend. 1992. Surface moisture and satellite microwave observations in semi-arid southern Africa. *Water Resources Research* 28:829–839.

Paloscia, S., P. Pampaloni, L. Chiarantini, P. Coppo, S. Gagliani, and G. Luzi. 1993. Mulitfrequency passive microwave remote sensing of soil moisture and roughness. *International Journal of Remote Sensing* 14(3): 467–483.

Paltridge, G. W., and R. M. Mitchell. 1990. Atmospheric and viewing angle correction of vegetation indices and grassland fuel moisture content derived from NOAA-AVHRR. *Remote Sensing of Environment* 31:121–135.

Pampaloni, P., and S. Paloscia. 1986. Microwave emission and plant water content: A comparison between field measurement and theory. *IEEE Transactions on Geoscience and Remote Sensing* 24:900–905.

Park, A. B., R. N. Colwell, and V. F. Meyers. 1968. Resource survey by satellite: Science fiction coming true. In *Yearbook of agriculture*, 13–19. Washington D.C.: U.S. Government Printing Office.

Patel, N. K., N. Ravi, R. R. Navalgund, R. R. Dash, K. C. Dash, and S. Patnaik. 1991. Estimation of rice yield using IRS-1A digital data in coastal tract of Orissa. *International Journal of Remote Sensing* 12:2,259–2,266.

Pedley, M. I., and P. J. Curran. 1991. Per-field classification: An example using SPOT HRV imagery. *International Journal of Remote Sensing* 12(11): 2,181–2,192.

Pedrycz, W. 1990. Fuzzy sets in pattern recognition: Methodology and methods. *Pattern Recognition* 23(1/2): 121–146.

Pelgrum, H., and W. G. M. Bastiaanssen. 1996. An intercomparison of techniques to determine the area-averaged latent heat flux from individual in situ observations: A remote sensing approach using the European Field Experiment in a Desertification-Threatened Area data. *Water Resources Research* 32(9): 2,775–2,786.

Penman, H. L. 1948. Natural evaporation from open water, bare soil and grass. *Proceedings Royal Society, London*, Series A, 193:120–146.

Perry, C. J. 1996. Quantification and measurement of a minimum set of indicators of the performance of irrigation systems. International Irrigation Management Institute, Colombo, Sri Lanka. Duplicated. 11 p.

Perry, E. M., and T. N. Carlson. 1988. Comparison of active microwave soil water content with infrared surface temperatures and surface moisture availability. *Water Resources Research* 24:1,818–1,824.

Perry, E. M., and M. S. Moran. 1994. An evaluation of atmospheric corrections of radiometric surface temperatures for a semiarid rangeland watershed. *Water Resources Research* 30:1,261–1,269.

Pestemalci, V., U. Dinc, I. Yegingil, M. Kandirmaz, M. A. Cullu, N. Ozturk, and E. Aksoy. 1995. Acreage estimation of wheat and barley fields in the province of Adana, Turkey. *International Journal of Remote Sensing* 16(6): 1,075–1,085.

Petty, G. W. 1995. The status of satellite-based rainfall estimation over land. *Remote Sensing of Environment* 51:125–137.

Pinker, R. T. 1985. Determination of surface albedo from satellites. *Advances in Space Research* 5:333–343.

Pinker, R. T., and J. A. Ewing. 1987. Simulations of the GOES visible sensor to changing surface and atmospheric conditions. *Journal of Geophysical Research* 92(D4): 4,001–4,009.

Pinker, R. T., R. Frouin, and Z. Li. 1995. A review of satellite methods to derive surface shortwave irradiance. *Remote Sensing of Environment* 51:105–124.

Pinter, P. J., K. E. Fry, G. Guinn, and J. R. Mauney. 1983. Infrared thermometry: A remote sensing technique for predicting yield in water-stressed cotton. *Agricultural Water Management* 6:385–395.

Pinty, B., and D. Ramond. 1987. A method for the estimate of broadband directional surface albedo from a geostationary satellite. *Journal of Climate and Applied Meteorology* 26:1,709–1,722.

Pinty, B., and M. M. Verstraete. 1992. GEMI: A non-linear index to monitor global vegetation from satellites. *Vegetatio* 101:15–20.

Prata, A. J. 1993. Land surface temperature derived from the Advanced Very High Resolution Radiometer and the Along-Track Scanning Radiometer: 1. Theory. *Journal of Geophysical Research–Atmospheres* 98(D9): 16,689–16,702.

Preuss, H. J., and F. Geleyn. 1984. Surface albedos derived from satellite data and their impact on forecast models. *Archiv fuer Meteorologie, Geophysik, und Bioklimatologie, Serie A* 29: 345–356.

Price, J. C. 1984. Land surface temperature measurements from the split window channels of the NOAA-7 Advanced Very High Resolution Radiometer. *Journal of Geophysical Research* 89(D5): 7,231–7,237.

Price, J. C. 1990. Using spatial context in satellite data to infer regional scale evapotranspiration. *IEEE Transactions on Geoscience and Remote Sensing* 28:940–948.

Priestley, C. H. B., and R. J. Taylor. 1972. On the assessment of surface heat flux and evapotranspiration using large scale parameters. *Monthly Weather Review* 100:81–92.

Qi, J., A. L. Chehbouni, A. R. Huete, Y. H. Kerr, and S. Sorooshian. 1994. A modified soil adjusted vegetation index (MSAVI). *Remote Sensing of Environment* 48:119–126.

Qi. J., A. R. Huete, M. S. Moran, A. Chehbouni, and R. D. Jackson. 1993. Interpretation of vegetation indices derived from multitemporal SPOT images. *Remote Sensing of Environment* 44:89–101.

Quarmby, N. A., M. Milnes, T. L. Hindle, and N. Silleos. 1993. The use of multi-temporal NDVI measurements from AVHRR data for crop yield estimation and prediction. *International Journal of Remote Sensing* 14(2): 199–210.

Ragan, R. M., and T. J. Jackson. 1980. Runoff synthesis using Landsat and SCS model. *Journal of the Hydraulic Division, ASCE* 106:667–678.

Rajan, M. S. 1991. *Remote sensing and geographic information system for natural resource management.* Manila: Asian Development Bank. 202 p.

Rambal, S., B. Lacaze, and T. Winkel. 1990. Testing an area-weighted model for albedo or surface temperature of mixed pixels in Mediterranean woodlands. *International Journal of Remote Sensing* 11:1,495–1,499.

Rango, A. 1990. Remote sensing of water resources: Accomplishments, challenges and relevance to global monitoring. In *International Symposium on Remote Sensing and Water Resources: Proceedings,* 3–16. Enschede, Netherlands: International Association of Hydrogeologists.

Rango, A., A. Feldman, T. George, and R. Ragan. 1983. Effective use of Landsat data in hydrologic models. *Water Resources Bulletin* 19(2): 165–174.

Rao, B. R., R. S. Dwivedi, L. Venkataratnam, T. Ravishankar, S. S. Thammappa, G. P. Bhargava, and A. N. Singh. 1991. Mapping the magnitude of sodicity in part of the Indo-Gangetic plains of Uttar Pradesh, Northern India using Landsat data. *International Journal of Remote Sensing* 12: 419–425.

Raschke, E., and M. Rieland. 1989. Downward solar radiation from geostationary satellite data. *Weather* 44:311–314.

Raschke, E., T. H. vonder Haar, W. Bandeen, and M. Pasternaak. 1973. The annual radiation balance of the earth atmosphere system during 1969–1970 from Nimbus 3 measurements. *Journal of Atmospheric Science* 30:341–364.

Rasmussen, M. S. 1992. Assessments of millet yields and production in northern Burkino Faso using integral NDVI from the AVHRR. *International Journal of Remote Sensing* 18:3,431–3,442.

Raupach, M. R. 1994. Simplified expressions for vegetation roughness length and zero-plane displacement as functions of canopy height and area index. *Boundary-Layer Meteorology* 71:211–216.

Reginato, R. J., R. D. Jackson, and P. J. Pinter. 1985. Evapotranspiration calculated from remote multispectral and ground station meteorological data. *Remote Sensing of Environment* 18:75–89.

Rejmankova, E., D. R. Roberts, A. Pawley, S. Manguin, and J. Polanco. 1995. Predictions of adult *Anopheles albimanus* densities in villages based on distances to remotely sensed larval habitats. *American Journal of Tropical Medicine and Hygiene* 53(5): 482–488.

Richards, J. A. 1986. *Remote sensing digital image analysis: An introduction.* Berlin: Springer-Verlag. 281 p.

Richardson, A. J., and C. L. Wiegand. 1977. Distinguishing vegetation from soil background information. *Photogrammetric Engineering and Remote Sensing* 43:1,541–1,552.

Ritchie, J. T. 1972. Model for predicting evaporation from a row crop with incomplete cover. *Water Resources Research* 8(5): 1,204–1,213.

Roerink, G. J., W. G. M. Bastiaanssen, J. Chambouleyron, and M. Menenti. 1997. Relating crop water consumption to irrigation water supply by remote sensing. *Water Resources Management* 11(6): 445-465.

Rogers, D. J. 1991. Satellite imagery, tsetse and trypanosomiasis in Africa. *Preventive Veterinary Medicine* 11:201–220.

Rondeaux, G. 1995. Vegetation monitoring by remote sensing: A review of biophysical indices. *Photo-Interpretation* no. 3:197–216.

Rondeaux, G., M. Steven, and F. Baret. 1996. Optimization of soil-adjusted vegetation indices. *Remote Sensing of Environment* 55:95–107.

Roo, A. P. J. de. 1996. The LISEM Project. *Hydrological Processes* 10:1,021–1,025.

Rosema, A. 1990. Comparison of Meteosat-based rainfall and evapotranspiration mapping in the Sahel region. *International Journal of Remote Sensing* 11(12): 2,299–2,309.

Rosenthal, W. D., J. C. Harlan, and B. J. Blanchard. 1982. Case study—estimating antecedent precipitation index from Heat Capacity Mapping Mission day thermal infrared data. *Hydrological Sciences Journal* 27:415–426.

Rossow, W. B., and Y. C. Zhang. 1995. Calculation of surface and top of atmosphere radiative fluxes from physical quantities based on ISCCP data sets: 2. Validation and first results. *Journal of Geophysical Research–Atmospheres* 100(D1): 1,167–1,197.

Rubio, E., V. Caselles, and C. Badenas. 1996. Emissivity measurements of several soils and vegetation types in the 8-14 mm waveband: Analysis of two field methods. *Remote Sensing of Environment* 59(3): 490–521.

Rudorff, B. F. T., and G. T. Batista. 1991. Wheat yield estimation at the farm level using TM Landsat and agrometeorological data. *International Journal of Remote Sensing* 12:2,477–2,484.

Saha, S. K., M. Kudrat, and S. K. Bhan. 1990. Digital processing of Landsat TM data for wasteland mapping in parts of Aligarh District, Uttar Pradesh, India. *International Journal of Remote Sensing* 11:485–492.

Salisbury, J. W., and D. M. D'Aria. 1992a. Emissivity of terrestrial materials in the 8–14 mm atmospheric window. *Remote Sensing of Environment* 42:83–106.

Salisbury, J. W., and D. M. D'Aria. 1992b. Infrared (8–14 mm) remote sensing of soil particle size. *Remote Sensing of Environment* 42:157–165.

Satterlund, D. R. 1979. An improved equation for estimating longwave radiation from the atmosphere. *Water Resources Resources* 15:1,649–1,650.

Saunders, R. W. 1990. The determination of broad band surface albedo from AVHRR visible and near-infrared radiances. *International Journal of Remote Sensing* 11:49–67.

Schmetz, P., J. Schmetz, and E. Raschke. 1986. Estimation of daytime downward longwave radiation at the surface from satellite and grid point data. *Theoretical and Applied Climatology* 37:136–149.

Schmugge, T. J., and F. Becker. 1991. Remote sensing observations for the monitoring of land-surface fluxes and water budgets. In *Land surface evaporation: Measurement and parameterization*, ed. T. J. Schmugge and J.-C. André, 337–347. New York: Springer-Verlag. 424 p.

Schmugge, T. J., F. Becker, and Z. L. Li. 1991. Spectral emissivity variations observed in airborne surface temperature measurements. *Remote Sensing of Environment* 35:95–104.

Schmugge, T. J., J. R. Wang, and G. Asrar. 1988. Results from the Push Broom Microwave Radiometer flights near the Konza Prairie in 1985. *IEEE Transactions on Geoscience and Remote Sensing* 26:590–596.

Schotten, C. G. J., W. W. L. van Rooy, and L. L. F. Janssen. 1995. Assessment of the capabilities of multi-temporal ERS-1 SAR data to discriminate between agricultural crops. *International Journal of Remote Sensing* 16(14): 2,619–2,637.

Schreier, G., K. Maeda, and B. Guindon. 1991. Three spaceborne SAR sensors: ERS-1, JERS-1 and RADARSAT: Competition or synergism? *Geographical Information Systems* 4:20–27.

Schultz, G. A. 1988. Remote sensing in hydrology. *Journal of Hydrology* 100:239–265.

Schultz, G. A. 1993. Hydrological modelling based on remote sensing information. *Advances in Space Research* 13:149–166.

Schuurmans, W., and G. Pichel. 1996. Management of water delivery systems (RIBASIM/OMIS). In *Dutch experience in irrigation water management modelling*, ed. B. J. van den Broek, 87–102. Report 123. Wageningen, Netherlands: DLO-Winand Staring Centre.

Seckler, D., U. Amarasinghe, D. Molden, R. De Silva, and R. Barker. 1998. *World water demand and supply, 1990 to 2025: Scenario's and issues*. Research Report 19. Colombo: International Irrigation Management Institute.

Seguin, B., and B. Itier. 1983. Using midday surface temperature to estimate daily evaporation from satellite thermal IR data. *International Journal of Remote Sensing* 4:371–383.

Seguin, B., E. Assad, J. P. Freteaud, J. Imbernon, Y. Kerr, and J. P. Lagouarde. 1989. Use of meteorological satellites for water balance monitoring in Sahelian regions. *International Journal of Remote Sensing* 10:1,101–1,117.

Sellers, P. J., M. D. Heiser, and F. G. Hall. 1992. Relations between surface conductance and spectral vegetation indices at intermediate (100 m^2–15 km^2) length scales. *Journal of Geophysical Research–Atmospheres* 97(D17): 19,033–19,059.

Sellers, P. J., B. W. Meeson, F. G. Hall, G. Asrar, R. E. Murphy, R. A. Schiffer, F. P. Bretherton, R. E. Dickinson, R. G. Ellingson, C. B. Field, K. F. Huemmrich, C. O. Justice, J. M. Melack, N. T. Roulet, D. S. Schimel, and P. D. Try. 1995. Remote sensing of the land surface for studies of global change: Models-algorithms-experiments. *Remote Sensing of Environment* 51:3–26.

Sellers, P. J., S. I. Rasool, and H.-J. Bolle. 1990. A review of satellite data algorithms for studies of the land surface. *Bulletin American Meteorological Society* 717(10): 1,429–1,447.

Settle, J. J., and S. A. Briggs. 1987. Fast maximum likelihood classification of remotely sensed imagery. *International Journal of Remote Sensing* 8:723–734.

Sharma, K. D., M. Menenti, J. Huygen, and P. C. Fernandez. 1996. Distributed numerical rainfall-runoff modelling in an arid region using Thematic Mapper data and a geographical information system. *Hydrological Processes* 10:1,229–1,242.

Sharma, R. C., and G. P. Bhargava. 1988. Landsat imagery for mapping saline soils and wet lands in north-west India. *International Journal of Remote Sensing* 9:39–44.

Sharma, T., K. S. Sudha, N. Ravi, R. R. Navalgund, Tomar, K. P. Tomar, N. V. K. Chakravarty, and D. K. Das. 1993. Procedures for wheat yield prediction using Landsat MSS and IRS-1A data. *International Journal of Remote Sensing* 14:2,509–2,518.

Shibayama, M., and T. Akiyama. 1991. Estimating grain yield of maturing rice canopies using high spectral resolution reflectance measurements. *Remote Sensing of Environment* 36:45–53.

Shibayama, M., W. Takahashi, S. Morinaga, and T. Akiyama. 1993. Canopy water deficit detection in paddy rice using a high resolution field spectroradiometer. *Remote Sensing of Environment* 45:117–126.

Shih, S. F., and E. Y. Chen. 1984. On the use of GOES thermal data to study effects of land uses on diurnal temperature fluctuation. *Journal of Climate and Applied Meteorology* 23(3): 426–433.

Shih, S. F., and J. D. Jordan. 1993. Use of Landsat thermal-IR data and GIS in soil moisture assessments. *Journal of Irrigation and Drainage Engineering* 119(5): 868–879.

Shutko, A. M. 1991. Present and future applications of land surface remote sensing by microwave radiometry. *Preventive Veterinary Medicine* 11:289–292.

Siderius, W. 1991. *The use of remote sensing for irrigation management with emphasis on IIMI research concerning salinity, waterlogging and cropping patterns.* Mission Report. Enschede, Netherlands: International Institute for Aerospace Survey and Earth Sciences. 97 p.

Simmer, C. 1996. Retrieval of precipitation from satellites. In *Radiation and water in the climate system: Remote measurements,* ed. E. Raschke, 249–276. Berlin: Springer-Verlag.

Singh, A. N., and R. S. Dwivedi. 1989. Delineation of salt-affected soils through digital analysis of Landsat MSS data. *International Journal of Remote Sensing* 10:83–92.

Singh, R. P., and S. K. Srivastav. 1990. Mapping waterlogged and salt affected soils using microwave radiometers. *International Journal of Remote Sensing* 11:1,879–1,887.

Singh, R., R. C. Goyal, S. K. Saha, and R. S. Chikara. 1992. Use of satellite spectral data in crop yield estimation surveys. *International Journal of Remote Sensing* 13:2,583–2,592.

Smith, R. C. G., and B. J. Choudhury. 1990. Relationship of multispectral satellite data to land surface evaporation from the Australian continent. *International Journal of Remote Sensing* 11(11): 2,069–2,088.

Sobrino, J. A., C. Coll, and V. Caselles. 1991. Atmospheric correction for land surface temperature using NOAA-11 AVHRR channels 4 and 5. *Remote Sensing of Environment* 38:19–34.

Soer, G. J. R. 1980. Estimation of regional evapotranspiration and soil moisture conditions using remotely sensed crop surface temperatures. *Remote Sensing of Environment* 9:27–45.

Soil Conservation Service. 1972. Hydrology. Section 4 in *National engineering handbook.* Washington D. C: U.S. Department of Agriculture. 762 p.

Sriramany, S., and V. V. N. Murthy. 1996. A real-time water allocation model for large irrigation systems. *Irrigation and Drainage Systems* 10:109–129.

Staples, G., and J. Hurley. 1996. Rice crop monitoring in Zhaoqing, China using RADARSAT SAR: Initial results. Paper A-1 in *Proceedings of the 17th Asian Conference on Remote Sensing.* Colombo: Survey Department. 5 p.

Steven, M. D. 1993. Satellite remote sensing for agricultural management: Opportunities and logistic constraints. *Photogrammetry and Remote Sensing* 48(4): 29–34.

Steven, M. D., and J. A. Clark. 1990. *Applications of remote sensing in agriculture.* London : Butterworths. 404 p.

Steven, M. D., P. V. Biscoe, and K. W. Jaggard. 1983. Estimation of sugar-beet productivity from reflection in the red and infra-red spectral bands. *International Journal of Remote Sensing* 4:325–339.

Steven, M. D., T. J. Malthus, F. M. Jaggard, and B. Andrieu. 1992. Monitoring responses of vegetation to stress. In *Remote sensing from research to operation: Proceedings of the 18th Annual Conference*

of the Remote Sensing Society, University of Dundee, 15–17 September 1992, ed. A. P. Cracknell and R. A. Vaughan, 369–377. Nottingham, U.K.: Remote Sensing Society.

Stewart, J. B., H. A. R. de Bruin, J. Garatuza-Payan, and C. J. Watts. 1995. Use of satellite data to estimate hydrological variables for Northwest Mexico. In *Remote sensing in action: Proceedings of the 21st Annual Conference of the Remote Sensing Society, University of Dundee, 11–14 September 1995,* ed. P. J. Curran and Y. C. Robertson, 91–98. Nottingham, U.K.: Remote Sensing Society.

Stewart, J. B., T. Engman, R. A. Feddes, and Y. Kerr, eds. 1996. *Scaling up hydrology using remote sensing.* New York: John Wiley. 255 p.

Strahler, A. H. 1980. The use of prior probabilities in maximum likelihood classification of remotely sensed data. *Remote Sensing of Environment* 10:135–163.

Stuhlmann, R. 1996. Clouds and the radiative heating of the earth surface-atmosphere system. In *Radiation and water in the climate system: Remote measurements,* ed. E. Raschke, 151–174. Berlin: Springer-Verlag.

Stum, J., B. Pinty, and D. Ramond. 1985. A parameterization of broadband conversion factors for Meteosat visible radiances. *Journal of Climate and Applied Meteorology* 24:1,377–1,382.

Sutherland, R. A. 1986. Broadband and spectral (2–18 μm) emissivity of some natural soils and vegetation. *Journal of Atmospheric Oceanic Technology* 3:199–202.

Taconet, O., R. Bernard, and D. Vidal-Madjar. 1986. Evapotranspiration over an agricultural region using a surface flux temperature model based on NOAA-AVHRR data. *Journal of Climate and Applied Meteorology* 25:284–307.

Takashima, T., and K. Masuda. 1987. Emissivities of quartz and Sahara dust powders in the infrared region (7–17 mm). *Remote Sensing of Environment* 23:51–63.

Tarpley, J. D. 1979. Estimating incident solar radiation at the surface from geostationary satellite data. *Journal of Applied Meteorology* 18:1,172–1,181.

Tennakoon, S. B., V. V. N. Murthy, and A. Eiumnoh. 1992. Estimation of cropped area and grain yield of rice using remote sensing data. *International Journal of Remote Sensing* 13:427–439.

Thiruvengadachari, S. 1981. Satellite sensing of irrigation pattern in semiarid areas: An Indian study. *Photogrammetric Engineering and Remote Sensing* 46(5): 657–666.

Thiruvengadachari, S., and H. R. Gopalkrishna. 1995. Satellite aided regional vegetation dynamics over India: A case study in Karnataka State. In *Global Change Studies: Scientific results from the 1994 Geosphere-Biosphere program of the Indian Space Research Organisation,* 167–191. ISRO-GBP-SR-42-94. Bangalore, India: Department of Space.

Thiruvengadachari, S., and R. Sakthivadivel. 1997. *Satellite remote sensing techniques to aid irrigation system performance assessment: A case study in India.* Research Report 9. Colombo: International Irrigation Management Institute. 23 p.

Thiruvengadachari, S., Jonna, P. V. Raju, C. S. Murthy, and J. Harikishan. 1995. Satellite remote sensing (SRS) and geographic information system (GIS) applications to aid irrigation system rehabilitation and management. In *46th International Executive Council: ICID-FAO workshop on irrigation scheduling.* Rome: Italian National Committee on Irrigation and Drainage.

Thiruvengadachari, S., C. S. Murthy, and P. V. Raju. 1997. Remote sensing study of Bhakra Canal Command Area, Haryana State, India. Water Resources Group, National Remote Sensing Agency, Hyderabad, India. 82 p. Duplicated.

Thome, R., H. E. Yanez, and J. M. Zuluaga. 1988. Determinación del área bajo riego en la provincia de Mendoza. In *Mecanismos de aprovechamiento hídrico en la région Andina: Imagenes satélitarias y modelos de simulacion,* ed. M. Menenti, 203–227. Mendoza, Argentina: Instituto Nacional de Ciencia y Técnicas Hídricas. .

Thomson, M. C., S. J. Connor, P. J. M. Milligan, and S. P. Flasse. 1996. The ecology of malaria—as seen from Earth-observation satellites. *Annals of Tropical Medicine and Parasitology* 90(3): 243–264.

Timmerman, K. B. 1989. *Standardization of the albedo.* Internal Note 26. Wageningen, Netherlands: DLO-Winand Staring Centre. 29 p.

Townshend, J. R. G. 1984. Agricultural land cover discrimination using Thematic Mapper spectral bands. *International Journal of Remote Sensing* 5(4): 681–698.

Troufleau, D., A. Vidal, A. Beaudin, M. S. Moran, M. A. Weltz, D. C. Goodrich, J. Washburne, and A. F. Rahman. 1994. Using optical-microwave synergy for estimating surface energy fluxes over semi-arid rangeland. In *Sixth International Symposium on Physical Measurement and Signatures in Remote Sensing, Val d'Isère, France, 17-21 January 1994,* 1167–1174. Toulouse, France: Centre National Etudes Spatiales.

Tucker, C. J. 1979. Red and photographic infrared linear combination for monitoring vegetation. *Remote Sensing of Environment* 8:127–150.

Tucker, C. J., B. N. Holben, J. H. Eglin, and J. E. McMurtrey. 1980. Relationship of spectral data to grain yield variation. *Photogrammetric Engineering and Remote Sensing* 46(5): 657–666.

Tucker, C. J., B. N. Holben, J. H. Eglin, and J. E. McMurtrey. 1981. Remote sensing of total dry matter accumulation in winter wheat. *Remote Sensing of Environment* 11:171–189.

Tuzet, A. 1990. A simple method for estimating downward longwave radiation from surface and satellite data by clear sky. *International Journal of Remote Sensing* 11:125–131.

Ulaby, F., A. Aslam, and C. Dobson. 1982. Effects of vegetation cover on the radar sensitivity to soil moisture. *IEEE Transactions on Geoscience and Remote Sensing* 20(4): 476–481.

Ulivieri, C., M. Castronuovo, M. M. Franciono, and A. Cardillo. 1994. A split window algorithm for estimating land surface temperature from satellites. *Advances in Space Research* 14(3): 59–65.

Ustin, S. L., W. W. Wallender, L. Costick, R. Lobato, S. N. Martens, J. Pinzon, and Q. F. Xiao. 1996. *Modeling terrestrial and aquatic ecosystem responses to hydrologic regime in a California watershed.* Davis, California USA: University of California. 33 p.

Valiente, J. A., M. Nunez, E. Lopez-Baeza, and J. F. Moreno. 1995. Narrow-band to broad-band conversion for Meteosat-visible channel and broad-band albedo using AVHRR-1 and 2 channels. *International Journal of Remote Sensing* 16(6): 1,147–1,166.

Valor, E., and V. Caselles. 1996. Mapping land surface emissivity from NDVI: Application to European, African and South American areas. *Remote Sensing of Environment* 57:167–184.

van de Griend, A. A., and M. Owe. 1993. On the relationship between thermal emissivity and the normalized difference vegetation index for natural surfaces. *International Journal of Remote Sensing* 14(6): 1,119–1,131.

van de Griend, A. A., M. Owe, M. Groen, and M. P. Stoll. 1991. Measurement and spatial variation of thermal infrared spatial emissivity in a savanna environment. *Water Resources Research* 27:371–379.

van den Hurk, B. J. J. M., W. G. M. Bastiaanssen, H. Pelgrum, and E. van der Meygaarden. 1997. Soil moisture assimilation for numerical weather prediction using evaporative fraction from remote sensing. *Journal of Applied Meteorology* 36:1,271-1,283.

van Dijk, A., and T. Wijdeveld. 1996. Water management and remote sensing. *Land and Water International* 84:12–15.

van Leeuwen, W. J. D., A. R. Huete, C. L. Walthall, S. D. Prince, A. Bégué, and J. L. Roujean. 1997. Deconvolution of remotely sensed spectral mixtures for retrieval of LAI, fAPAR and soil brightness. *Journal of Hydrology* 188–189(1–4): 697–724.

van Oevelen, P. J., D. H. Hoekman, and R. A. Feddes. 1996. Errors in estimation of areal soil water content from SAR. In *Scaling up in hydrology using remote sensing,* ed. J. B. Stewart, T. Engman, R. A. Feddes, and Y. Kerr, 207–220. New York: John Wiley.

Venkataratnam L. 1983. Monitoring of soil salinity in Indo-Gangetic plain of NW India using multidate Landsat data. In *Proceedings of the Seventeenth International Symposium on Remote Sensing of Environment, 9–13 May 1983, Ann Arbor, Michigan,* 369–377. Vol. I. Ann Arbor, Michigan, USA: Environmental Research Institute of Michigan.

Verhoef, W., M. Menenti, and S. Azzali. 1996. A colour composite of NOAA-AVHRR-NDVI based on time series analysis (1981–1992). *International Journal of Remote Sensing* 17(2): 231–235.

Vidal, A. 1991. Atmospheric and emissivity corrections of land surface temperature measured from satellite using ground measurements or satellite data. *International Journal of Remote Sensing* 12(12): 2,449–2,460.

Vidal, A., and A. Baqri. 1995. Management of large irrigation projects in Morocco. In *Use of remote sensing techniques in irrigation and drainage,* ed. A. Vidal and J. A. Sagardoy, 99–105. Water Reports 4. Rome: FAO.

Vidal, A., and A. Perrier. 1989. Analysis of a simplified relation used to estimate daily evapotranspiration from satellite thermal IR data. *International Journal of Remote Sensing* 10(8): 1,327–1,337.

Vidal, A., and A. Perrier. 1990. Irrigation monitoring by following the water balances from NOAA-AVHRR thermal infrared data. *IEEE Transactions on Geoscience and Remote Sensing* 28:949–954.

Vidal, A., and J. A. Sagardoy, eds. 1995. *Use of remote sensing techniques in irrigation and drainage.* Water Reports 4. Rome: FAO. 202 p.

Vidal, A., P. Maure, H. Durand, and P. Strosser. 1996. Remote sensing applied to irrigation system management: Example of Pakistan. In *EURISY Colloquium: Satellite Observation for Sustainable Development in the Mediterranean Area,* 132–142. Paris: Promotion of Education and Information Activities for the Advancement of Space Technology and its Applcation in Europe.

Vincent, B., E. Frejefond, A. Vidal, and A. Baqri. 1995. Drainage performance assessment using remote sensing in the Gharb Plain, Morocco. In *Use of remote sensing techniques in irrigation and drainage,* ed. A. Vidal and J. A. Sagardoy, 155–164. Water Reports 4. Rome: FAO.

Vincent, B., A. Vidal, D. Tabbet, A. Baqri, and M. Kuper. 1996. Use of satellite remote sensing for the assessment of waterlogging or salinity as an indication of the performance of drained systems. In *Evaluation of performance of subsurface drainage systems: 16th Congress on Irrigation and Drainage, Cairo, Egypt, 15–22 September 1996,* ed. B. Vincent, 203–216. New Delhi: International Commission on Irrigation and Drainage.

Visser, T. N. M. 1989. Appraisal of the implementation of water allocation policies. ICW Nota 1963. Wageningen, Netherlands: ICW (Instituute voor Cultuurtechnick en Waterhuishouding). 54 p.

Visser, T. N. M. 1990. *Assessment of the green areas of Riyadh.* Report 21. Wageningen, Netherlands: DLO-Winand Staring Centre. 43 p.

Vorosmarty, C. L., C. J. Willmot, B. J. Choudhury, A. L. Schloss, T. K. Stearns, S. M. Robeson, and T. J. Dorman. 1996. Analyzing the discharge regime of a large tropical river through remote sensing, ground-based climatic data and modeling. *Water Resources Research* 32(10): 3,137–3,150.

Waddington, G., and F. Lamb. 1990. Using remote sensing images in commercial agriculture. *Advanced Imaging*: 5(9): 46–49.

Wan, Z., and J. Dozier. 1989. Land surface temperature measurements from space: Physical principles and inverse modelling. *IEEE Transactions on Geoscience and Remote Sensing* 27: 268–278.

Wang, F. 1990. Fuzzy supervised classification of remote sensing images. *IEEE Transactions on Geoscience and Remote Sensing* 28(2): 194–201.

Wang, J. R., and T. J. Schmugge. 1980. An empirical model for the complex dielectric permittivity of soils as a function of water content. *IEEE Transactions on Geoscience and Remote Sensing* 18:288–295.

Wang, J., Y. Ma, L. Jia, K. Sahaski, E. Ohtaki, T. Maitani, O. Tsukamoto, and Y. Mitsuta. 1994. Downward sensible heat flux during daytime observed in the oasis station. In *Proceedings of International Symposium on HEIFE,* ed. Y. Mitsuta, 449–457. Kyoto, Japan: Disaster Prevention Research Institute, Kyoto University.

Wang, J., Y. Ma, M. Menenti, W. G. M. Bastiaanssen and Y. Mitsuta. 1995. The scaling-up of processes in the heterogeneous landscape of HEIFE with the aid of satellite remote sensing. *Journal of the Meteorological Society of Japan* 73(6): 1,235–1,244.

Watson, K. 1992a. Two-temperature method for measuring emissivity. *Remote Sensing of Environment* 42:117–121.

Watson, K. 1992b. Spectral ratio method for measuring emissivity. *Remote Sensing of Environment* 42:113–116.

Watts, C. J., J. C. Rodriguez, H. A. R. de Bruin, A. R. van den Berg, J. Garatuza-Payan, and J. B. Stewart. 1995. Estimation of incoming solar radiation using satellite data. In *Remote sensing in action: Proceedings of the 21st Annual Conference of the Remote Sensing Society, 11 to 14 September 1995,* 903–910. Nottingham, UK: Remote Sensing Society.

Weiss, A., and J. M. Norman. 1985. Partitioning solar radiation into direct and diffuse, visible and near-infrared components. *Agricultural and Forest Meteorology* 34:205–213.

Wetzel, P. J., D. Atlas, and R. Woodward. 1984. Determining soil moisture from geosynchronous satellite infrared data: A feasibility study. *Journal of Climate and Applied Meteorology* 23:375–391.

Whitlock, C. H., T. P. Charlock, W. F. Staylor, R. T. Pinker, I. Laszlo, A. Ohmua, H. Gilgen, T. Konzelman, R. C. DiPasquale, C. D. Moats, S. R. LeCroy, and N. A. Ritchey. 1995. First global WCRP shortwave surface radiation budget datasets. *Bulletin of the American Meteorology Society* 76:905–922.

Wiegand, C. L., J. H. Everitt, and A. J. Richardson. 1992. Comparison of multispectral video and SPOT-1 HRV observations for cotton affected by soil salinity. *International Journal of Remote Sensing* 13(8): 1,511–1,525.

Wijk, W. R. van, and D. A. de Vries. 1954. Evapotranspiration. *Netherlands Journal of Agricultural Science* 2:105–119.

Williams, V. L., W. R. Philipson, and W. D. Philpot. 1987. Identifying vegetable crops with Landsat Thematic Mapper data. *Photogrammetric Engineering and Remote Sensing* 53:187–191.

Williamson, H. D. 1989. The discrimination of irrigated orchard and vine crops using remotely sensed data. *Photogrammetric Engineering and Remote Sensing* 55:77–82.

Wit, C. T. de. 1958. *Transpiration and crop yields.* Verslagen van Landbouwkundige Onderzoekingen 64.6. Wageningen, Netherlands: Instituut voor Biologisch en Scheikundig Onderzoek van Lanbouwgewassen. 88 p.

Wittmeyer, I. L., and T. H. vonder Haar. 1994. Analysis of the global ISCCP TOVS water vapor climatology. *Journal of Climate* 7:325–333.

WMO (World Meteorological Organization). 1988. *Concept of the Global Energy and Water Experiment (GEWEX).* Report WCRP 5. Geneva, Switzerland. 130 p.

Wolters, W., A. W. Zevenbergen, and M. G. Bos. 1991. Satellite remote sensing in irrigation. *Irrigation and Drainage Systems* 5:307–323.

Wong, C. L., and W. R. Blevin. 1967. Infrared reflectances of plant leaves. *Australian Journal of Biological Science* 20:501–512.

Wood, E. F., and V. Lakshmi. 1993. Scaling water and energy fluxes in climate systems, three land-atmospheric modeling experiments. *Journal of Climate* 6(5): 839–857.

Wood, E. F., D. S. Lin, M. Mancini, D. Thongs, P. A. Troch, T. J. Jackson, J. S. Famiglietta, and E. T. Engman. 1993. Intercomparisons between passive and active microwave remote sensing and hydrological modelling for soil moisture. *Advances in Space Research* 13(5): 167–176.

Wright, J. L. 1982. New evapotranspiration crop coefficients. *Journal of the Irrigation and Drainage Division, ASCE* 108:57–74.

Wukelic, G. E., D. E. Gibbons, L. M. Martucci, and H. P. Foote. 1989. Radiometric calibration of Landsat Thematic Mapper thermal band. *Remote Sensing of Environment* 28:339–347.

Xia, Li. 1994. A two-axis vegetation index (TWVI). *International Journal of Remote Sensing* 15:1,447–1,458.

Xinmei, H., T. J. Lyons, R. C. G. Smith, and J. M. Hacker. 1995. Estimation of land surface parameters using satellite data. In *Passive microwave remote sensing of land-atmosphere interactions*, ed. B. J. Choudhury, Y. H. Kerr, E. G. Njoku, and P. Pampaloni, 387–399. Utrecht, Netherlands: VSP Publishing.

Yamagata, Y. C., and T. Akiyama. 1988. Flood damage analysis using multi-spectral Landsat Thematic Mapper data. *International Journal of Remote Sensing* 9:503–514.

Zevenbergen, A. W., A. Rango, J. C. Ritchie, E. T. Engman, and R. H. Hawkins. 1988. Rangeland runoff curve numbers as determined from Landsat MSS data. *International Journal of Remote Sensing* 9:495–502.

Zhang, L., R. Lemeur, and J. P. Gourtorbe. 1995. A one-layer resistance model for estimating regional evapotranspiration using remote sensing data. *Agricultural and Forest Meteorology* 77:241–261.

Zhang, Y. C., W. B. Rossow, and A. A. Lacis. 1995. Calculation of surface and top of atmosphere radiative fluxes from physical quantities based on ISCCP data sets: 1. Method and sensitivity to input data uncertainties. *Journal of Geophysical Research–Atmospheres* 100(D1): 1,149–1,165.

Zhong, Q., and Y. H. Li. 1988. Satellite observation of surface albedo over the Qinghai-Xizang plateau region. *Advances in Atmospheric Science* 5:57–65.

Zimmerman, H. J. 1991. *Fuzzy set theory and its applications*, 2nd ed. Dordrecbt, Netherlands: Kluwer. 399 p.

Zuluaga, J. M. 1990. Remote sensing applications in irrigation management in Mendoza, Argentina. In *Remote sensing in evaluation and management of irrigation*, ed. M. Menenti, 37–58. Mendoza, Argentina: Instituto Nacional de Ciencia y Técnicas Hídricas.